JARA|FIT Fundamentals of Future Information Technology

UNIVERSITÀ DEGLI STUDI DI PERUGIA

JÜLICH FORSCHUNGSZENTRUM

The 6th IEEE Magnetics Society Summer School

JUNE 9-14, 2013 ASSISI, ITALY

IEEE

MAGNETICS

Spintronics

Daniel E. Bürgler

Peter Grünberg Institute, Electronic Properties (PGI-6) and Jülich-Aachen Research Alliance (JARA-FIT)
Forschungszentrum Jülich, Germany

Assisi June 11, 2013

Overview: Spin transfer processes for spintronics

Introduction

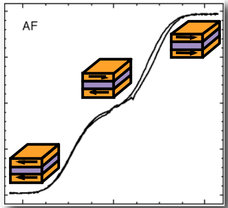

Interlayer exchange coupling

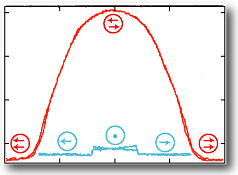

Giant and tunneling magnetoresistance

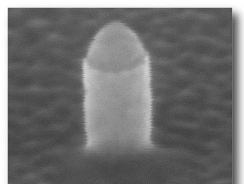

Current-induced magnetization dynamics

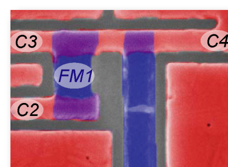

Pure spin current

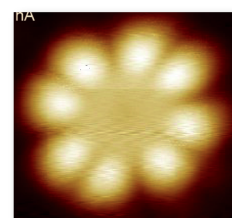

Magnetic molecules
(Time permitting)

Conclusions

Conduction electrons in a solid

Conduction electrons move with Fermi velocity ($v_F \approx 10^6$ m/s) and undergo random scattering from defects, phonons, electrons

Relaxation time $\tau \approx 10^{-14}$ - 10^{-15} s $\Rightarrow$ Mean free path $\lambda = v_F\tau \approx 1$ - 10 nm

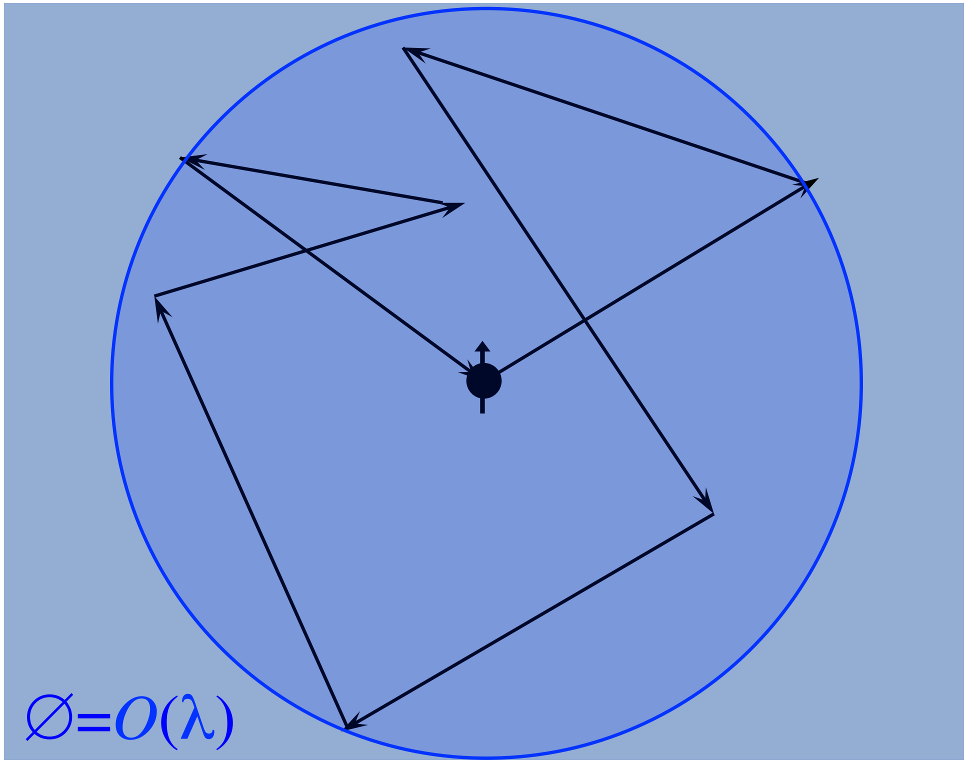

$\Rightarrow$ Conduction electrons experience the environment on a length scale given by the mean free path λ

Drift velocity

An electric field $\boldsymbol{E}$ superimposes a much lower drift velocity ($v_D \approx 10^3$-10^4 m/s) in the direction of the electric field:

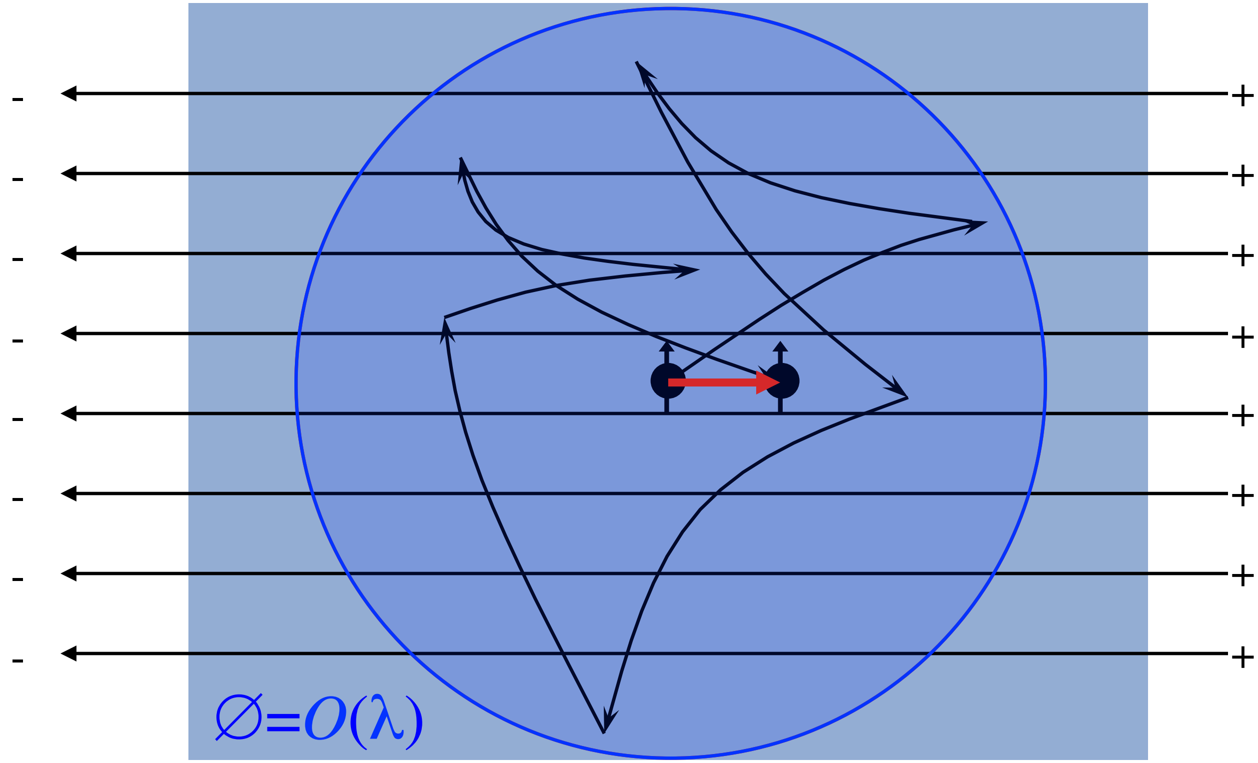

$\boldsymbol{E}$-field:
$\boldsymbol{F} = q\boldsymbol{E} = m\boldsymbol{a}$

⇒ $\boldsymbol{E}$-field induces net transport of electrons, *i.e.* electrical current
⇒ Diffusive transport for $d >> \lambda$ or ballistic transport for $d < \lambda$

Electrons in a multilayer

Consider multilayer with layer thicknesses less than λ.

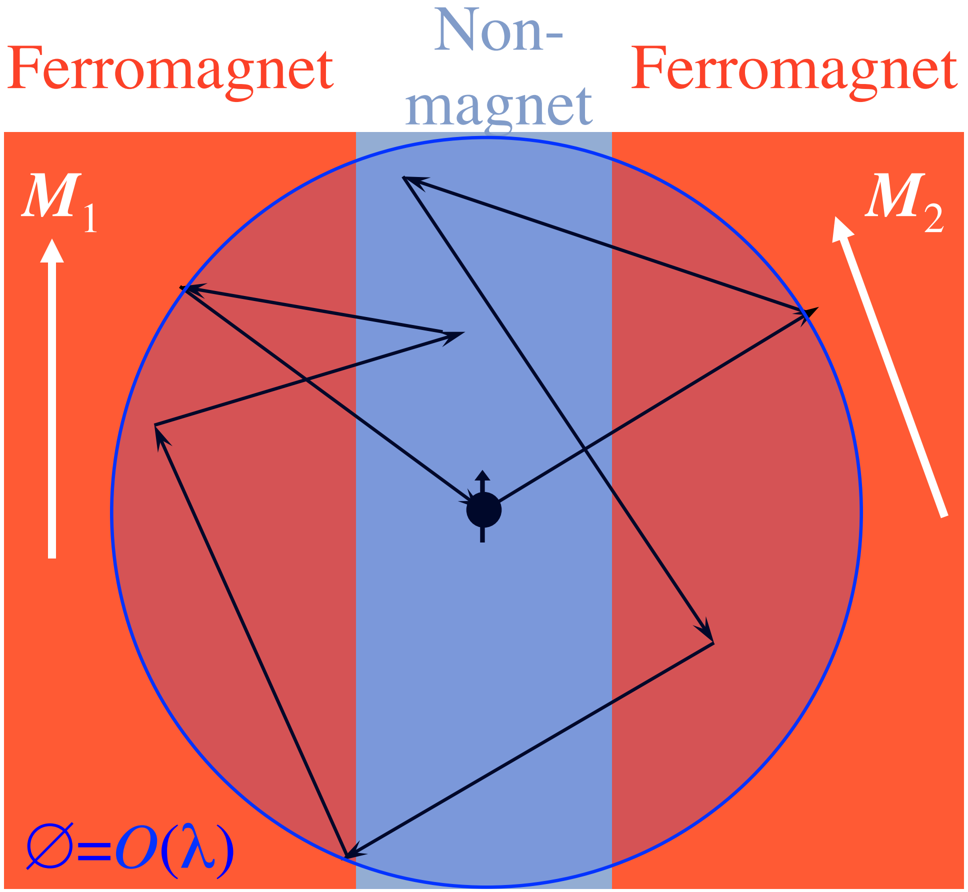

⇒ Conduction electrons experience both magnetic layer

⇒ Static spin-transfer processes

Spin-flip scattering is less probable than momentum scattering
Spin-flip length exceeds to mean free path L

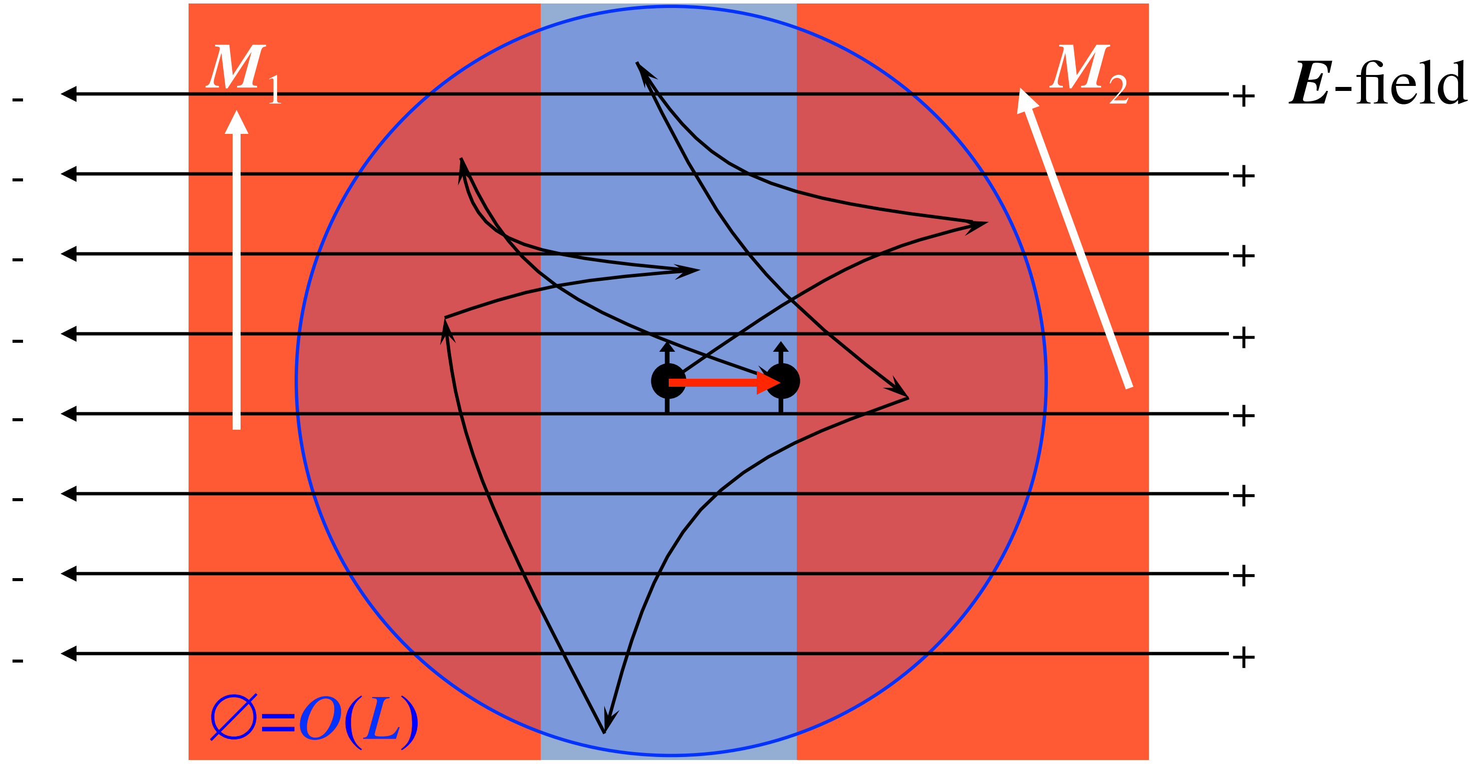

$\Rightarrow$ ***E***-field gives rise to net charge and/or spin currents
$\Rightarrow$ Dynamic spin-transfer processes

Definition of spintronics

- Spintronics (magnetoelectronics) comprises all spin-dependent electronic transport phenomena.
  $\Rightarrow$ Novel fundamental physics

- Spintronics make use of the spin degree of freedom of the electron in addition to (or instead of) its charge.
  $\Rightarrow$ Spin transport *versus* charge transport

- Spintronics is a new paradigm of electronics based on the spin degree of freedom of the electron.
  $\Rightarrow$ Novel prospects for applications in information technology

Spin-resolved density of states (SDOS)

Electrical transport is due to charge carriers close to the Fermi edge E_F ($\Delta E \approx kT$)

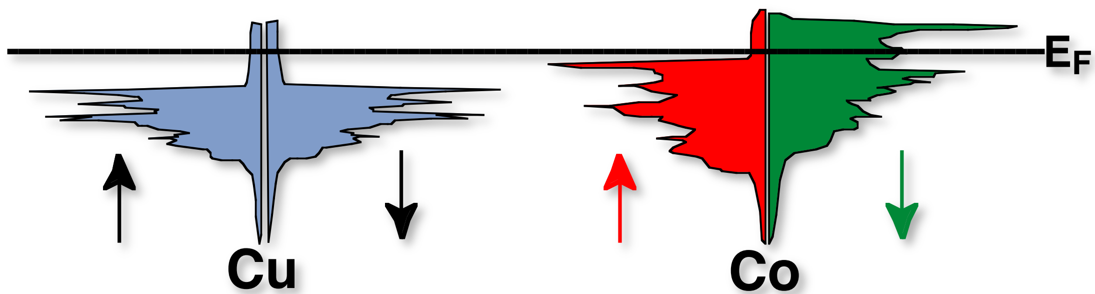

Unequal DOS for spin-up and spin-down in ferromagnets lead to a polarization of the current

IMPORTANT: Distinguish

1) Total occupation number for the two spin orientations: $N_\uparrow$ and $N_\downarrow$

$\Rightarrow$ Majority and minority spins; magnetization $M \propto (N_\uparrow - N_\downarrow)$

2) Density of states at the Fermi edge $E_{F:}$ $N_\uparrow(E_F)$ and $N_\downarrow(E_F)$

$\Rightarrow$ Polarization P at E_F

Spin polarization

An imbalance of spin-up and spin-down electrons (*e.g.* in a ferromagnet) can give rise to a spin-polarized current $\Rightarrow$ Spin-transport.

The spin polarization $P_{current}$ of a current is defined as

$$P_{current} = \frac{J^{\uparrow} - J^{\downarrow}}{J^{\uparrow} + J^{\downarrow}} \quad ; \quad \left| P_{current} \right| \leq 1 \quad ; \quad J^{\uparrow,\downarrow}: \text{current densities}$$

However, $J^{\uparrow,\downarrow}$ cannot be measured directly.

$\Rightarrow$ Various, system and experiment dependent "definitions" of spin polarization are used instead

Various definitions of spin polarization

$$P_{current} = \frac{J^{\uparrow} - J^{\downarrow}}{J^{\uparrow} + J^{\downarrow}} \quad ; \quad \left|P_{current}\right| \le 1 \quad ; \quad J^{\uparrow,\downarrow}\text{: current densities}$$

Popular, but only for ground state valid definition (no current) :

$$P = \frac{N^{\uparrow}(E_F) - N^{\downarrow}(E_F)}{N^{\uparrow}(E_F) + N^{\downarrow}(E_F)} \quad ; \quad |P| \le 1 \quad ; \quad N^{\uparrow,\downarrow}(E_F)\text{: SDOS at Fermi edge}$$

Ballistic transport: $J \propto \langle Nv \rangle \Rightarrow P_{Nv} = \dfrac{\langle Nv \rangle^{\uparrow} - \langle Nv \rangle^{\downarrow}}{\langle Nv \rangle^{\uparrow} + \langle Nv \rangle^{\downarrow}}$

Diffusive transport: $J \propto \langle Nv^2 \rangle \Rightarrow P_{Nv^2} = \dfrac{\langle Nv^2 \rangle^{\uparrow} - \langle Nv^2 \rangle^{\downarrow}}{\langle Nv^2 \rangle^{\uparrow} + \langle Nv^2 \rangle^{\downarrow}}$

$v^{\uparrow,\downarrow}$: velocity ; $\langle ... \rangle^{\uparrow,\downarrow}$ integral over Fermi surface of up or down states

$\Rightarrow$ Spin polarization is NOT a uniquely defined quantity

I.I. Mazin, Phys. Rev. Lett. **83**, 1427 (1999)

Spin relaxation

In contrast to the charge the spin of an electron is not conserved.

Electrons in a solid undergo random scattering. Most scattering event are spin-conserving but change the momentum
$\Rightarrow$ momentum scattering, relaxation time τ

Some (1 in $N \approx 10^3$) scattering events transfer angular momentum (e.g. to the lattice by spin-orbit coupling) and flip the spin
$\Rightarrow$ spin-flip scattering, relaxation time $\tau_{SF} >> \tau$

$\Rightarrow$ After $N = \tau_{SF} / \tau$ scattering events the spin-flip occurs. The characteristic length scale is the spin diffusion length λ_{SF}:

$\lambda_{SF} = v_F \tau_{SF} \approx$ 1-10 nm for Py
50 nm for Co
100 nm for Cu
>10 μm for 2-DEG GaAs/GaAlAs or Si

Spin diffusion length

Total path to spin-flip:

$$L_{SF} = N\lambda = \lambda\, \tau_{SF} / \tau$$

Spin diffusion length λ_{SF} in a random walk model:

$$\lambda_{SF} = \sqrt{\frac{N}{3\lambda}} = \lambda\sqrt{\frac{\tau_{SF}}{3\tau}}$$

⇒ The spin state of an electron in a solid relaxes within a spin diffusion length of typically few to several 100 nm (for metals)

⇒ Need for nanostructures

⇒ Spintronics is a nanotechnology

Decay of spin polarization

An imprinted (injected) spin polarization P decays due to spin-flip processes to the equilibrium polarization P_0:

$$P(x) = P_0 + (P - P_0)\exp(-x/\lambda_{SF})$$

Consider a ferromagnet with $P_0 \neq 0$. The unequal density of final states for the two spin directions yields asymmetric spin-flip scattering probabilities. Simple model:

$$\lambda_{SF}(P_0) = \lambda_{SF} / (1-P_0^{\,2})^{1/2} \qquad \Rightarrow \qquad P = \pm 1 : \lambda_{SF}(P_0) = \infty$$

All electrons are majority electrons. Spin-flip is forbidden because there are no minority states at near the Fermi level.

$\Rightarrow$ Strongly polarized materials show less spin relaxation

$\Rightarrow$ Intense search for ferromagnetic half-metals

Overview

Introduction

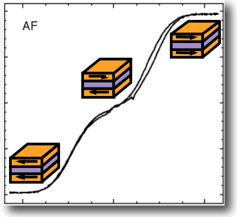

Interlayer exchange coupling

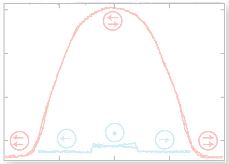

Giant and tunneling magnetoresistance

Current-induced magnetization dynamics

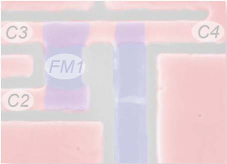

Pure spin current

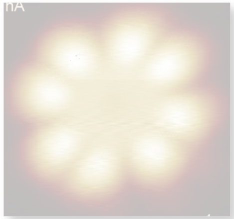

Magnetic molecules

Conclusions

Once upon a time, in the early 1980's …

Peter Grünberg

"What happens if
I bring two ferromagnets close
–I mean *really* close–
together?"

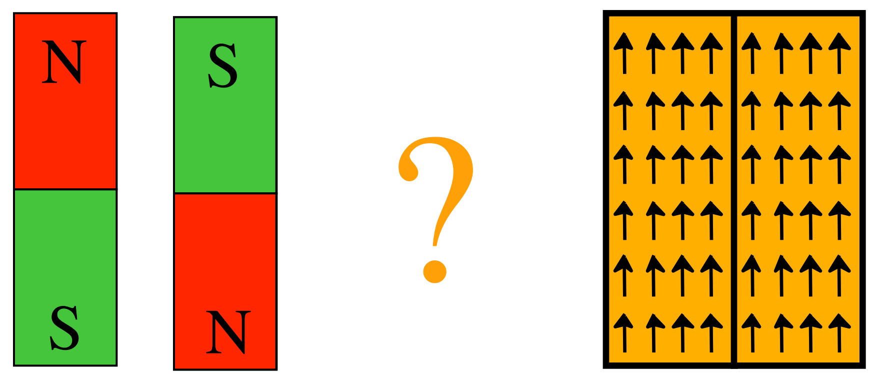

Phenomenology of Magnetic Interlayer Coupling

Consider two ferromagnetic layers separated by a thin spacer layer:

Ferromagnet / Non-Ferromagnet / Ferromagnet

The ferromagnetic layers interact across the spacer and align …

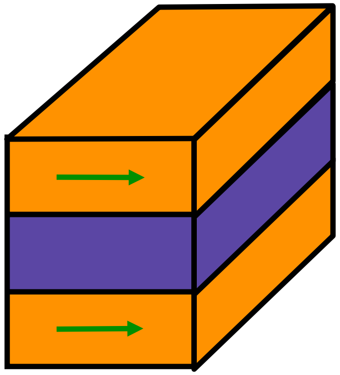

… parallel …

“ferromagnetic coupling”

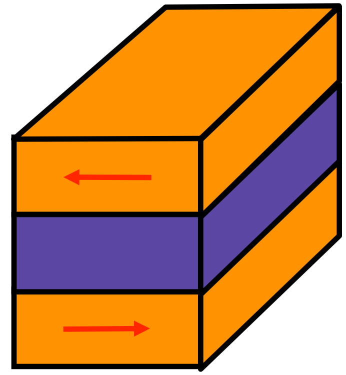

… antiparallel …

“antiferromagnetic coupling”

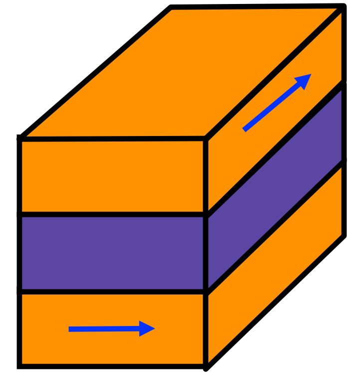

… at 90°…

“biquadratic or 90°-coupling”

Outline: Interlayer exchange coupling

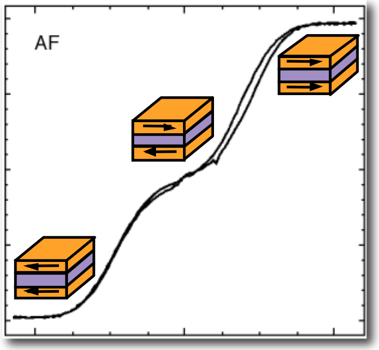

- Phenomenology of interlayer coupling
- Measurement by MOKE
- Physical picture for oscillatory bilinear coupling
- Biquadratic coupling
- Example: Morphology and "Fermiology"
- Applications
- Conclusions

Phenomenological description

Contribution of IEC to the areal free energy density :

$$E = -J_1 \cos(\Delta\Theta) - J_2 \cos^2(\Delta\Theta)$$

"bilinear" "biquadratic"

$\Delta\theta$ is the angle between the magnetizations of the two coupled layers.

J_1 and J_2 are parameters describing the coupling:

$J_1 > 0$: FM coupling

$J_1 < 0$: AF coupling

J_2 dominant and $J_2 < 0$: 90^o coupling

Note: $J_1(D)$ oscillates as a function of the spacer thickness D

Oscillatory interlayer exchange coupling

- only occurs for thin spacers with a thickness of a few nm
- is observed for many metallic spacer layers
  (see [1] for a "periodic table of interlayer coupling")
- oscillates as a function of the spacer thickness *D*

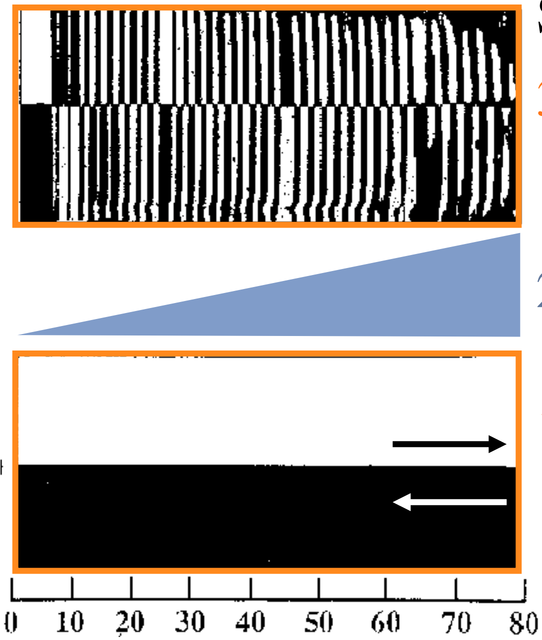

Cr spacer thickness *D* (ML)

Scanning electron microscopy with spin analysis (SEMPA) [2]:

3) Domain picture of Fe
layer grown on Cr wedge

2) Wedge-shaped Cr spacer

1) Domain picture of Fe
single crystal (whisker)
with two domains

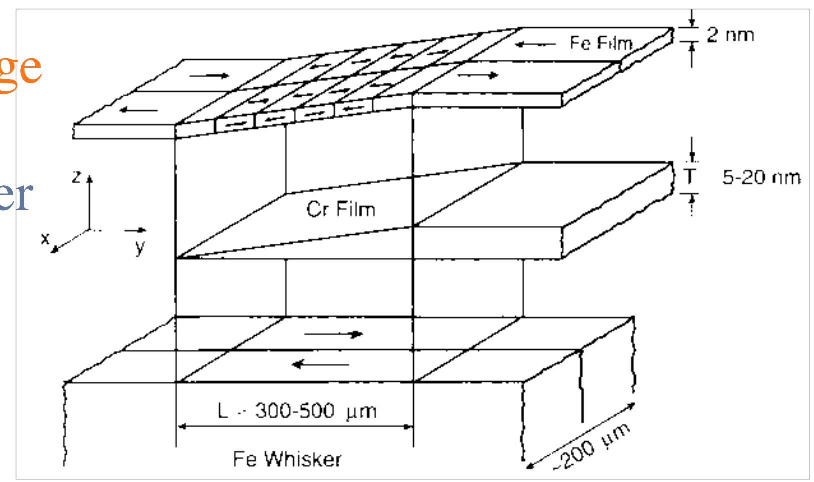

[1] S.S.P. Parkin, Phys. Rev. Lett. **67**, 3958 (1991)
[2] D.T. Pierce *et al*., Phys. Rev. B **49**, 14564 (1994)

Outline: Interlayer exchange coupling

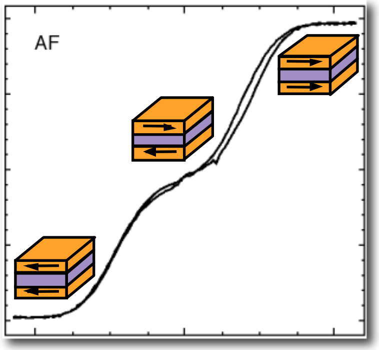

- Phenomenology of interlayer coupling
- Measurement by MOKE
- Physical picture for oscillatory bilinear coupling
- Biquadratic coupling
- Example: Morphology and "Fermiology"
- Applications
- Conclusions

MOKE setup

The magneto-optical Kerr effect is a simple means to measure hysteresis loops of thin films and multilayers. Any other method (*e.g*. SQUID, VSM, etc.) yielding hysteresis loops or sensitive to a local effective field (FMR, BLS) can be used to determine interlayer coupling.

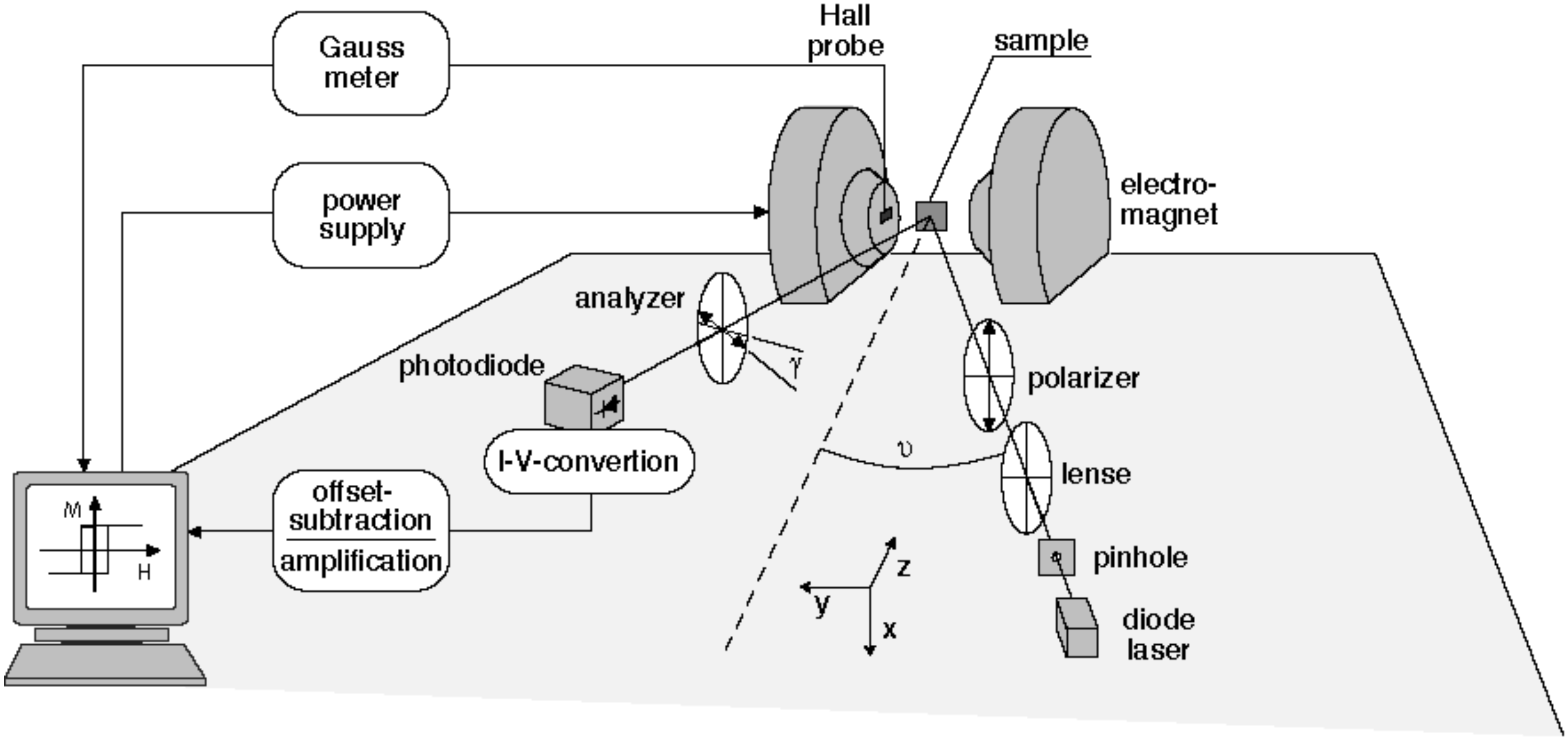

Typical hysteresis loops for different types of interlayer coupling

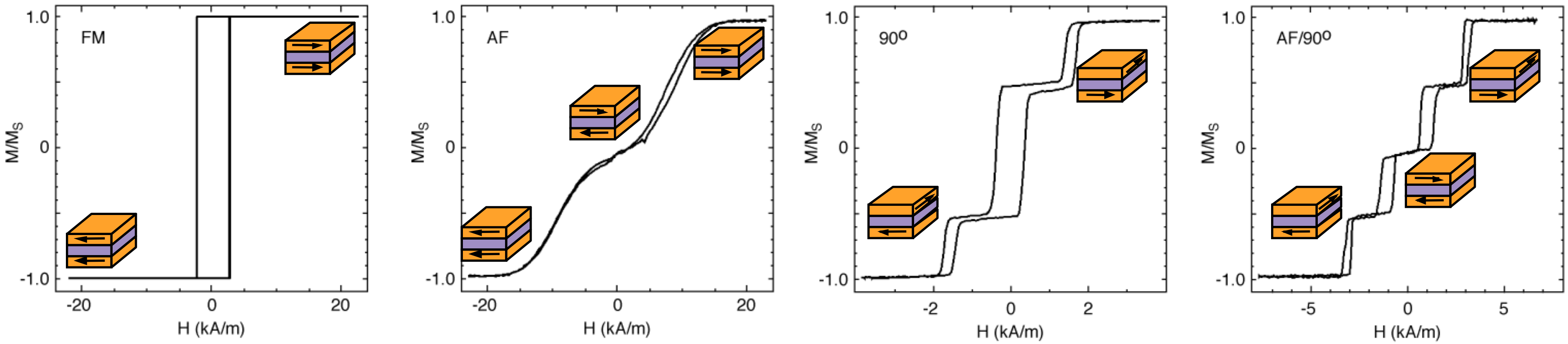

FM coupling
or
decoupled

AF coupling

90° coupling

Dominant
90° plus AF
coupling

The saturation and switching fields are approximate measures for the coupling strength

BUT: A quantitative determination of the coupling needs fitting.

Phenomenological *ansatz* for a coupled trilayer

$$
\begin{aligned}
E(\Theta_1,\Theta_2) = & \qquad\qquad\qquad \text{Free energy per area =}\\
& - HM_S[d_1\cos(\Theta_1) + d_2\cos(\Theta_2)] \qquad \text{Zeemann energy}\\
& + \frac{1}{4}[K_1 d_1 \sin^2(2\Theta_1) + K_2 d_2 \sin^2(2\Theta_2)] \qquad \text{+ in-plane anisotropy}\\
& - J_1\cos(\Theta_1 - \Theta_2) \qquad \text{+ bilinear coupling}\\
& - J_2\cos^2(\Theta_1 - \Theta_2) \qquad \text{+ biquadratic coupling}
\end{aligned}
$$

Fitting procedure: Determine for each field H the magnetization alignment (θ_1,θ_2) that minimizes the free energy E. Examples for Fe/Cr/Fe(001):

J_1 = -0.21 mJ/m^2

J_2 = -0.10 mJ/m^2

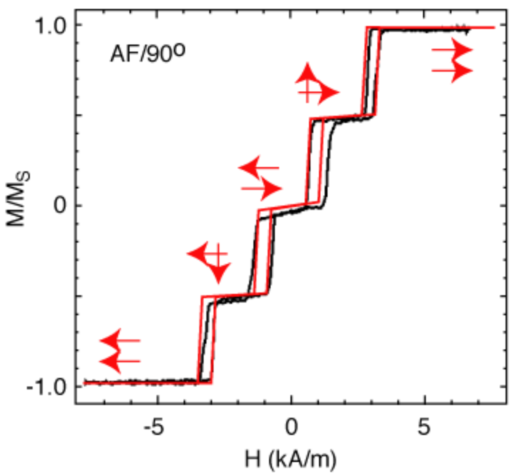

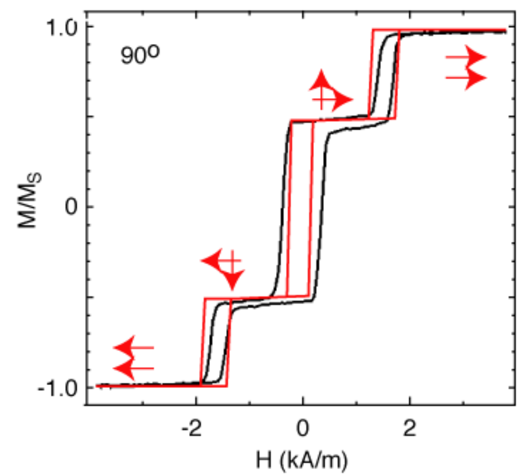

$J_1 + J_2 =$ -0.16 mJ/m^2

with

$J_1 < 2\,J_2$

Typical bilinear coupling strengths

Sample	Maximum strength $-J_1$ in mJ/m^2 (at spacer thickmann in nm)	Periods in ML and (nm)
Co/Cu/Co (100)	0.4 (1.2)	2.6 (0.47); 8 (1.45)
Co/Cu/Co (110)	0.7 (0.85)	9.8 (1.25)
Co/Cu/Co (111)	1.1 (0.85)	5.5 (1.15)
Fe/Au/Fe (100)	0.85 (0.82)	2.5 (0.51) ; 8.6 (1.75)
Fe/Cr/Fe (100)	> 1.5 (1.3)	2.1 (0.3); 12 (1.73)
Fe/Mn/Fe (100)	0.14 (1.32)	2 (0.33)
Co/Ru/Co (0001)	6 (0.6)	5.1 (1.1)
Co/Rh/Co (111)	34 (0.48)	2.7 (0.6)
Fe/Si/Fe (100)	6-8	---

Experimental values are often much smaller than theoretically predicted due to roughness, interdiffusion, etc.

Direct exchange in Fe: $J \approx \frac{k_B T_C}{a^2} = 170 \, \frac{\text{mJ}}{\text{m}^2}$; $T_C = 1040$ K, $a = 2.9$ Å

Outline: Interlayer exchange coupling

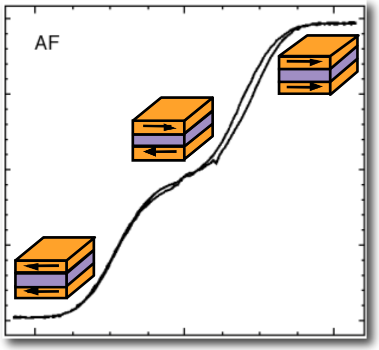

- Phenomenology of interlayer coupling
- Measurement by MOKE
- Physical picture for oscillatory bilinear coupling
- Biquadratic coupling
- Example: Morphology and "Fermiology"
- Applications
- Conclusions

Origin of bilinear coupling

Distinguish antiferromagnetic and paramagnetic/diamagnetic spacers:

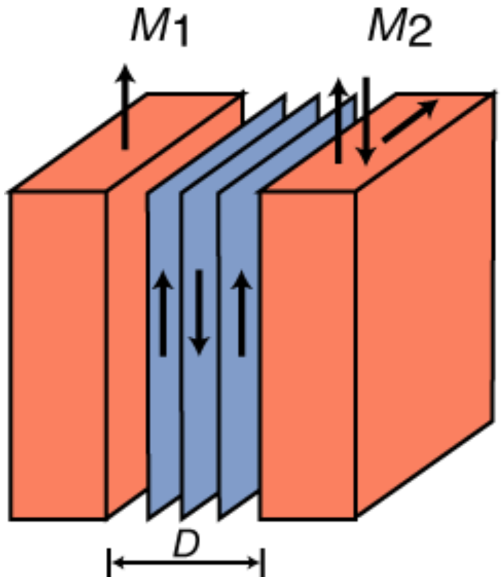

Direct exchange from layer to layer gives rise to oscillations with a period of two monolayers. Possible example: Cr(001) spacers ?

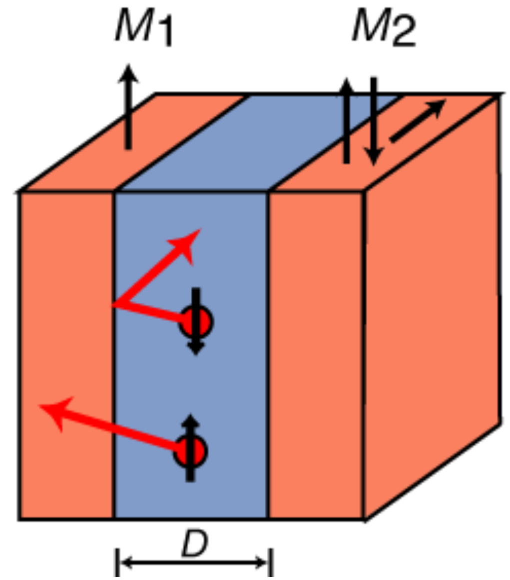

New explanation needed for diamagnetic/paramagnetic spacers without intrinsic magnetic order:

Conduction electrons in the spacer mediate the coupling!

First simple explanation: RKKY-oscillations

Ruderman, Kittel, Kasuya, and Yoshida considered in the 1950's magnetic impurities in a non-magnetic metal host :

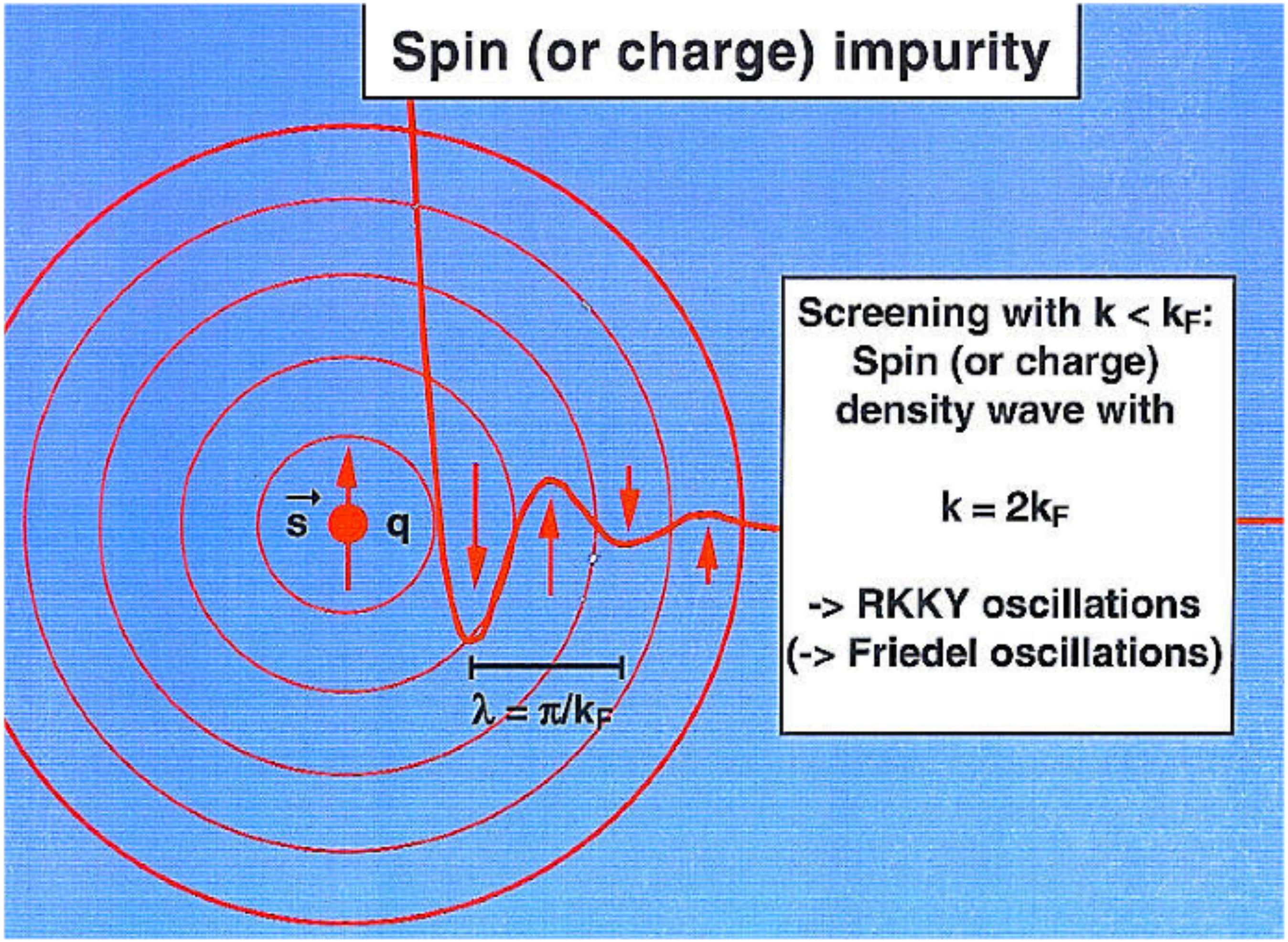

The interaction of two magnetic impurities is oscillating with their separation r and decays with r^3:

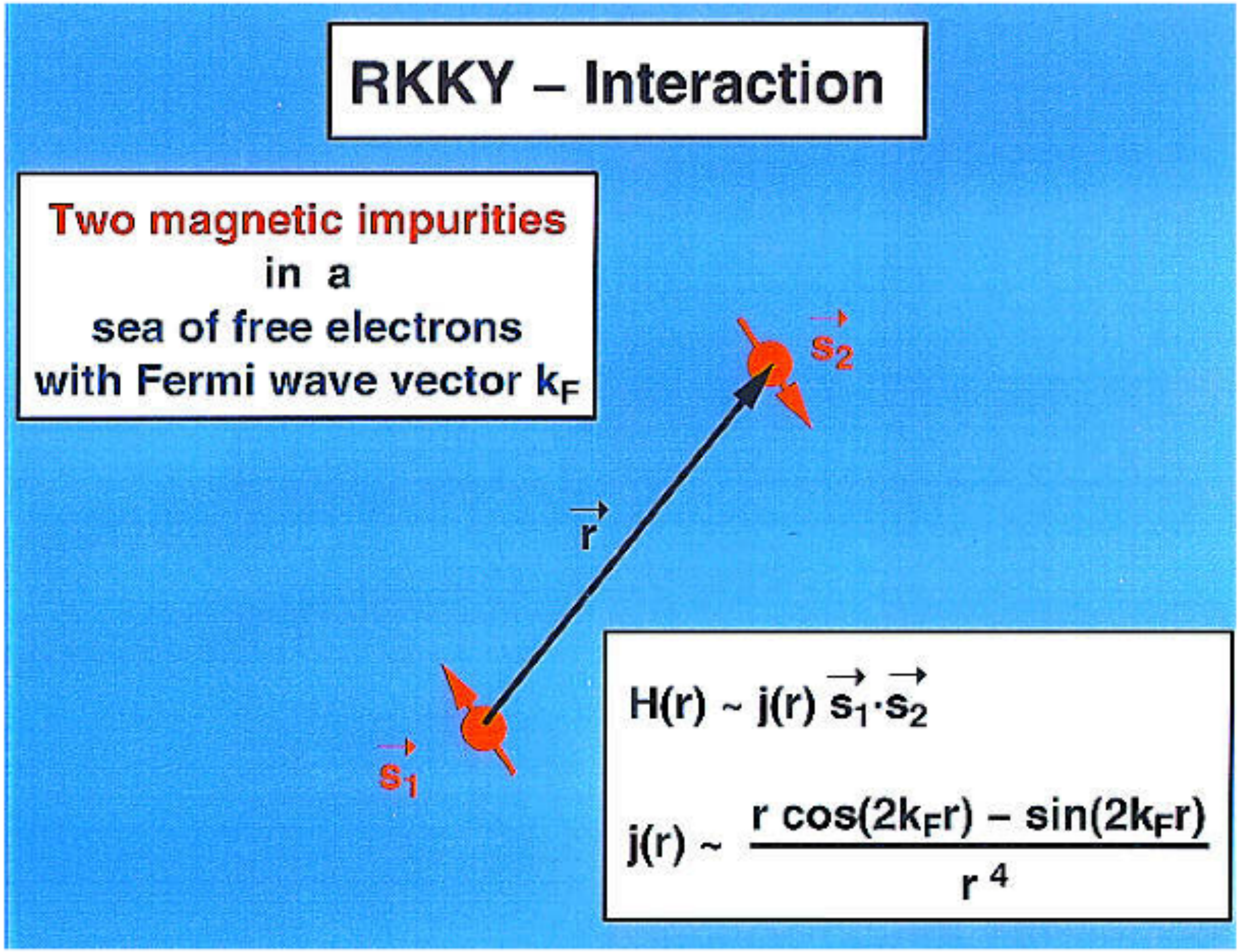

RKKY-model

Extension to two layers of "magnetic impurities": The interaction oscillates with with the layer separation z and decays with z^2:

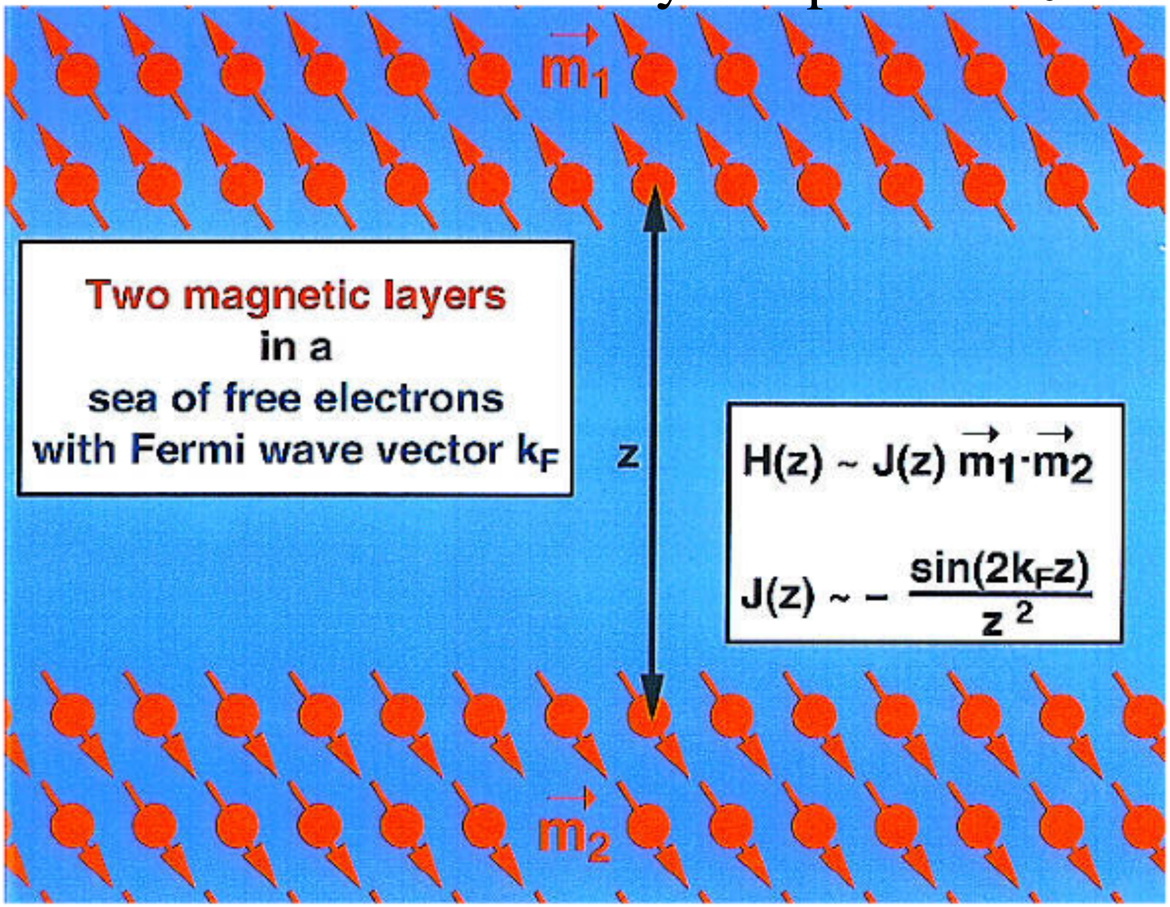

Periodicity of $J(z)$:

$Q = 2k_F$

⇒ Simple and intuitive, but not simply applicable to real spacer materials

Quantum interference model for bilinear coupling

Consider spin-dependent quantum well states (QWS) due to spin-dependent reflectivities at the interfaces between spacer and FM layers.

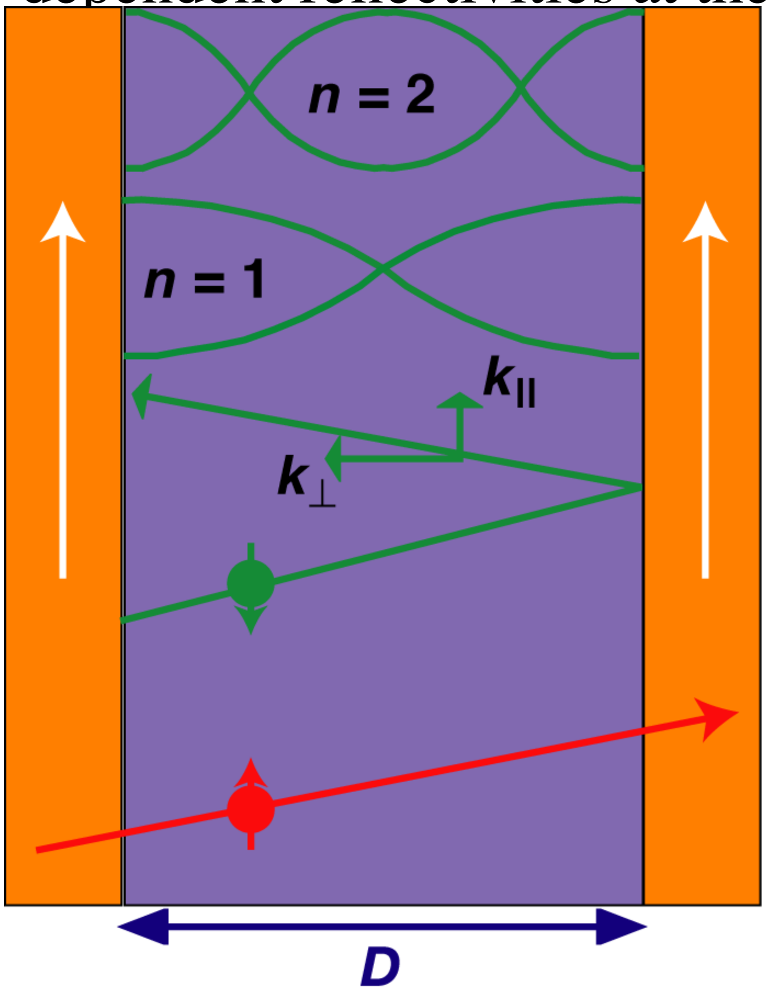

For a certain spacer thickness *D* there is a series of QWS fulfilling the condition:

$$D = n\frac{\lambda}{2} \quad ; \quad n = 1,2,3,\ldots \qquad \lambda = \frac{2\pi}{k_\perp}$$

$$\Rightarrow k_\perp^{(n)} = n\frac{\pi}{D} \quad ; \quad n = 1,2,3,\ldots$$

$$\Rightarrow \text{Period } \Delta D = \frac{\lambda}{2} = \frac{2\pi}{2k_\perp} \text{ for given } k_\perp$$

P. Bruno, Phys. Rev. B **52**, 411 (1995)

What is the origin of spin-dependent reflectivity?

Spin-dependent reflectivity arises from the "potential landscape" seen by the electrons due to the layered structure. The two spin channels experience different potential steps at the interfaces between the spacer and the FM layers.

Example Co / Cu / Co:

Similar band structure (low potential steps and low reflectivity) for majority electrons and shifted band structure (high potential step and high reflectivity) for minority electrons:

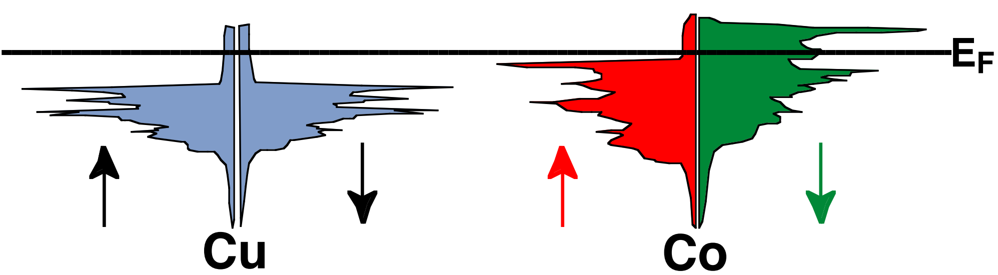

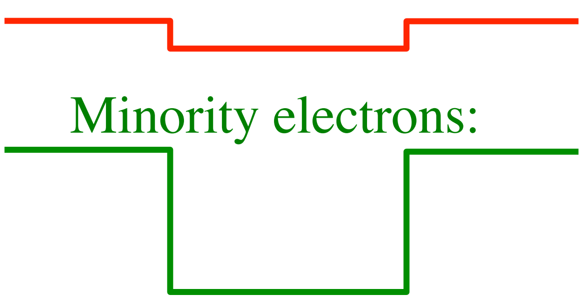

Spin-dependent “Spaghetti diagrams” of Co and Cu

Example Co / Cu / Co: Similar band structure for Cu and majority electrons; shifted band structure for minority electrons:

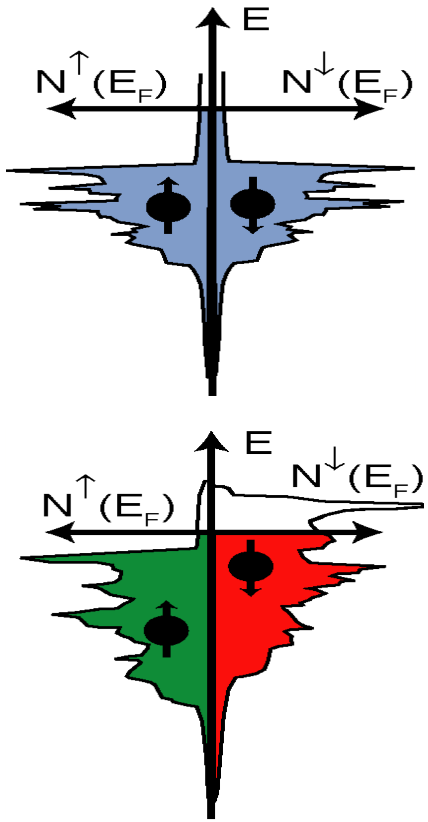

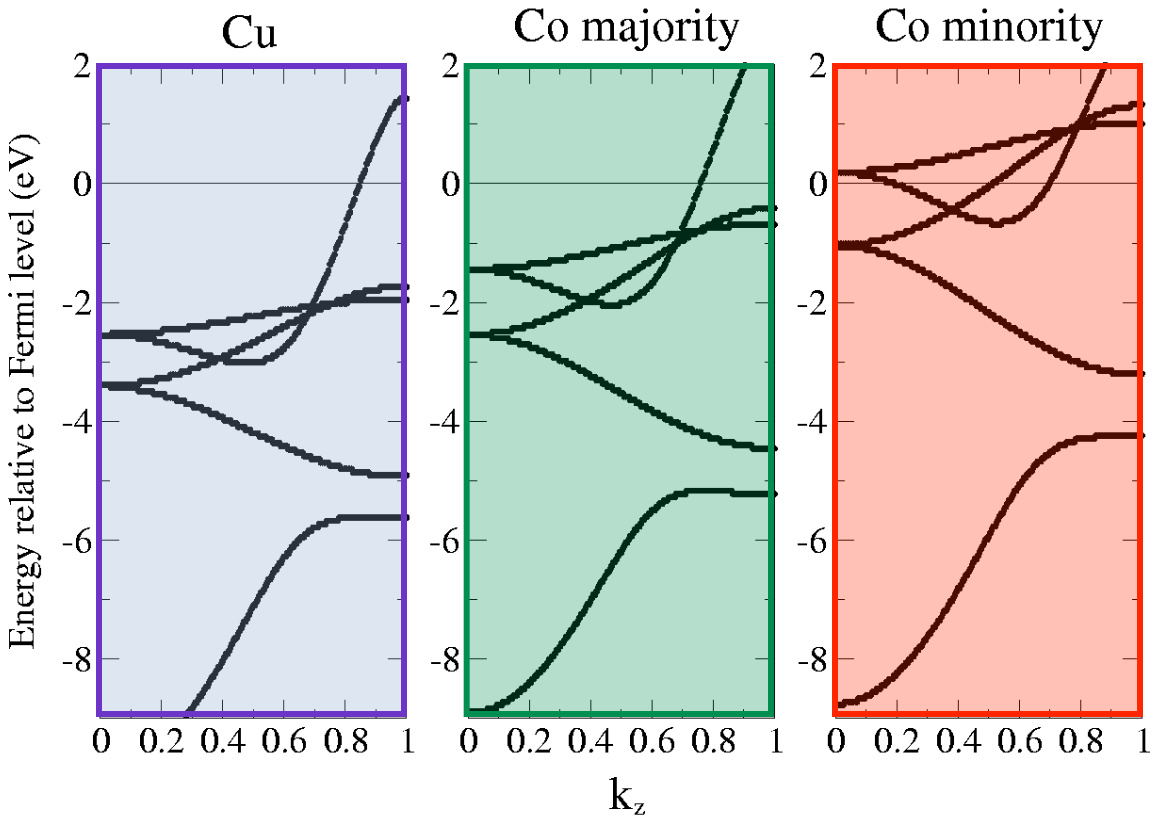

P. Lang *et al.*, Phys. Rev. B **53**, 9092 (1996)

Interlayer exchange coupling

- Consider static case without external $\boldsymbol{E}$-field
- Assume spin-dependent interface reflection

Parallel alignment:

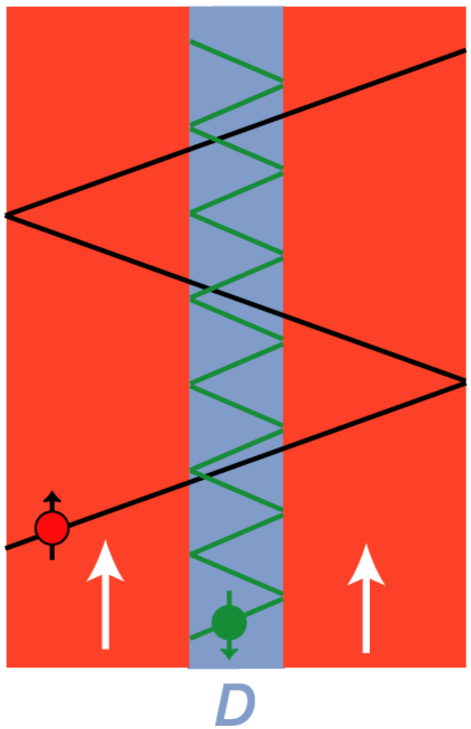

Antiparallel alignment:

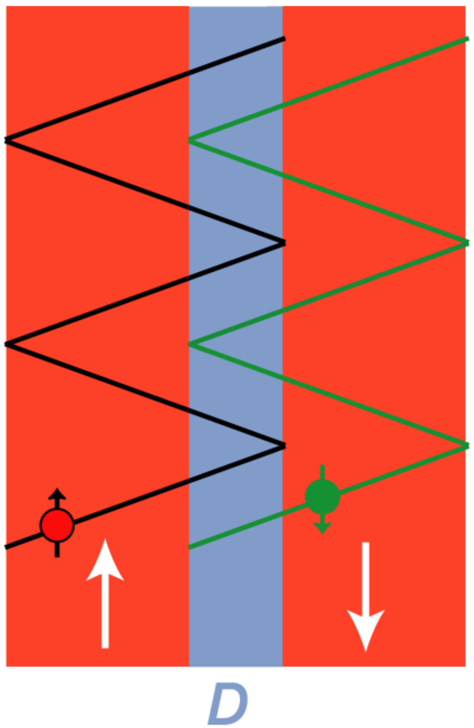

$\Rightarrow$ Formation of spin-dependent quantum well states (QWS) for parallel, but not for antiparallel alignment of the FM layers

Quantum well states

Energy of QWS related to $k_\perp$ is quantized. Energy levels shift when the spacer thickness D is varied.

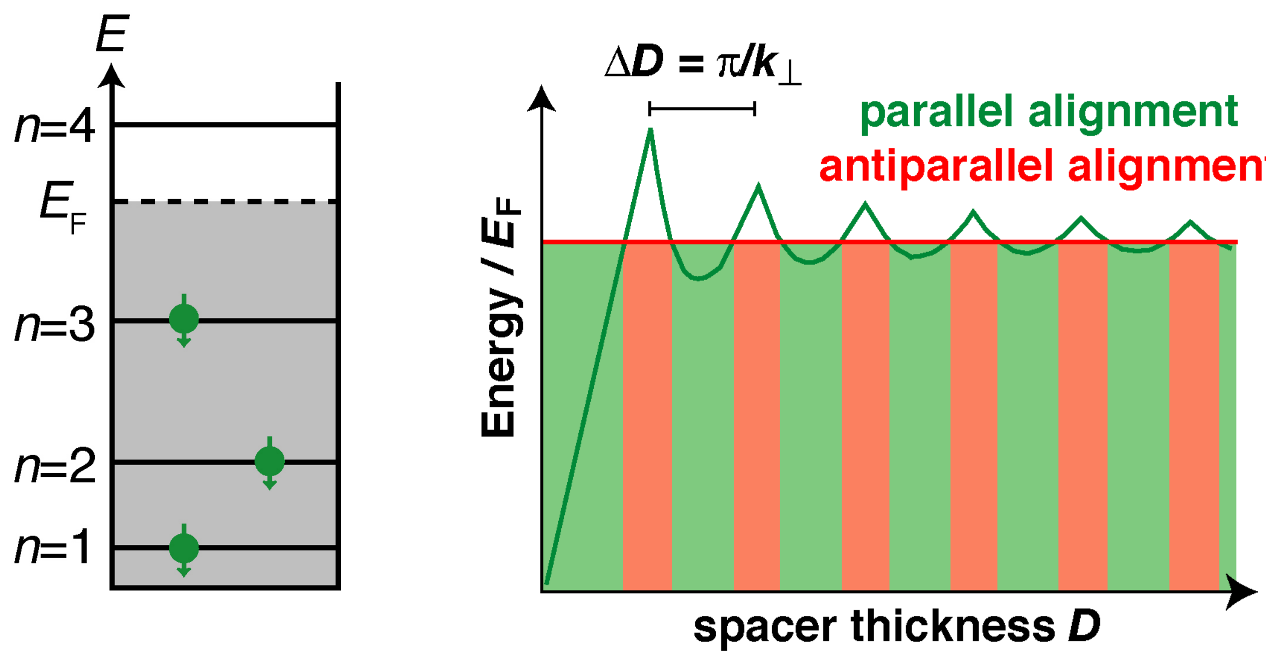

after
M. Stiles

⇒ Interlayer exchange coupling oscillates

as a function of the spacer thickness D

Example: Cu/Co(100)

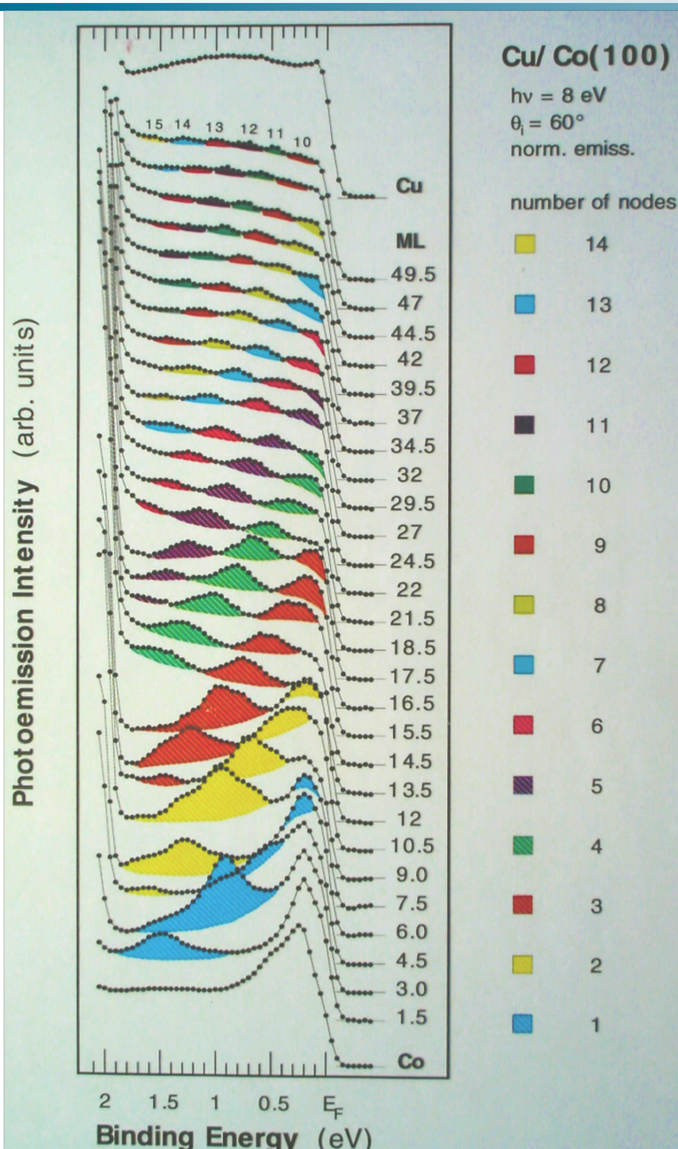

Angle-resolved photoemission:

The QWS shift up in energy with increasing D:

$$E \approx -k_{QWS}^{\;2}$$

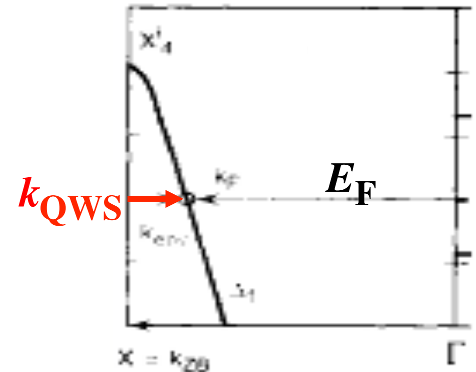

at upper band edge.

The QWS cross the E_F at regular interval of 5-6 atomic layer, exactly corresponding to the oscillation period *of J(D)*.

Spin-resolved spectra indicate that the QWS are mainly of minority (spin-down) character:

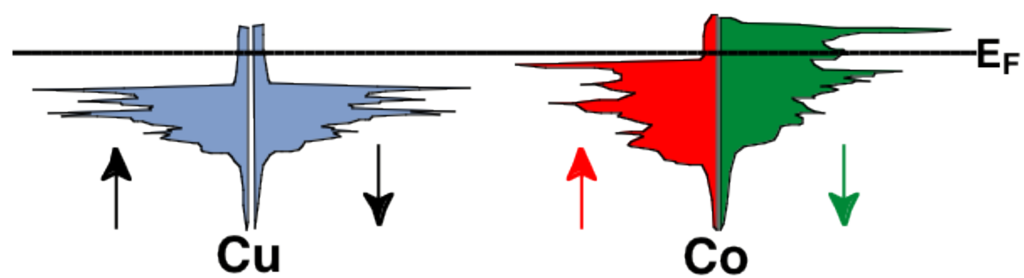

C. Carbone *et al*., Solid State Comm. **100**, 749 (1996)

Aliasing (or backfolding into the first Brillouin zone)

Typical ΔD are of the order of a few Å, *i.e.* interatomic distances

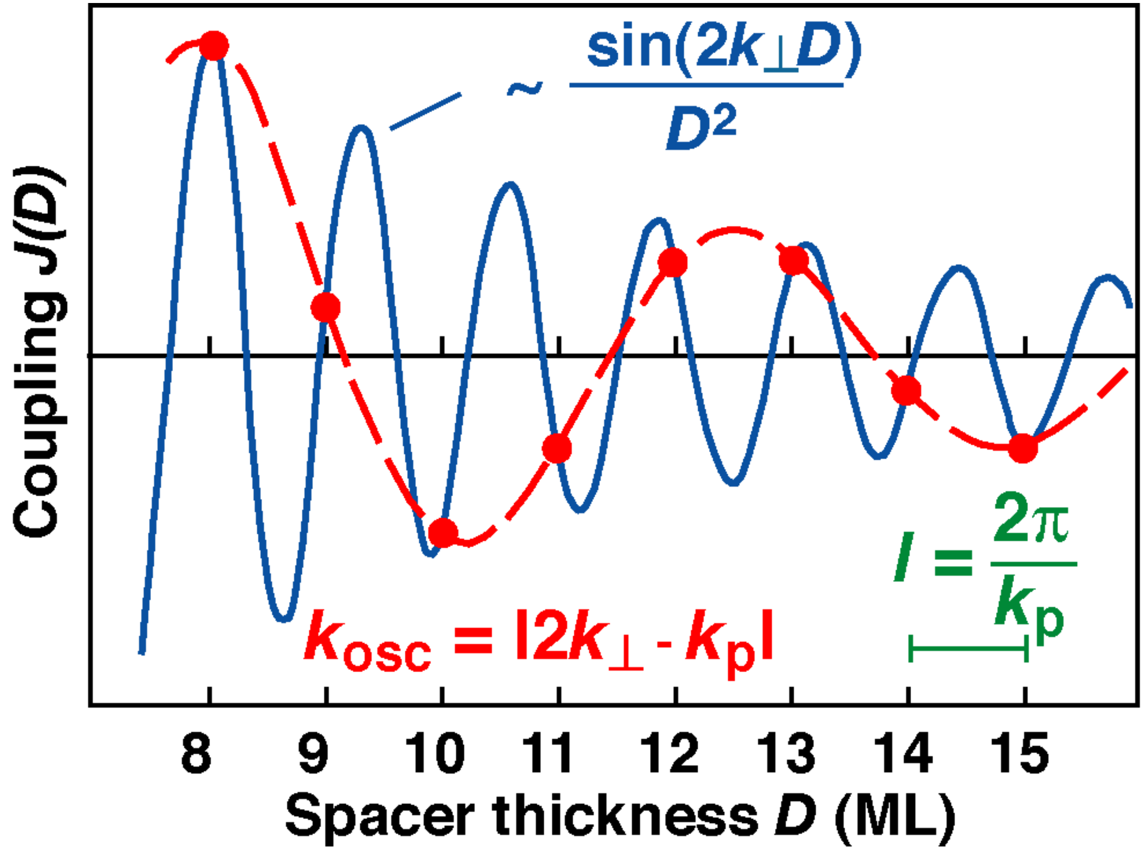

⇒ Each $k_\perp$ gives rise to an oscillation of *J(D)* with a periodicity given by

$$k_{osc} = |2k_\perp - k_p|$$

R. Coehoorn, Phys. Rev. B **44**, 9331 (1991)

Which $k_\perp$ are important?

$J(D)$ is dominated by $k_\perp$ with the highest density of states at E_F.

$\Rightarrow$ Consider $k_\perp$ at stationary point

$$k_{osc} = |2k_\perp - k_p|$$

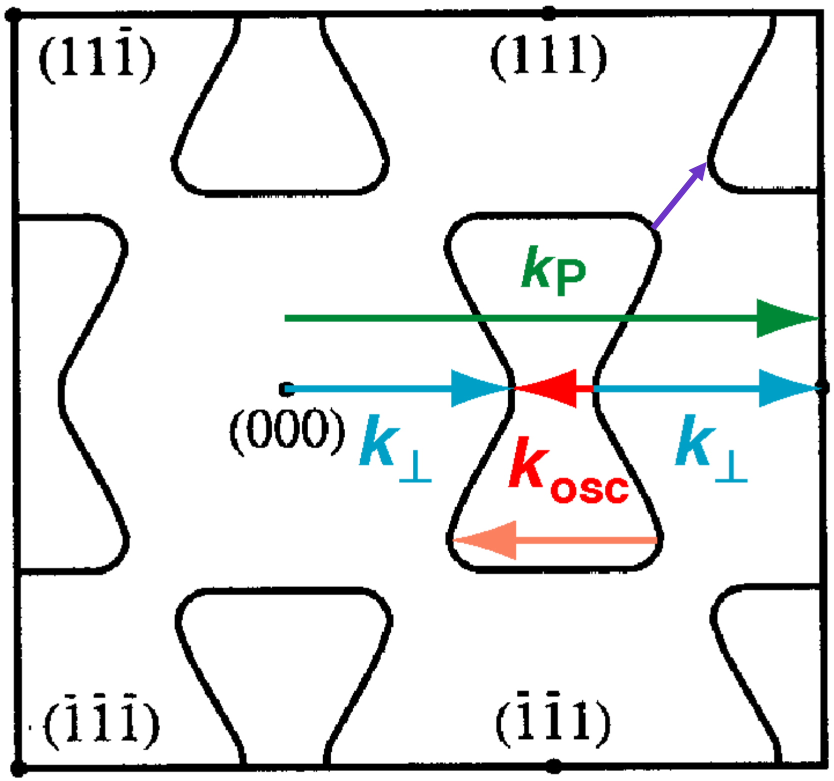

fcc(001) Fermi surface of a noble metal, *e.g.* Au(001)

Several stationary points may exist

$\Rightarrow$ $J(D)$ is a superposition of oscillations *e.g.* 2.5 and 8 ML for Au(001)

Real Fermi surfaces are non-spherical

$\Rightarrow$ Oscillations depend on growth direction

P. Bruno *et al*., Phys. Rev. Lett. **67**, 1602(1991)

Example Fe / Au / Fe(001)

Epitaxially grown Fe/Au/Fe(001)

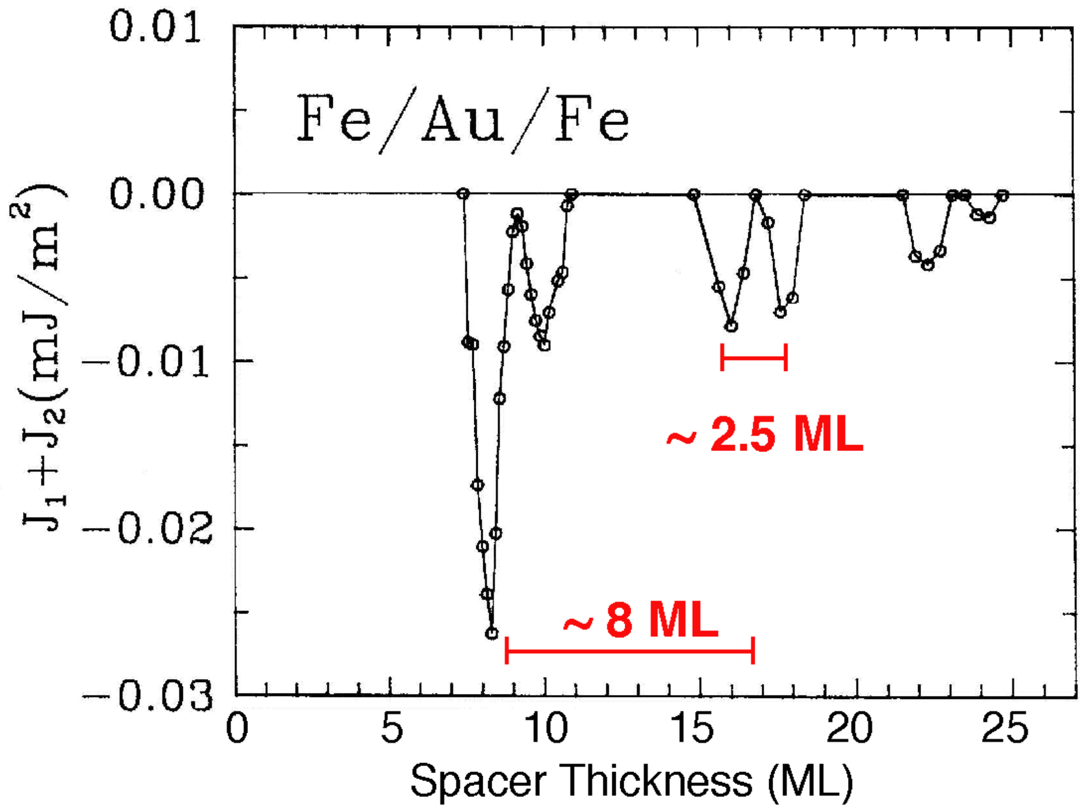

⇒ Oscillations periods are well described by the quantum interference model

A. Fuss *et al*., J. Magn. Magn. Mater. **103**, L221 (1992); P. Bruno, Phys. Rev. B **52**, 411 (1995)

Outline: Interlayer exchange coupling

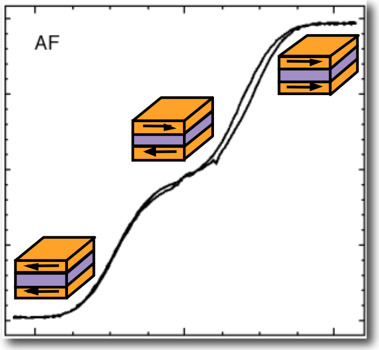

- Phenomenology of interlayer coupling
- Measurement by MOKE
- Physical picture for oscillatory bilinear coupling
- **Biquadratic coupling**
- Example: Morphology and "Fermiology"
- Applications
- Conclusions

Biquadratic or 90°-coupling

Biquadratic coupling is less well understood than bilinear coupling.

Intrinsic higher-order contributions are expected to be small.

Most models relate biquadratic coupling to extrinsic effects like:

- Interface roughness:
  - Fluctuation mechanism
  - Magnetic dipole mechanism
- Pinholes in the spacer
- Chemical intermixing
  - "Loose-spin" mechanism

Fluctuation mechanism

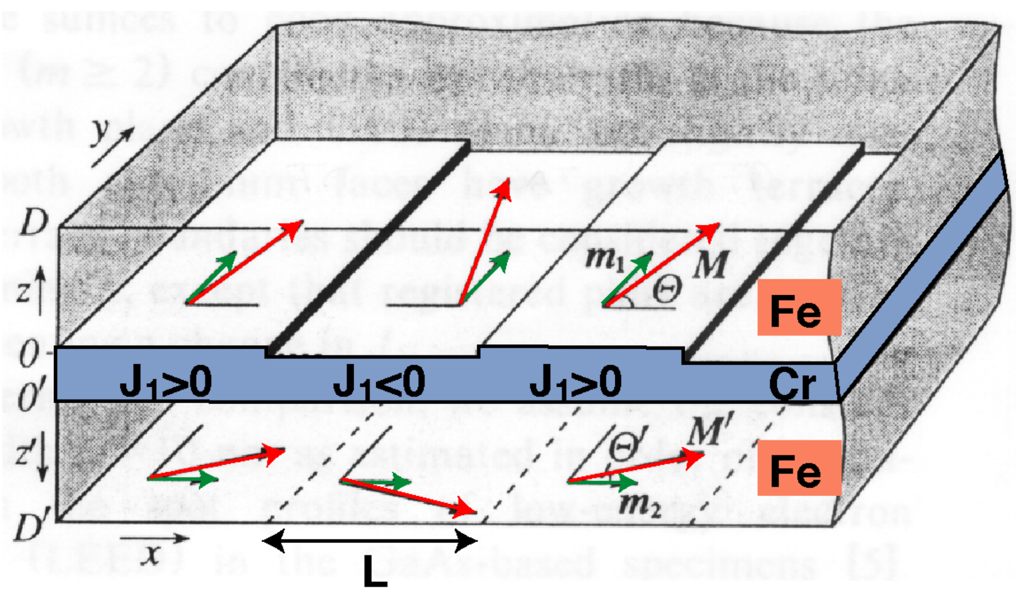

For a oscillation period of 2 ML J_1 locally changes sign at each step edge!

Examples for short oscillations:

- 2.5 ML for Au(100)
- 2.6 ML for Cu(100)
- 2 ML for Cr(100)
- 2 ML for Mn(100)

Competition between local fluctuations of the bilinear coupling due to spacer thickness fluctuations

and

direct exchange within the FM layers

on a lateral length scale shorter than the FM domain wall width.

Interface roughness can give rise to interlayer coupling of different types depending on the vertical correlation of the roughness

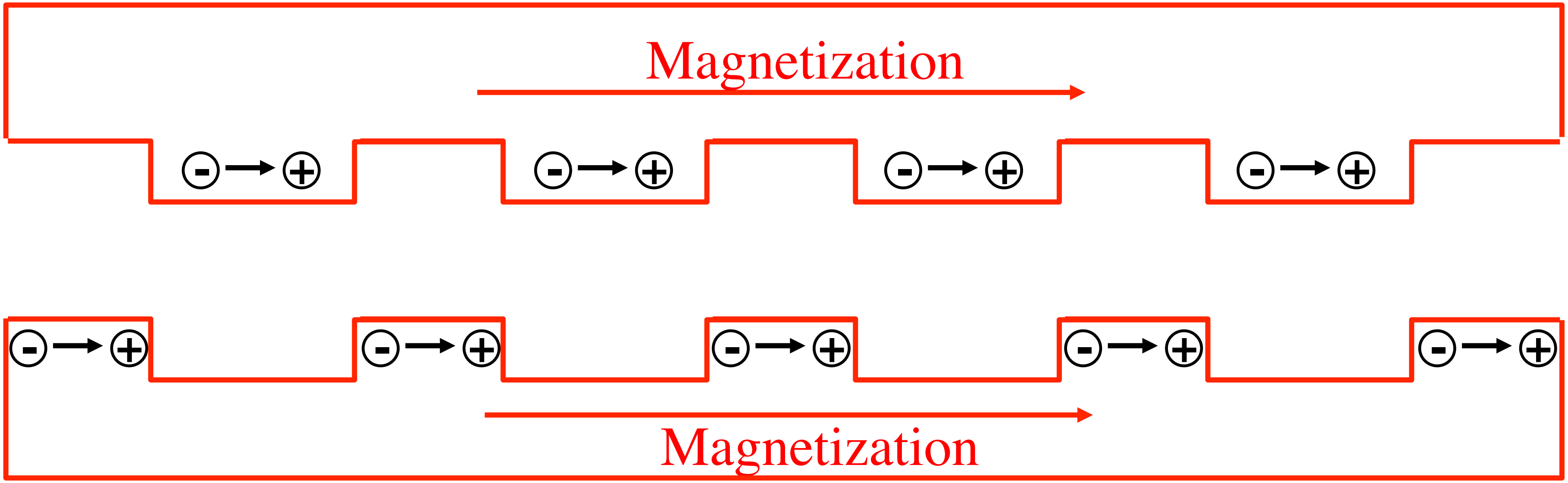

⇒ Ferromagnetic "orange-peel" coupling for correlated roughness

Magnetic dipole mechanism

Interface roughness can give rise to interlayer coupling of different types depending on the vertical correlation of the roughness

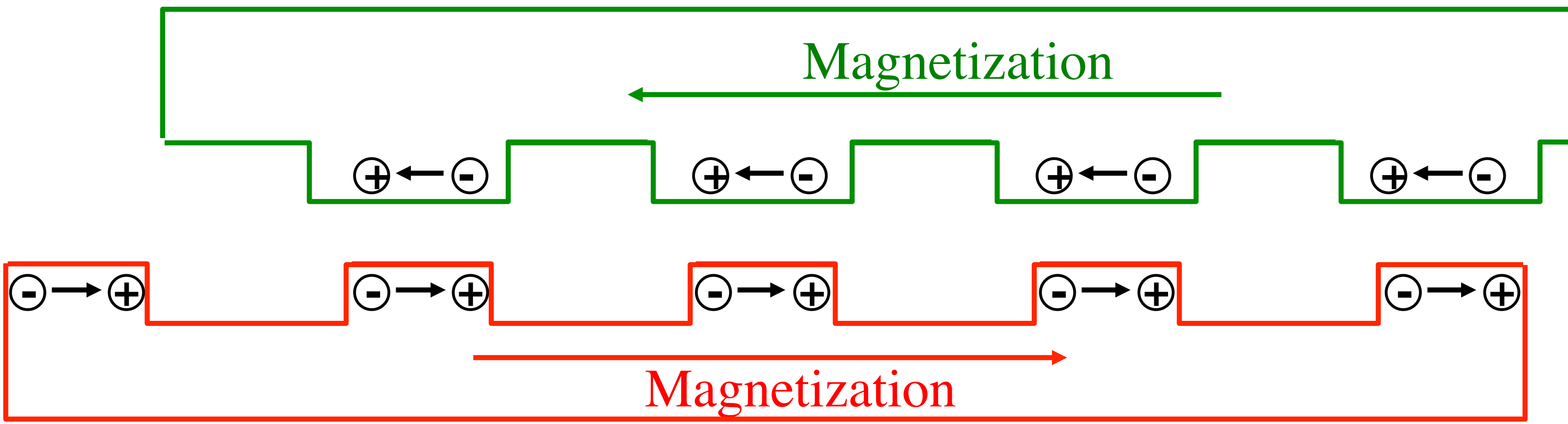

⇒ Antiferromagnetic “Néel” coupling for anti-correlated roughness

Magnetic dipole mechanism

Interface roughness can give rise to interlayer coupling of different types depending on the vertical correlation of the roughness

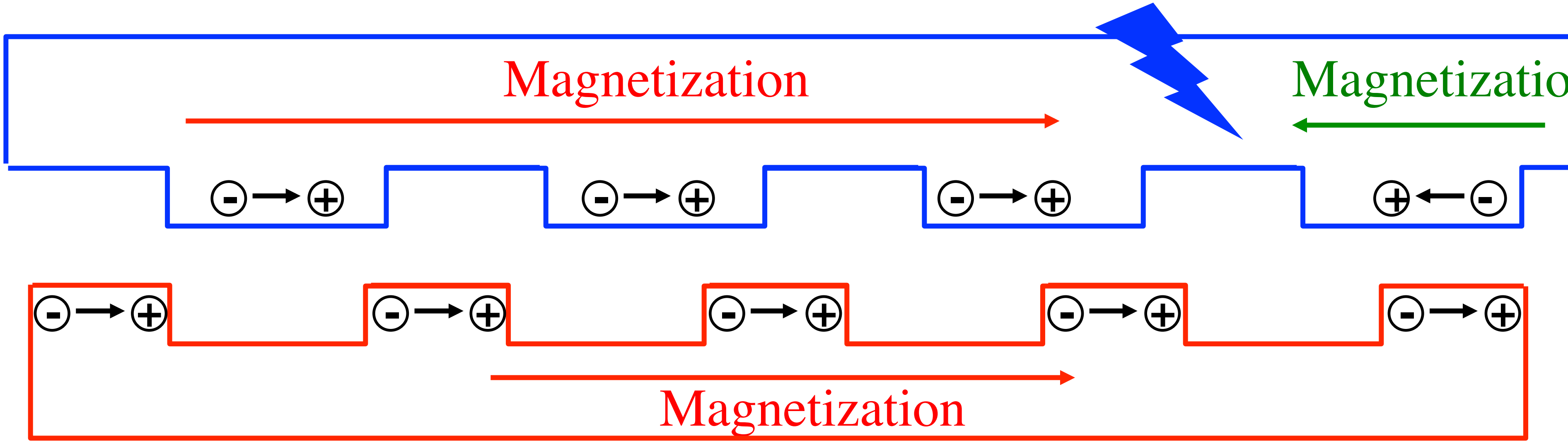

⇒ 90°-coupling for uncorrelated (random) roughness

Outline: Interlayer exchange coupling

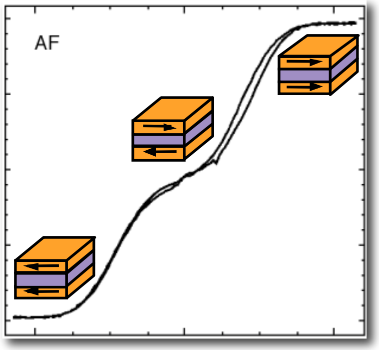

- Phenomenology of interlayer coupling
- Measurement by MOKE
- Physical picture for oscillatory bilinear coupling
- Biquadratic coupling
- Example: Morphology and "Fermiology"
- Applications
- Conclusions

Influence of interface roughness

Epitaxial Fe/Cr-wedge/Fe(001) grown at different substrate temperatures

STM images:

400 nm x 400nm

100 nm x 40 nm

Coupling *versus* spacer thickness (MOKE)

C.M. Schmidt, D.E. Bürgler *et al.*, Phys Rev. B **60**, 4158 (1999)

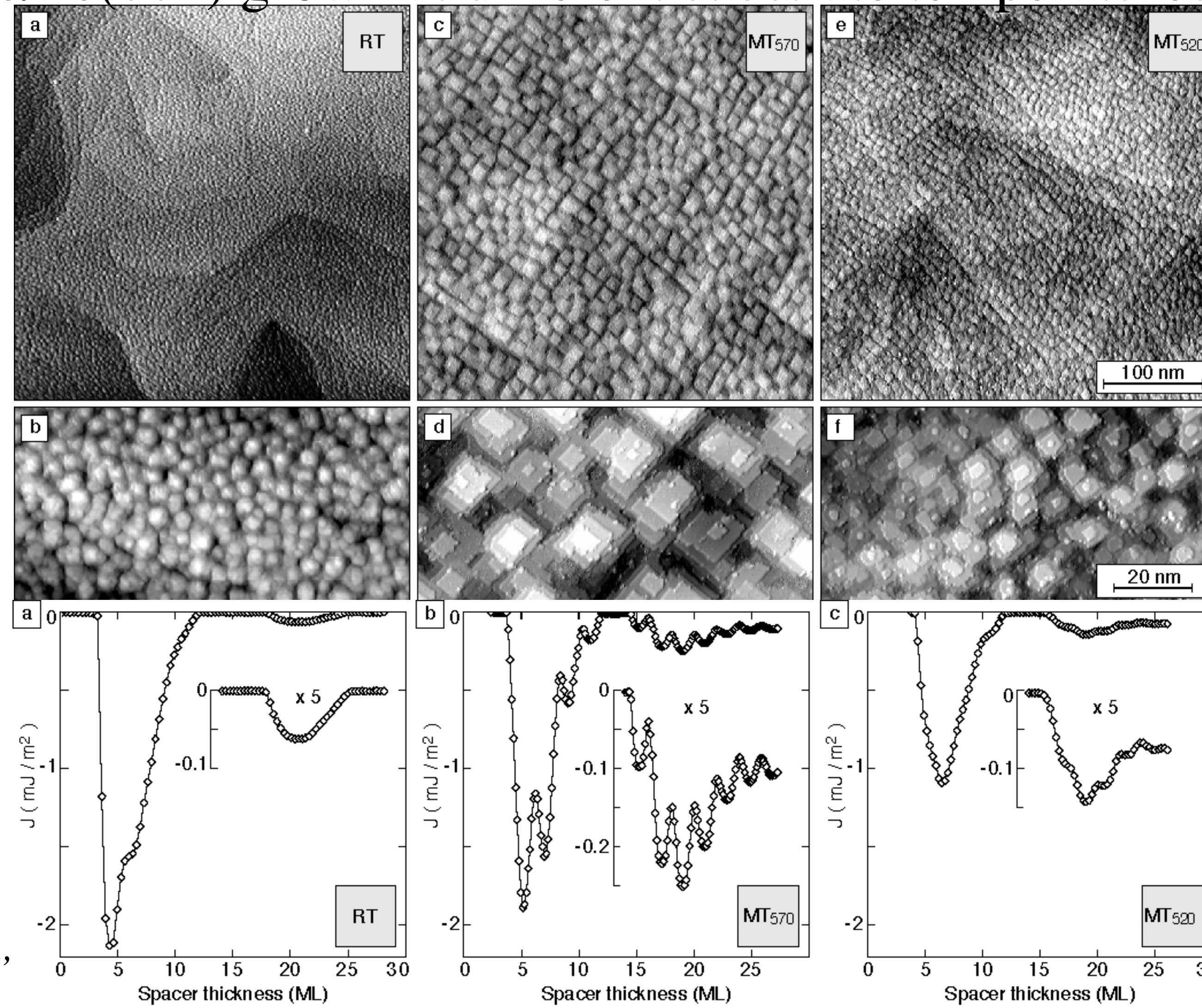

Influence of Fermi surface

Fe / Cr / Fe

compared with

Fe / Cr / Au / Fe(001)

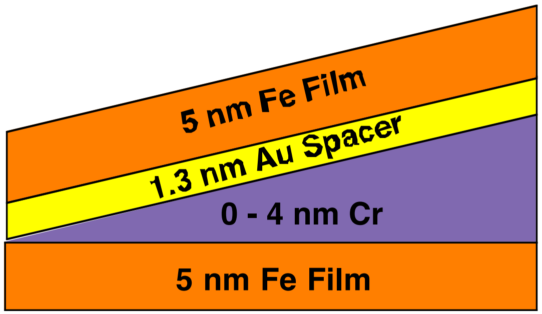

With additional Au layer:

- coupling strength decreases
- short-period oscillations still visible
- long-period oscillation disappeared

D.E. Bürgler *et al*., Phys. Rev. B **60**, R3732 (1999)

without Au

with Au

with Au

(thickness correction)

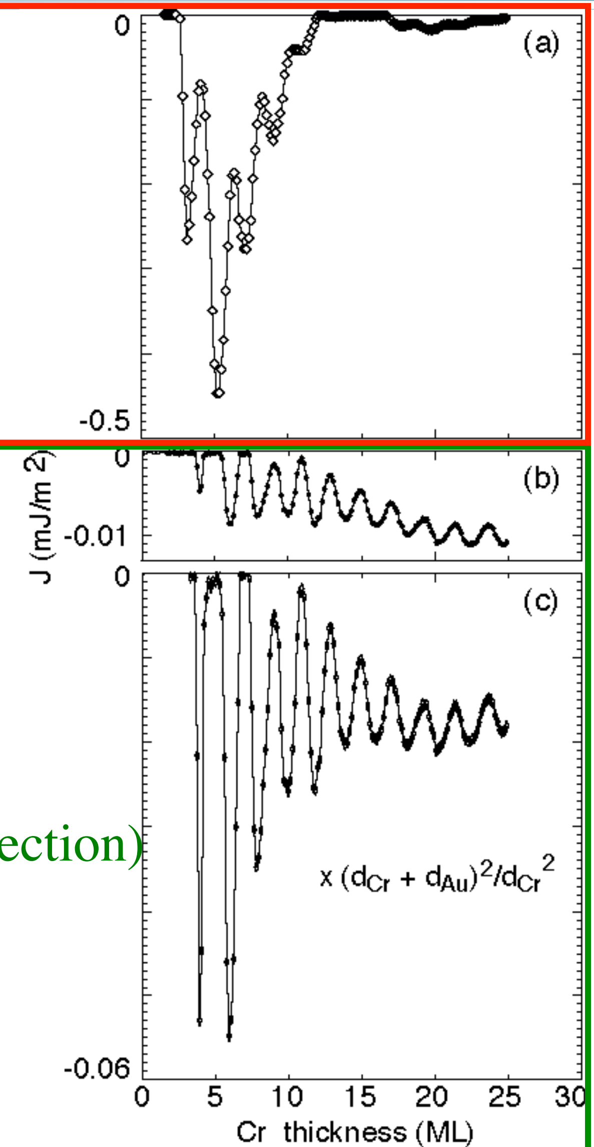

In-plane momentum conservation

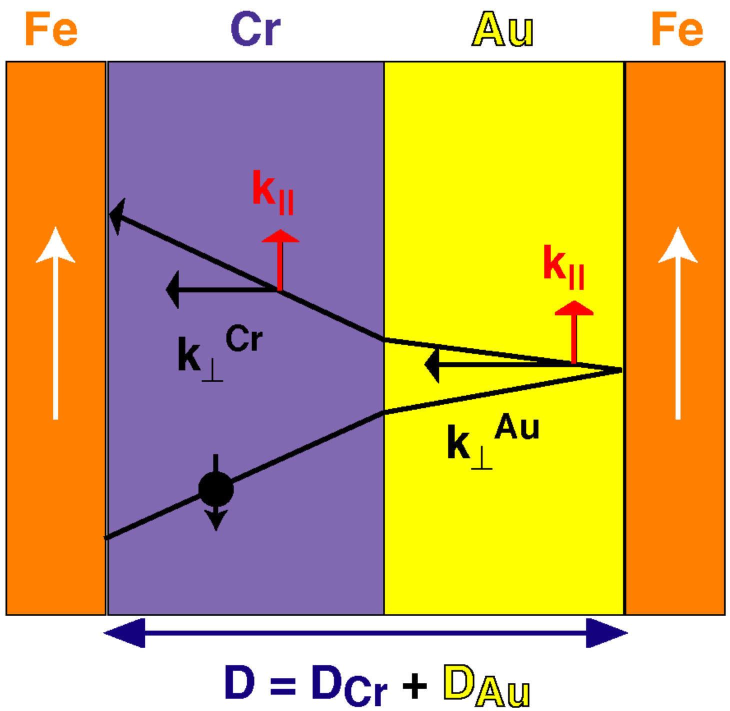

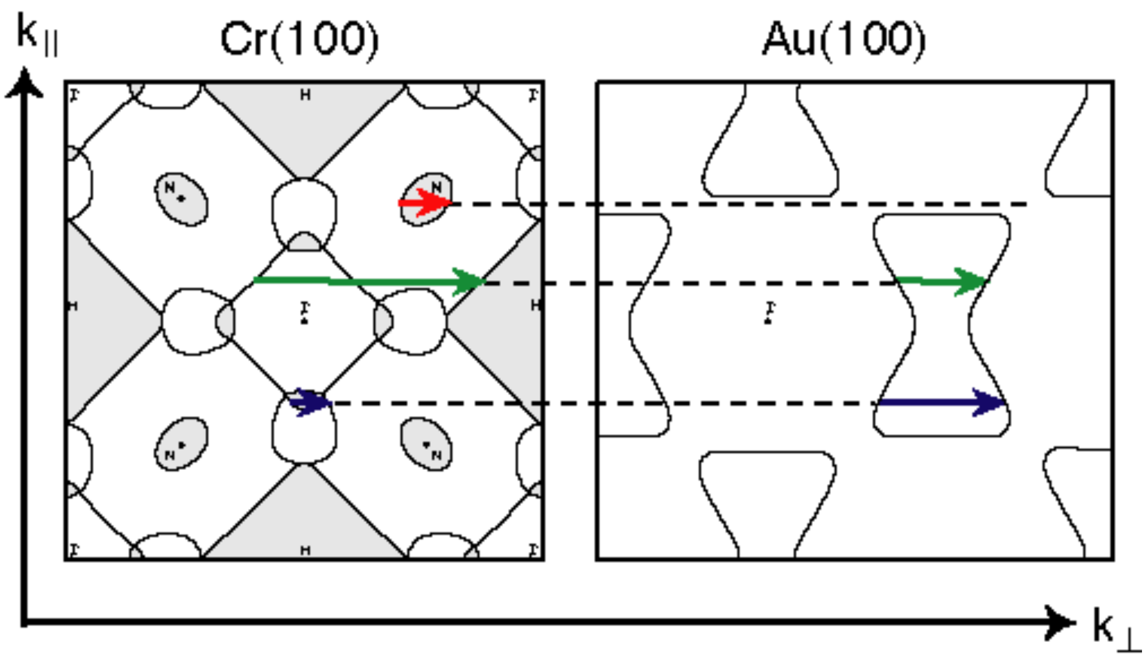

⇒ States giving rise to short-period oscillation can propagate in Au

⇒ States giving rise to long-period oscillation cannot propagate in Au

⇒ States near the X point do not mediate the long-period oscillation

D.E. Bürgler *et al.*, Phys. Rev. B **60**, R3732 (1999)

Outline: Interlayer exchange coupling

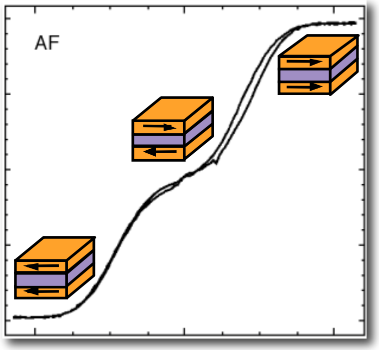

- Phenomenology of interlayer coupling
- Measurement by MOKE
- Physical picture for oscillatory bilinear coupling
- Biquadratic coupling
- Example: Morphology and "Fermiology"
- Applications
- Conclusions

Example: GMR-based angle sensor:

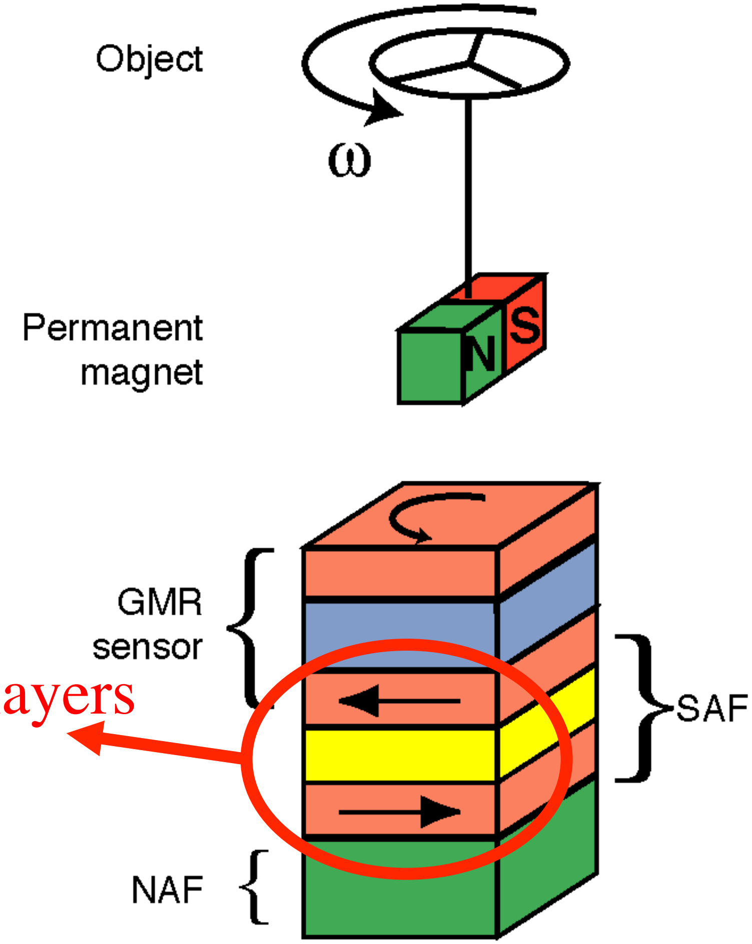

AF-coupled FM layers form a synthetic antiferromagnet

Example of a real layer structure:

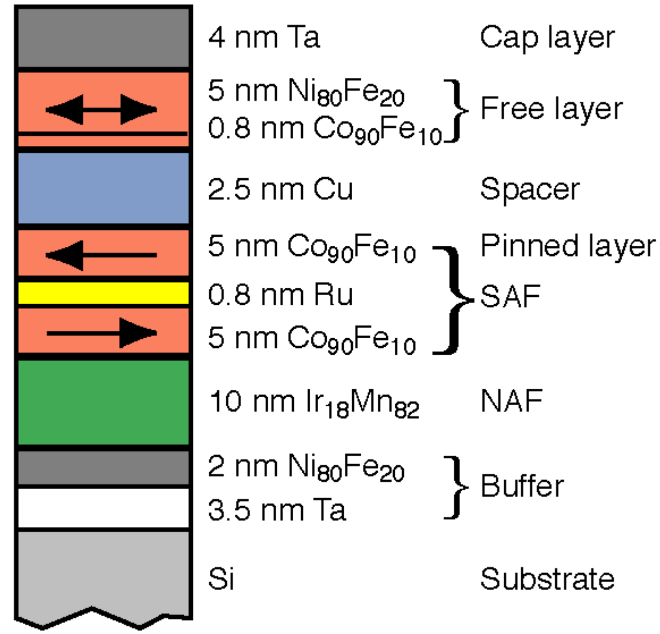

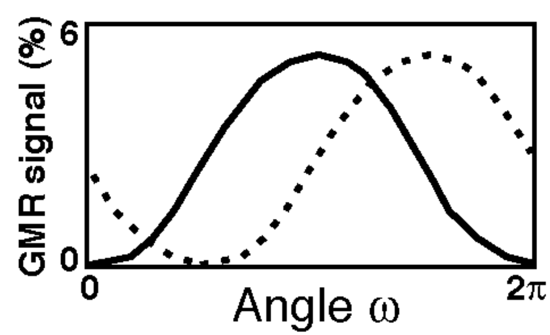

K.M.H. Lenssen *et al.*,
J. Appl. Phys. **85**, 5531 (1999)

NAF = natural antiferromagnet, SAF = synthetic antiferromagnet

Application: AFC media for harddisk drives (I)

Application of AF coupling in the disk media in order to push the superparamagnetic limit:

- Condition to increase storage density:

  Reduce magnetization density $M\,t$

- Condition to for long-time stability (10 years), *i.e.* to withstand superparamagnetism:

  Keep anisotropy energy large enough: $K_U V > 40\ k_B T$

- Condition given by max. field of write-heads:

  Keep writing field low enough: $H_{write} \approx K_U/M$

- Condition for sufficient signal-to-noise ratio:

  Reduce V in order to keep number of grains per bit constant.

E.E. Fullerton *et al*., Appl. Phys. Lett. **77**, 3806 (2000)

Application: AFC media for harddisk drives (II)

Idea: Use antiferromagnetically coupled trilayer with different FM layer thicknesses $t_1 < t_2$:

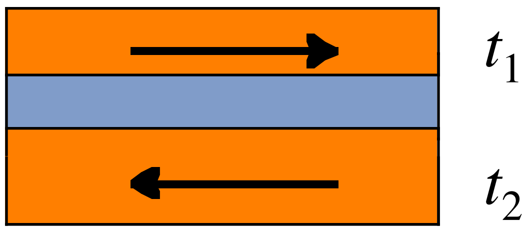

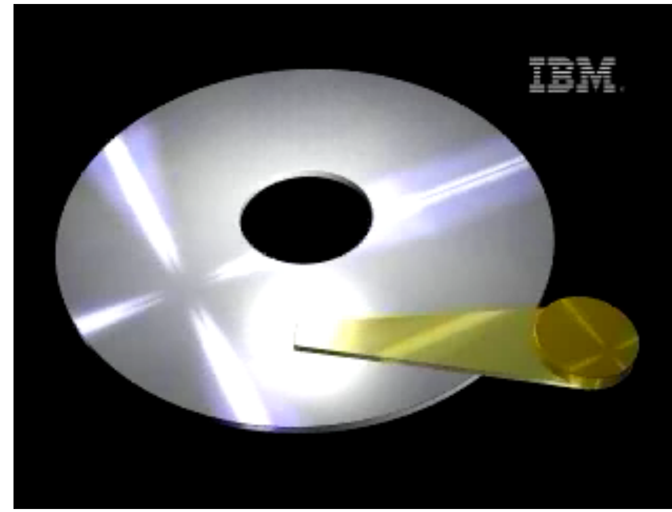

⇒ Reduced effective magnetization density: $M\,t = M\,(t_2 - t_1)$

⇒ Anisotropy energy not reduced: $K_U V = K_U(V_1 + V_2) \propto t_1 + t_2$

⇒ Slightly increased writing field: $H_{write} \approx H_c^{(1)} + H_{ex}$

⇒ Grain volume V can be decreased

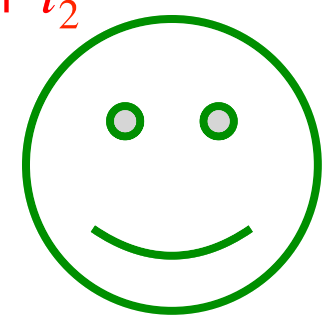

E.E. Fullerton *et al*., Appl. Phys. Lett. **77**, 3806 (2000)

Conclusions on IEC

- Bilinear magnetic interlayer exchange coupling across metallic spacer layers is well understood
- The quantum interference model predicts the oscillation periods with high precision
- Biquadratic coupling is due to extrinsic effects and, therefore, less well understood
- Interlayer exchange coupling has entered applications in sensors and harddisk drives
- Interlayer coupling paved the way for the discovery of the giant magnetoresistance effect (GMR)

For a review see: D.E. Bürgler *et al.*, in "Handbook of Magnetic Materials", Vol. 13, ed. by K.H.J. Buschow (Elsevier, 2001).

Overview

Introduction

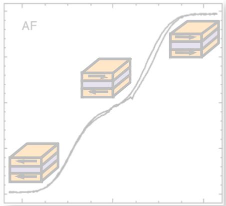

Interlayer exchange coupling

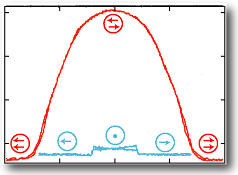

Giant and tunneling magnetoresistance

Current-induced magnetization dynamics

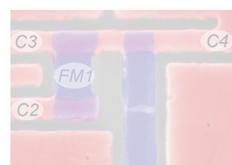

Pure spin current

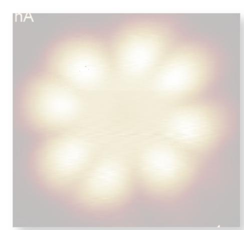

Magnetic molecules

Conclusions

Outline: Giant and tunneling magnetoresistance (GMR and TMR)

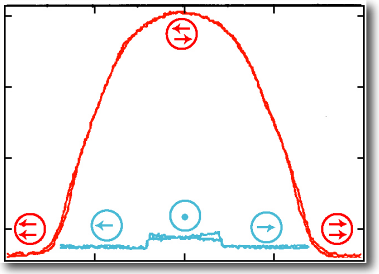

- Phenomenology of GMR
- Intermezzo: Ferromagnetic halfmetals
- Physical picture for GMR
- Applications of GMR
- Phenomenology of TMR
- Physical picture for TMR: Jullière and beyond
- Applications of TMR

Magnetic interlayer exchange coupling (IEC)

Consider two ferromagnetic layers separated by a thin spacer layer:
Ferromagnet / Non-Ferromagnet / Ferromagnet
The ferromagnetic layers interact across the spacer and align …

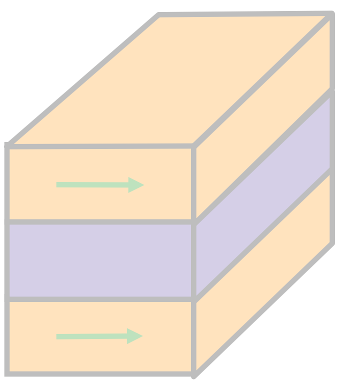

… parallel …
"ferromagnetic coupling"

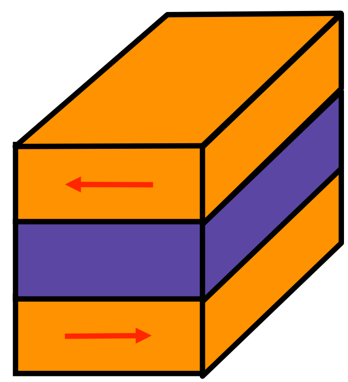

… antiparallel …
"antiferromagnetic coupling"

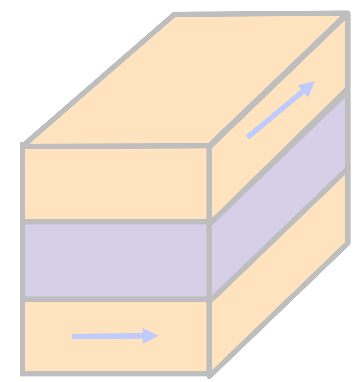

… at 90°…
"biquadratic or 90°-coupling"

P. Grünberg *et al*., Phys. Rev. Lett. **57**, 2442 (1986); M. Rührig *et al*., phys. stat. sol. (a) **125** , 635 (1991)

Control of magnetization alignment

Antiferromagnetic IEC provides a means to reversibly switch between antiparallel and parallel alignment by applying an external magnetic field ***H***

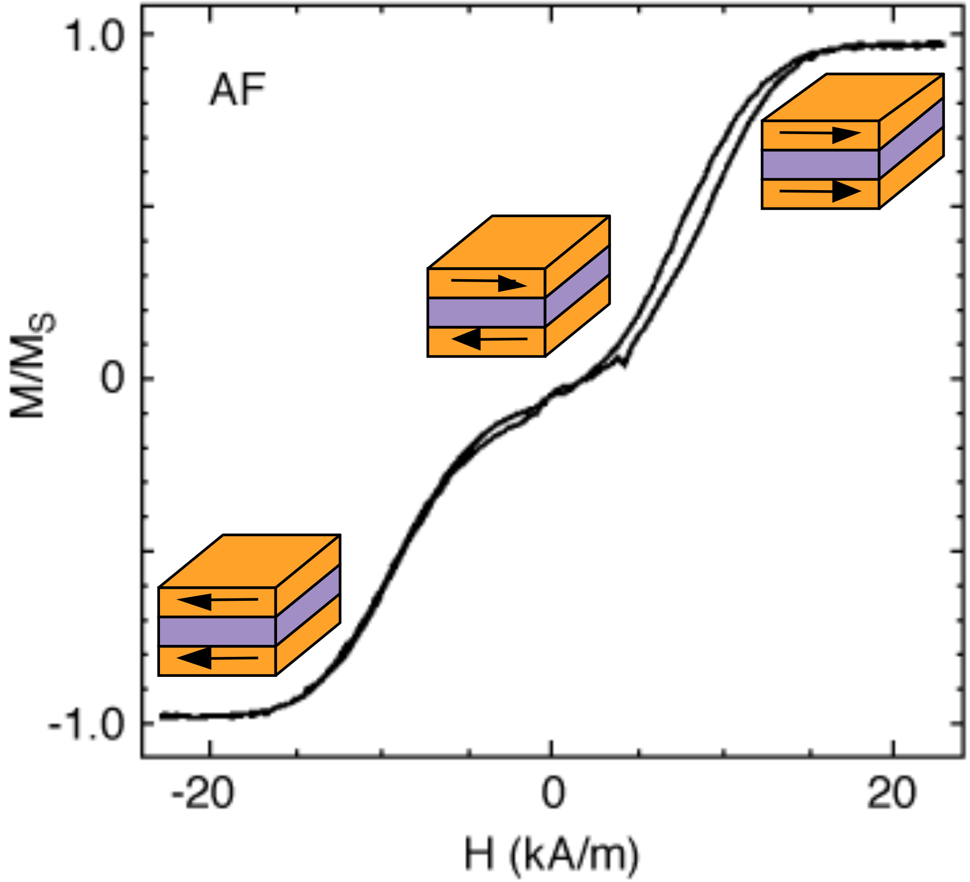

1988: … simultaneously, but independent …

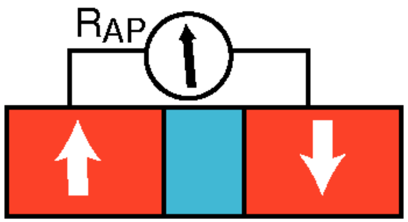

"Does the electrical resistance depend on the magnetization alignment?"

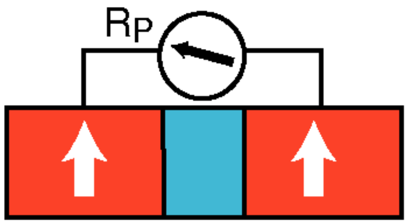

Albert Fert

Peter Grünberg

Giant magnetoresistance (GMR)

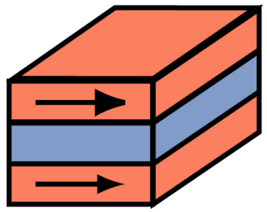

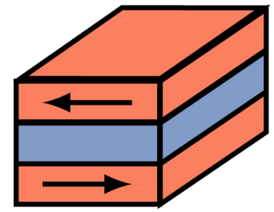

Ferromagnet
Metal
Ferromagnet

Electrical resistance: R_P <(>) R_{AP}

The electrical resistance depends on the relative magnetic alignment of the ferromagnetic layers

$$\mathrm{GMR} = \frac{R_{AP} - R_P}{R_P}$$

19% for trilayers @RT

80% for multilayers @ RT

GMR is much larger than the anisotropic magnetoresistance (AMR)

First observations of GMR

Both experiments employ antiferromagnetic interlayer coupling to achieve the antiparallel alignment

P. Grünberg, FZJ [1]

A. Fert, Paris-Sud [2]

(a) Fe/Cr/Fe trilayer: 1.5% @ 300 K

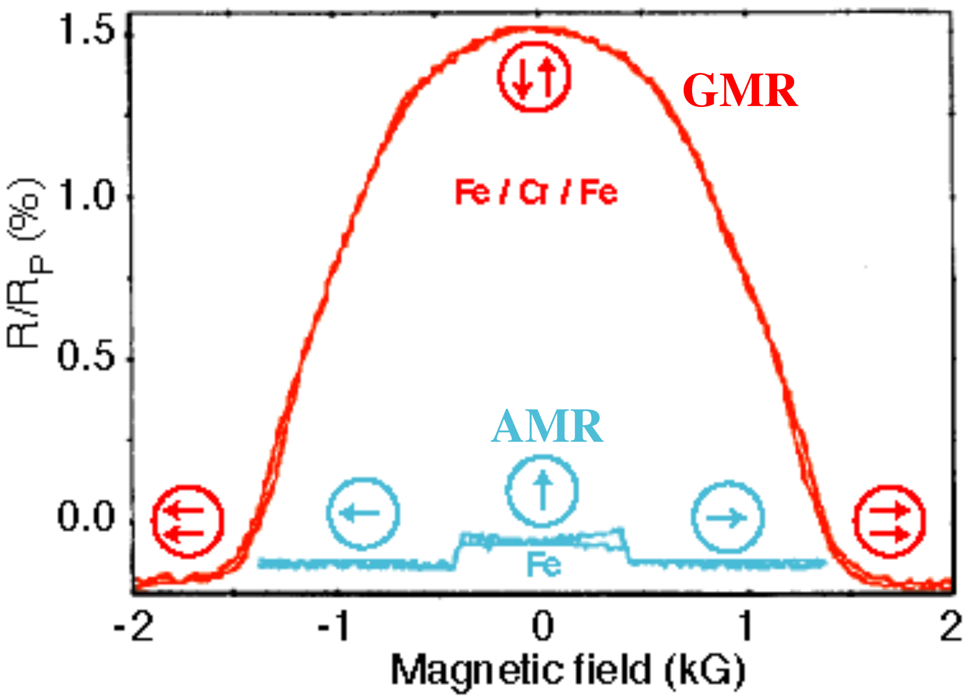

(b) Fe/Cr multilayers: 80% @ 4.2 K

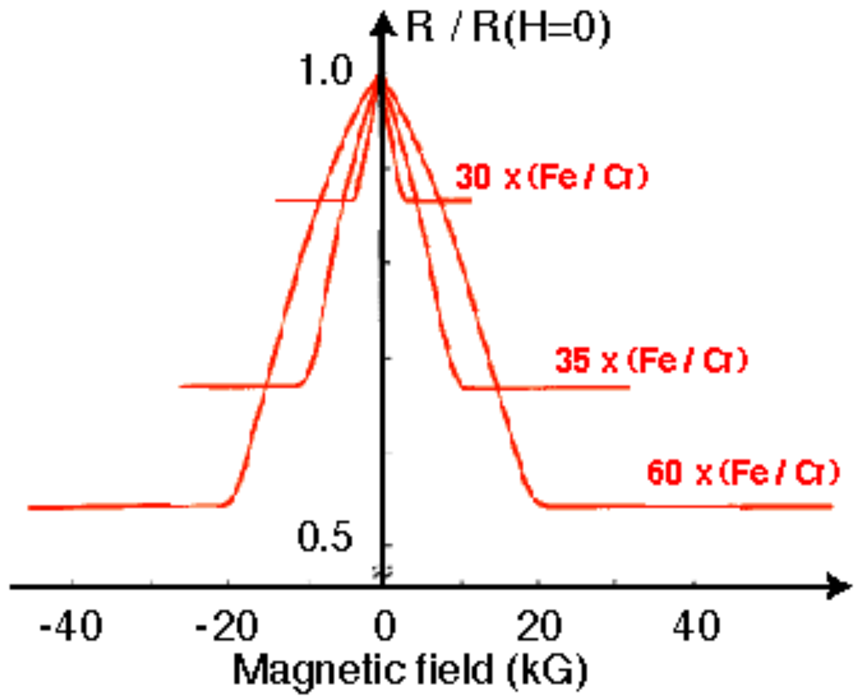

[1] G. Binasch, P. Grünberg *et al.*, Phys. Rev B **39**, 4828 (1989)
[2] M.N. Baibich, A. Fert *et al.*, Phys. Rev. Lett. **61**, 2472 (1988)

Normal magnetoresistance (MR):

In any metal the Lorentz force due to an applied field acts on the moving electrons and reduces the mean free path

$\Rightarrow$ Resistance increases with field (positive MR)

Spin disorder resistivity and negative MR:

In a ferromagnet spin disorder provides further scattering channels, *e.g.* stronger spin mixing

Especially relevant around T_c

$\Rightarrow$ Resistance decreases with field (negative MR)

Both effects are rather small and isotropic, *i.e.* they do not depend on the direction of the field with respect to the sample orientation

Retrospect: Anisotropic magnetoresistance (AMR)

Discovered 1857 by Lord Kelvin

Describes the dependence of the resistance for a current flowing parallel ($\rho_{||}$) or perpendicular ($\rho_{\perp}$) to the sample magnetization

⇒ Anisotropic with respect to the sample orientation

$$\mathrm{AMR} = \frac{\rho_{||} - \rho_{\perp}}{\rho_{||}}$$

For a thin film with in-plane magnetization
(θ angle between magnetization and current):

$$\rho(\theta) = \frac{\rho_{||} + \rho_{\perp}}{2} + (\rho_{||} - \rho_{\perp})(\cos^2\theta - \frac{1}{2})$$

⇒ π-periodic

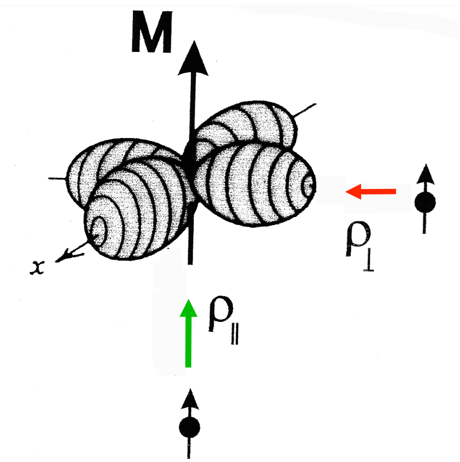

AMR originates from spin-orbit coupling and is 3% at most (Py)

Representative GMR ratios

Sample	$\Delta R{=}R_P$ (%)	Temperature (K)
$Fe(4.5)/Cr(12)_{50}$	220	1.5
	42	300
$Co(10)/Cu(10)_{100}$	80	300
Co(30)/Cu(19)/Co(25)	19	300
$Co_{90}Fe_{10}(40)/Cu(25)/Co_{90}Fe_{10}(8)\ldots$	7	300
NiFe(100)/Cu(25)/Co(22)	4.6	300
. . . CoFe/AgCu(15)/CoFe. . .	4–7	300
$Co(15)/Cu(12)_n$ CPP	170	4.2
$Co(12)/Cu(11)_{180}$ CPP	55	300

Geometry is CIP unless specially marked with CPP. Auxiliary layers which are not directly active in the GMR effect are mostly omitted. Numbers in brackets indicate the layer thicknesses in Å.

After P. Grünberg, Sensors and Actuators A **91**, 153 (2001)

Representative GMR ratios

Sample	$\Delta R/R_P$ (%)	Temperature (K)
$[Fe(4.5)/Cr(12)]_{50}$	220	1.5
	42	300
Co(10)/Cu(		00
Co(30)/Cu(1		00
$Co_{90}Fe_{10}(40$		00
NiFe(100)/C		00
…CoFe/Ag(		00
Co(15)/Cu(		.2
Co(12)/Cu(		300

Recent progress with Heusler alloys:
GMR in $Co_2MnSi/Ag/Co_2MnSi(100)$
39% GMR @ RT (67% @ 110 K)
due to high spin polarization
Fermi level

Y. Sakuraba *et al.*, Phys. Rev. B **82**, 094444 (2010)

Geometry is CIP unless specially marked with CPP. Auxiliary layers which are not directly active in the GMR effect are mostly omitted. Numbers in brackets indicate the layer thicknesses in Å.

After P. Grünberg, Sensors and Actuators A **91**, 153 (2001)

Outline: Giant and tunneling magnetoresistance (GMR and TMR)

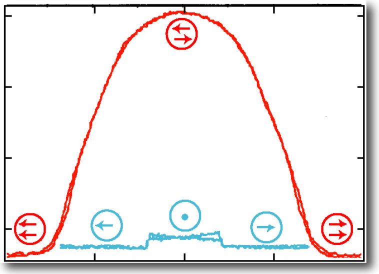

- Phenomenology of GMR
- Intermezzo: Ferromagnetic halfmetals
- Physical picture for GMR
- Applications of GMR
- Phenomenology of TMR
- Physical picture for TMR: Jullière and beyond
- Applications of TMR

Intermezzo: Ferromagnets halfmetalls

Not to be confused with:

Semimetal (e.g. Graphite): Vanishing gap, thus between metal and semiconductor

Halfmetal: Gap at the Fermi level for one spin direction, but no gap for the other spin direction

$\Rightarrow$ Requires spin splitting

$\Rightarrow$ Ferromagnetic material with $|P| = 100\%$

Materials:

Some oxides: CrO_2 with $|P| > 95\%$ form experiment at low T

Fe_3O_4 due to hopping of only one spin species

and Heusler alloys

Intermezzo: Properties of ferromagnetic halfmetals

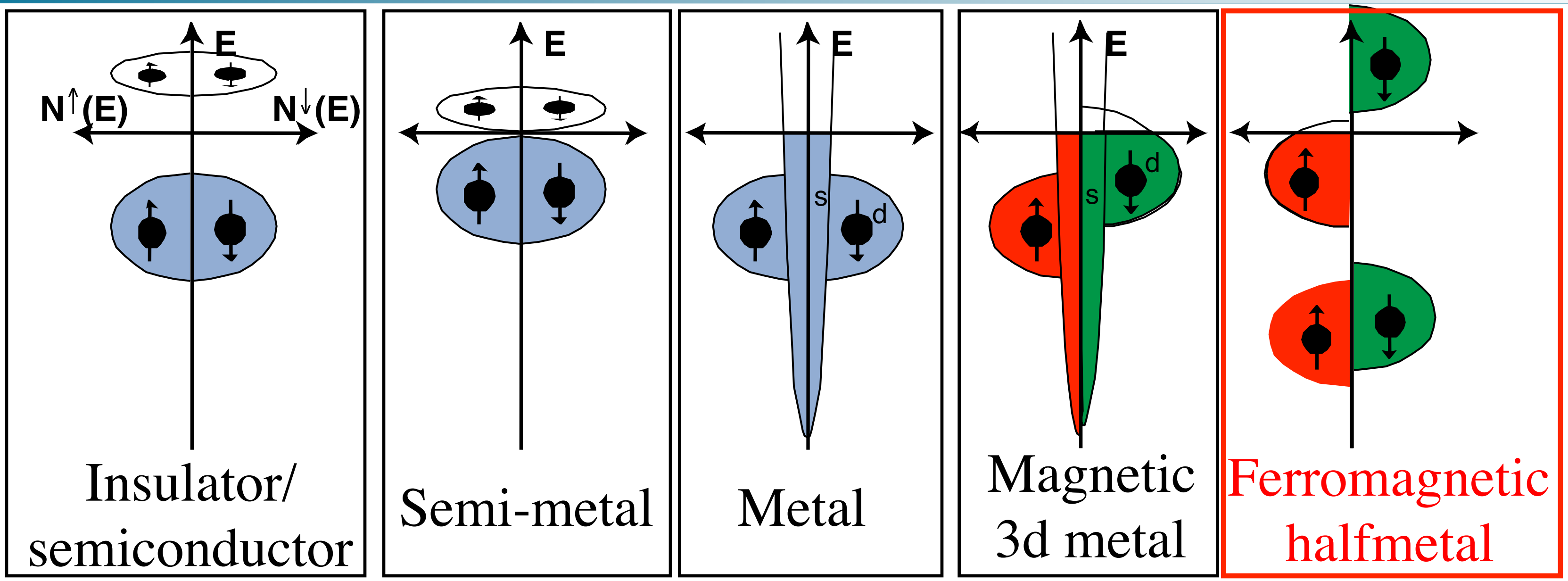

Only electrons of one spin species (spin-up) contribute to transport,
i.e. 100% spin polarization of conduction electrons

$\Rightarrow$ Infinite spin-flip length for spin-up

$\Rightarrow$ Zero spin-flip length for spin-down

$\Rightarrow$ Ideal electrodes for GMR, TMR, spin-injection, …

$\Rightarrow$ Ideal spin filter for current-induced magnetic switching

Intermezzo: Calculated spin-split DOS of NiMnSb

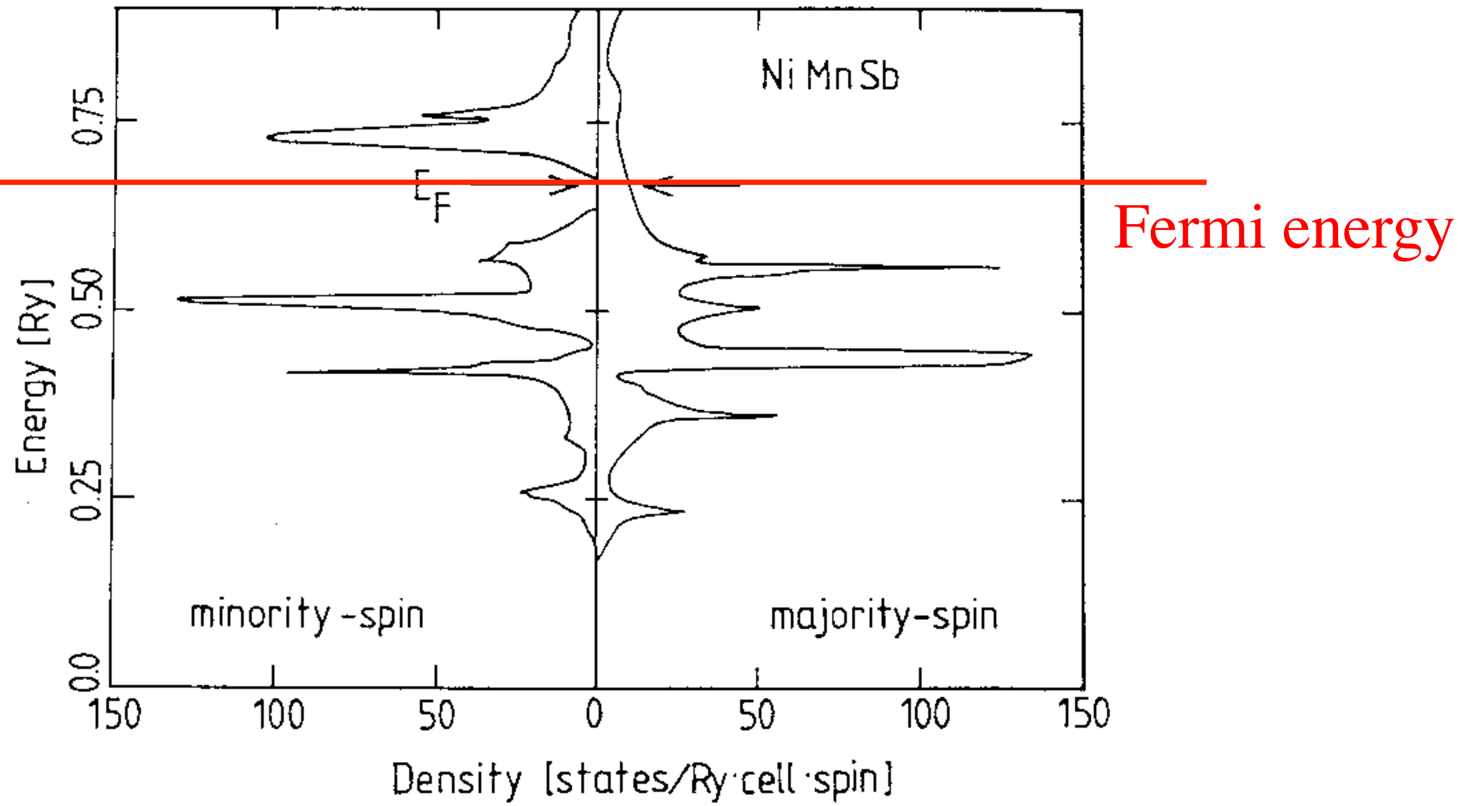

Experimental prove of half-metallicity is lacking for most predicted halfmetals. Problems: Stoichiometry

Chemical and structural disorder

Interface effects (surface states, bonding)

Back to GMR: Spin-valves

Interlayer coupling is no precondition for GMR.

The AP alignment can be achieved by other means, *e.g.* FM layers with different coercive fields $H_c^{(1)} < H_c^{(2)} \Rightarrow$ Pseudo spin-valve

Exchange bias effect acting at the interface between an antiferromagnet (AFM) and a FM layer $\Rightarrow$ Spin-valve

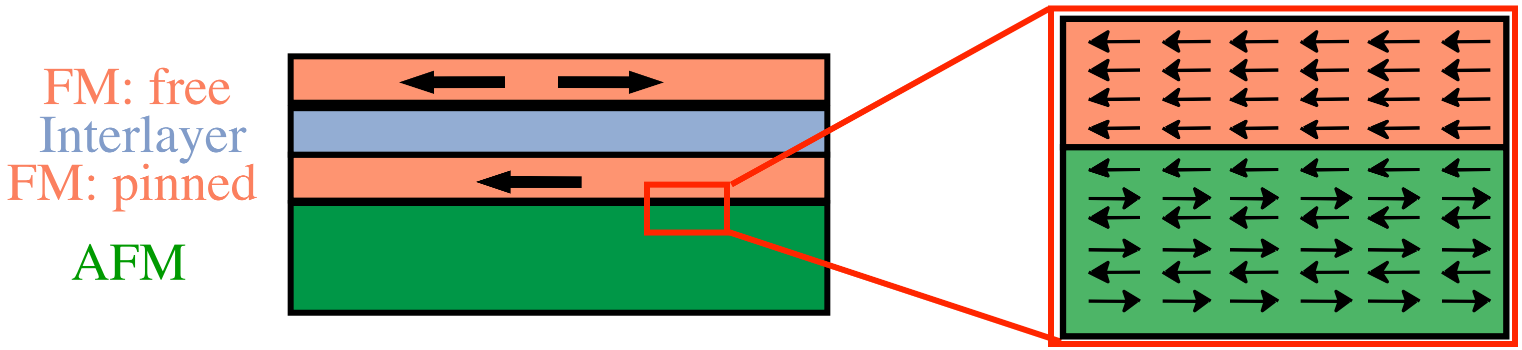

Exchange bias acts on the adjacent FM layer like an additional field H_E and shifts its magnetization loop on the field axis.

GMR of a spin-valve

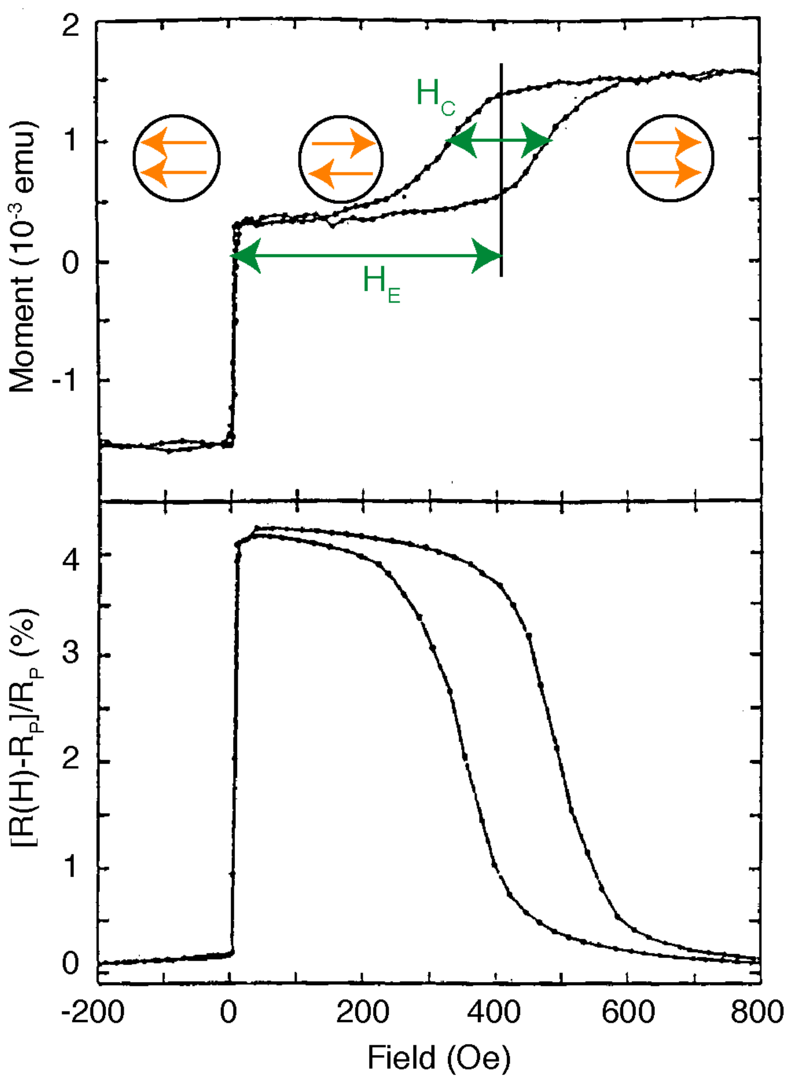

6 nm $Ni_{80}Fe_{20}$
2.2 nm Cu
4 nm $Ni_{80}Fe_{20}$
7 nm FeMn

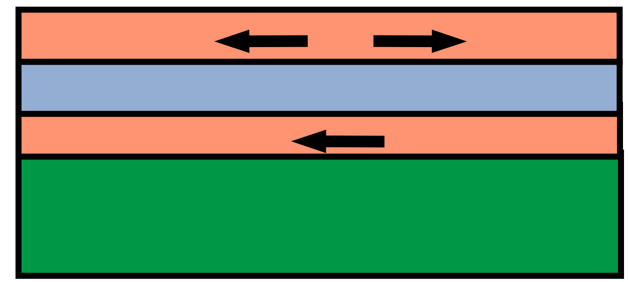

The steep slope at zero field makes spin-valves sensitive field sensors.

B. Dieny, J. Magn. Magn. Mater. **136**, 335 (1994)

Spin-valves II

1) AF-coupled system (multilayer)

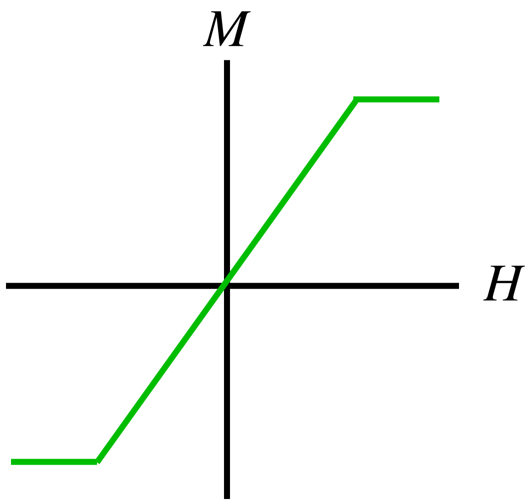

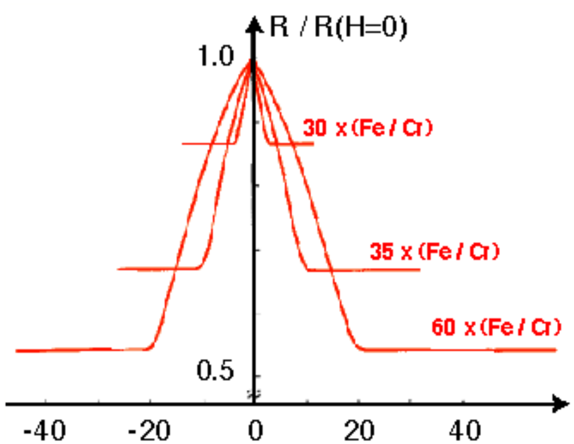

2) Pseudo spin-valve

$H_c^{(1)} < H_c^{(2)}$

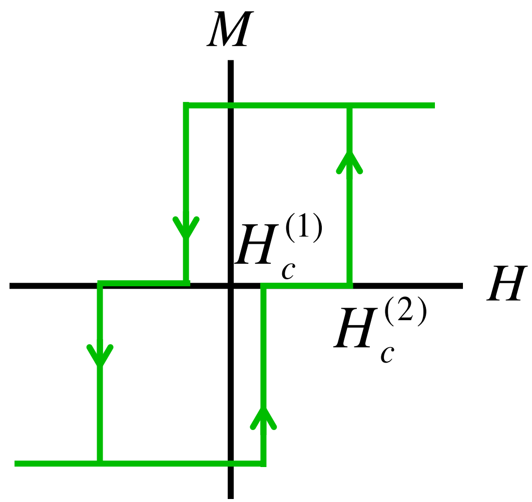

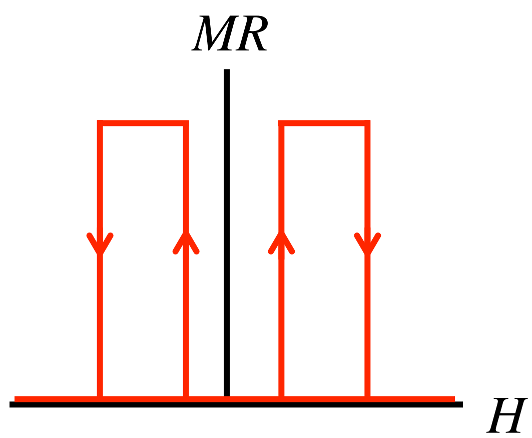

3) Spin-valve (exchange bias)

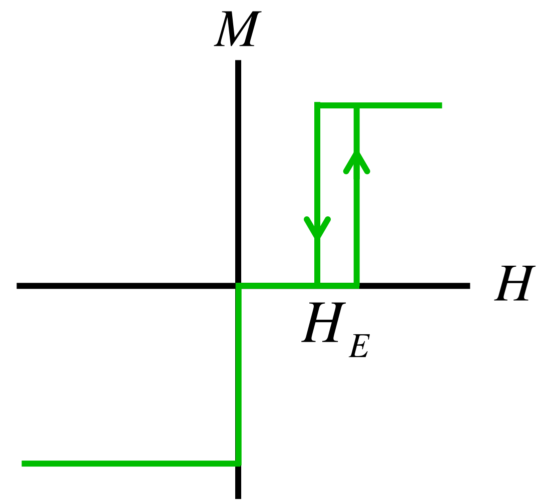

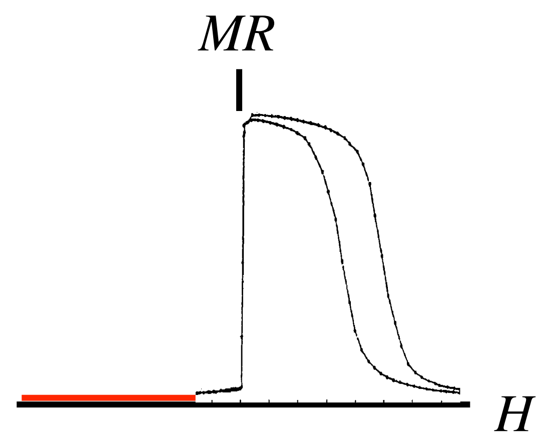

Outline: Giant and tunneling magnetoresistance (GMR and TMR)

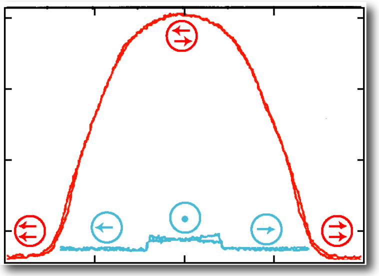

- Phenomenology of GMR
- Intermezzo: Ferromagnetic halfmetals
- Physical picture for GMR
- Applications of GMR
- Phenomenology of TMR
- Physical picture for TMR: Jullière and beyond
- Applications of TMR

Microscopic picture of GMR: Spin-dependent scattering

1) Spin-dependent scattering:
$r^{min} \neq r^{maj}$

2) Mott's two current model:
independent current channels for spin-up and spin-down (no spin-flip scattering)

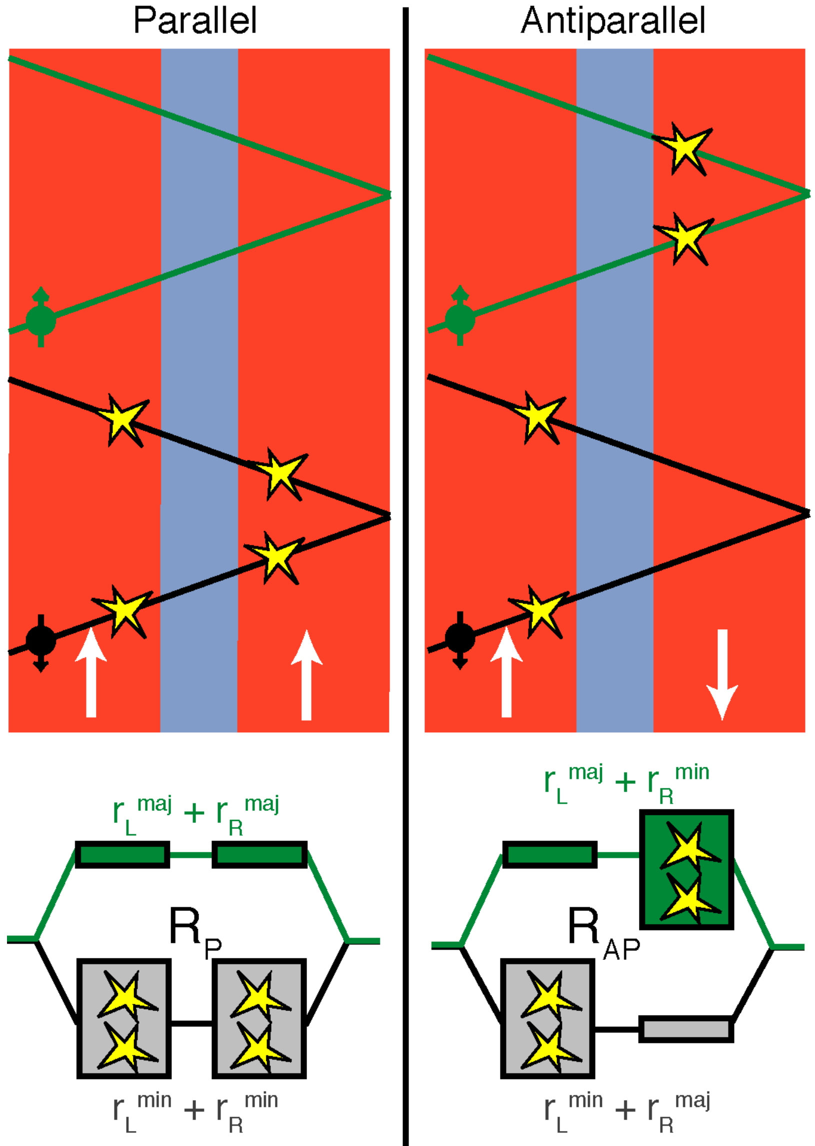

Microscopic picture of GMR: Scattering spin asymmetry

The origin of the spin-dependent scattering lies in the spin-split density of states (DOS) of 3d transition metals:

minority resistance $r^{min} \neq$ majority resistance r^{maj}

$$r^{maj,min} \propto [\mathrm{DOS}^{maj,min}(E_\mathrm{F})]^{-1}$$

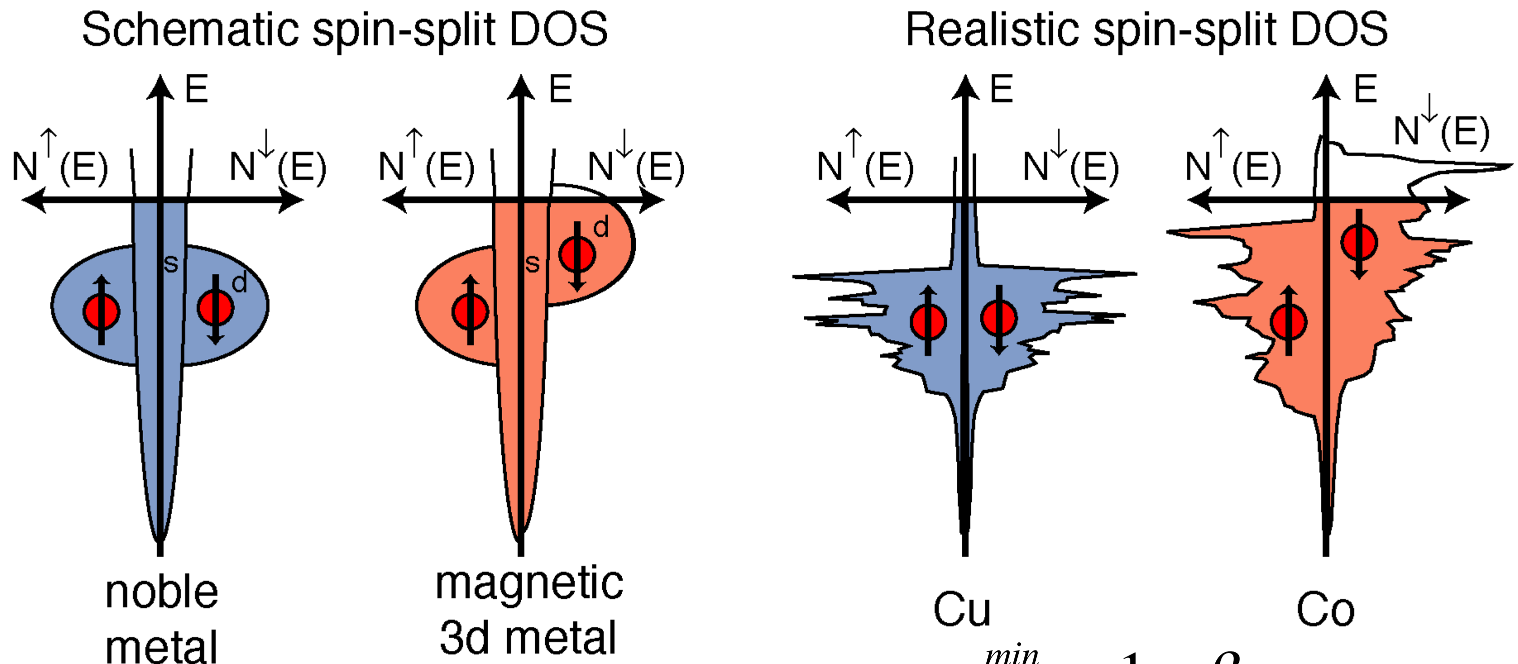

Scattering spin asymmetry parameter β: $\dfrac{r^{min}}{r^{maj}} = \dfrac{1+\beta}{1-\beta}$; $|\beta| \leq 1$

Normal and inverse GMR

Expressing the GMR ratio first by $r_{L,R}^{maj,min}$ and then $\beta_{L,R}$ one obtains:

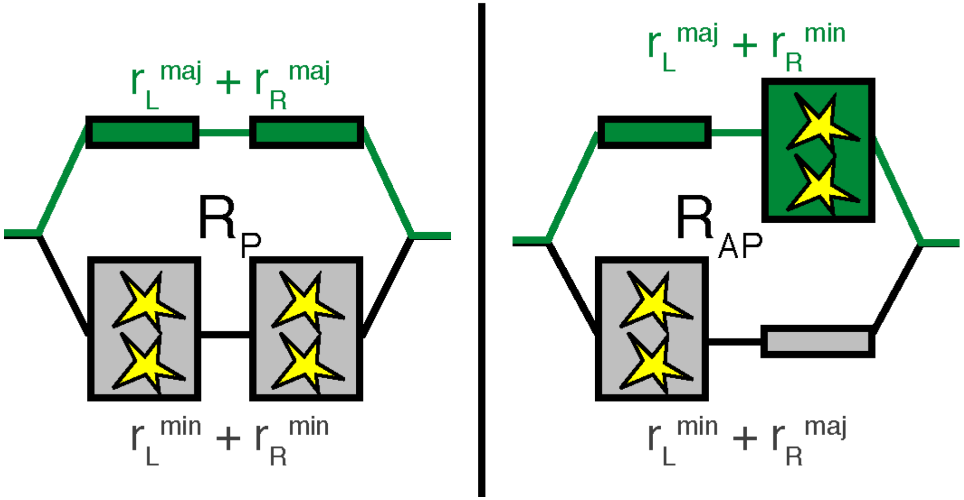

$$\frac{R_{AP} - R_P}{R_P} = C\beta_L\beta_R \quad ; \quad C > 0$$

$\Rightarrow$ Normal GMR for $\quad \beta_L\beta_R > 0$

Inverse GMR for $\quad \beta_L\beta_R < 0$

For symmetric systems $\beta_L = \beta_R$, and GMR is always normal

Normal and inverse GMR

Normal GMR:

$\beta_{L,R} > 0$ or $\beta_{L,R} < 0$

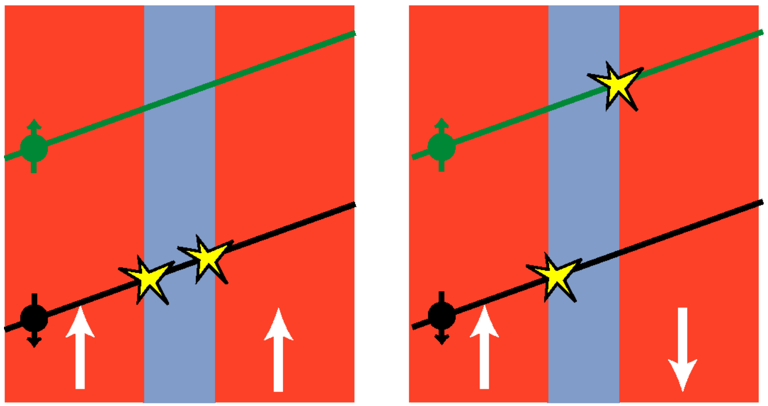

Inverse GMR:

$\beta_L > 0$ and $\beta_R < 0$ or *vice versa*

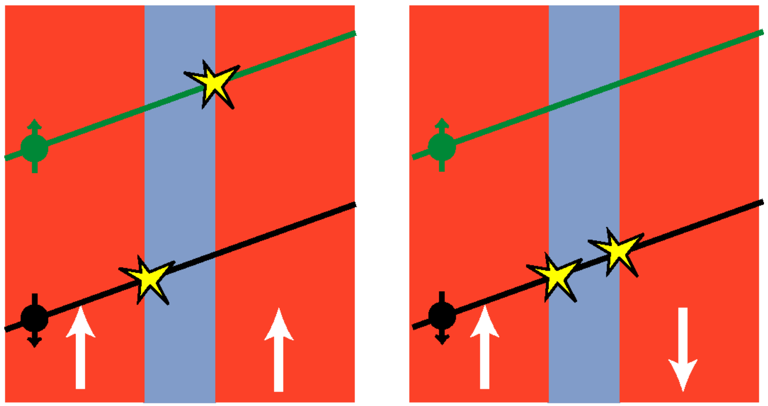

$\beta_L > 0$ and $\beta_R > 0$

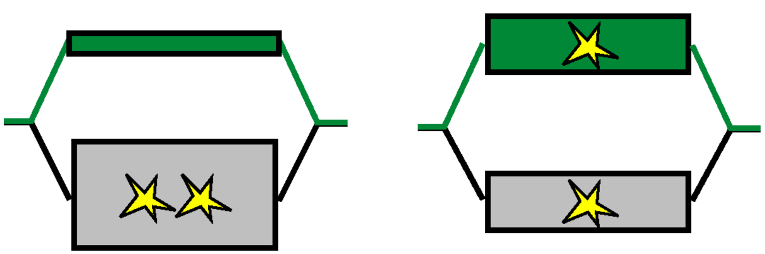

$\beta_L > 0$ and $\beta_R < 0$

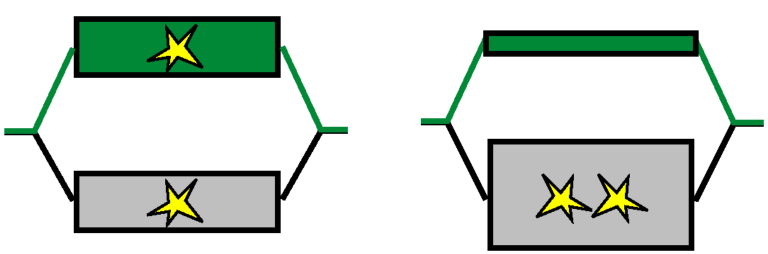

Relation to Slater-Pauling curve I

A. Barthélémy *et al.*, Handbook of Magnetic Materials **12** (1999)

The sign of the β' s of 3d transition metals and their alloys can be obtained from the Slater-Pauling curve:

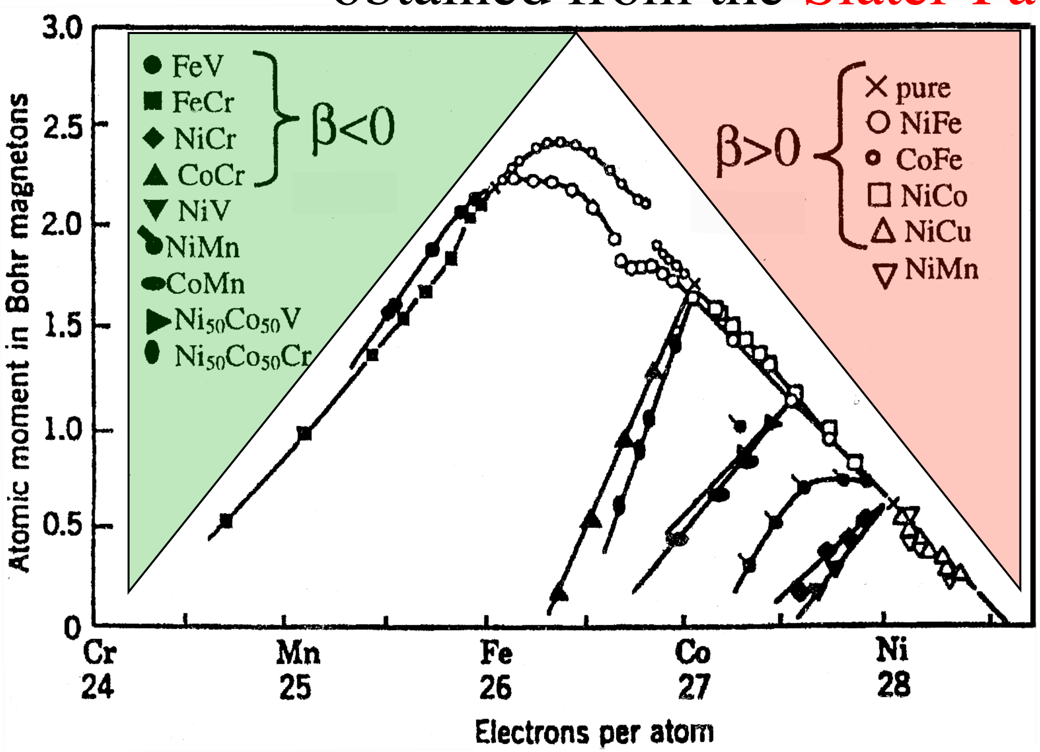

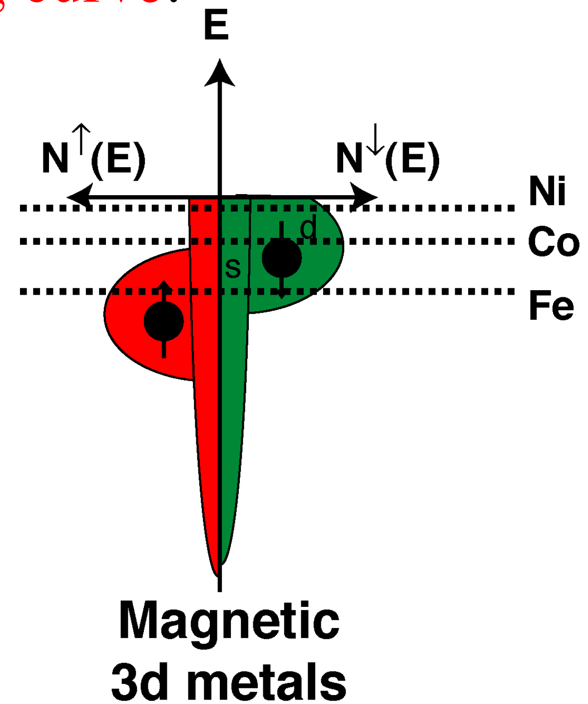

For positive slope: $N^{\uparrow} > N^{\downarrow} \Rightarrow r^{maj} > r^{\min} \Rightarrow \beta < 0$

For negative slope: $N^{\uparrow} < N^{\downarrow} \Rightarrow r^{maj} < r^{\min} \Rightarrow \beta > 0$

Relation to Slater-Pauling curve II

This rule holds for
bulk scattering spin asymmetries in AB alloys
as well as for
interface scattering spin asymmetries at A/B interfaces

($e.g.\ \beta < 0$ for CoCr bulk alloys and Co/Cr interfaces)

This rule is observed in many CIP and CPP
experiments and confirms
spin-dependent scattering
as the
predominant mechanism for GMR.

A. Barthélémy *et al.*, Handbook of Magnetic Materials **12** (1999)

Outline: Giant and tunneling magnetoresistance (GMR and TMR)

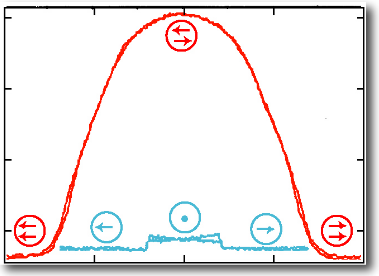

- Phenomenology of GMR
- Intermezzo: Ferromagnetic halfmetals
- Physical picture for GMR
- **Applications of GMR**
- Phenomenology of TMR
- Physical picture for TMR: Jullière and beyond
- Applications of TMR

Application of GMR: Magnetic field sensor

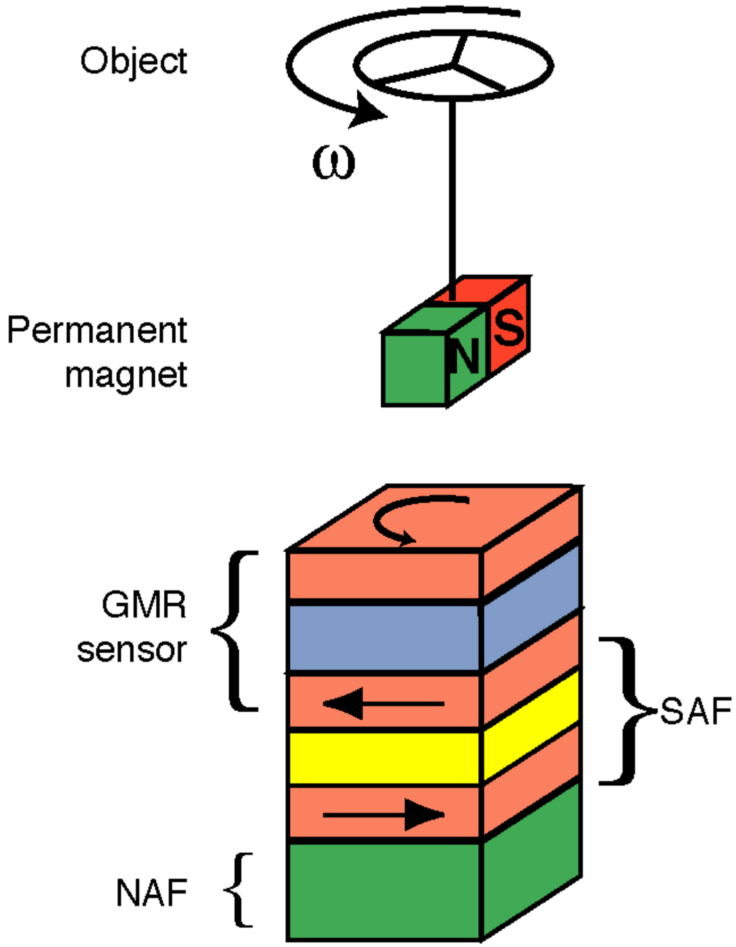

Example of a real layer structure [1]:

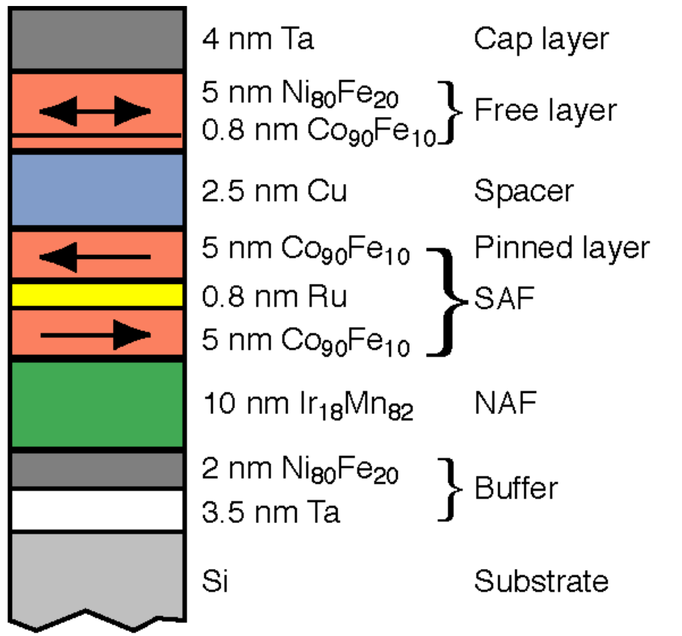

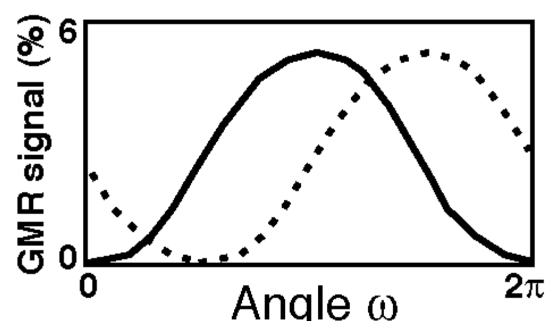

NAF = natural antiferromagnet, SAF = synthetic antiferromagnet

[1] K.M.H. Lenssen *et al.*, J. Appl. Phys. **85**, 5531 (1999)

Application of GMR: Read heads in hard-disk drives

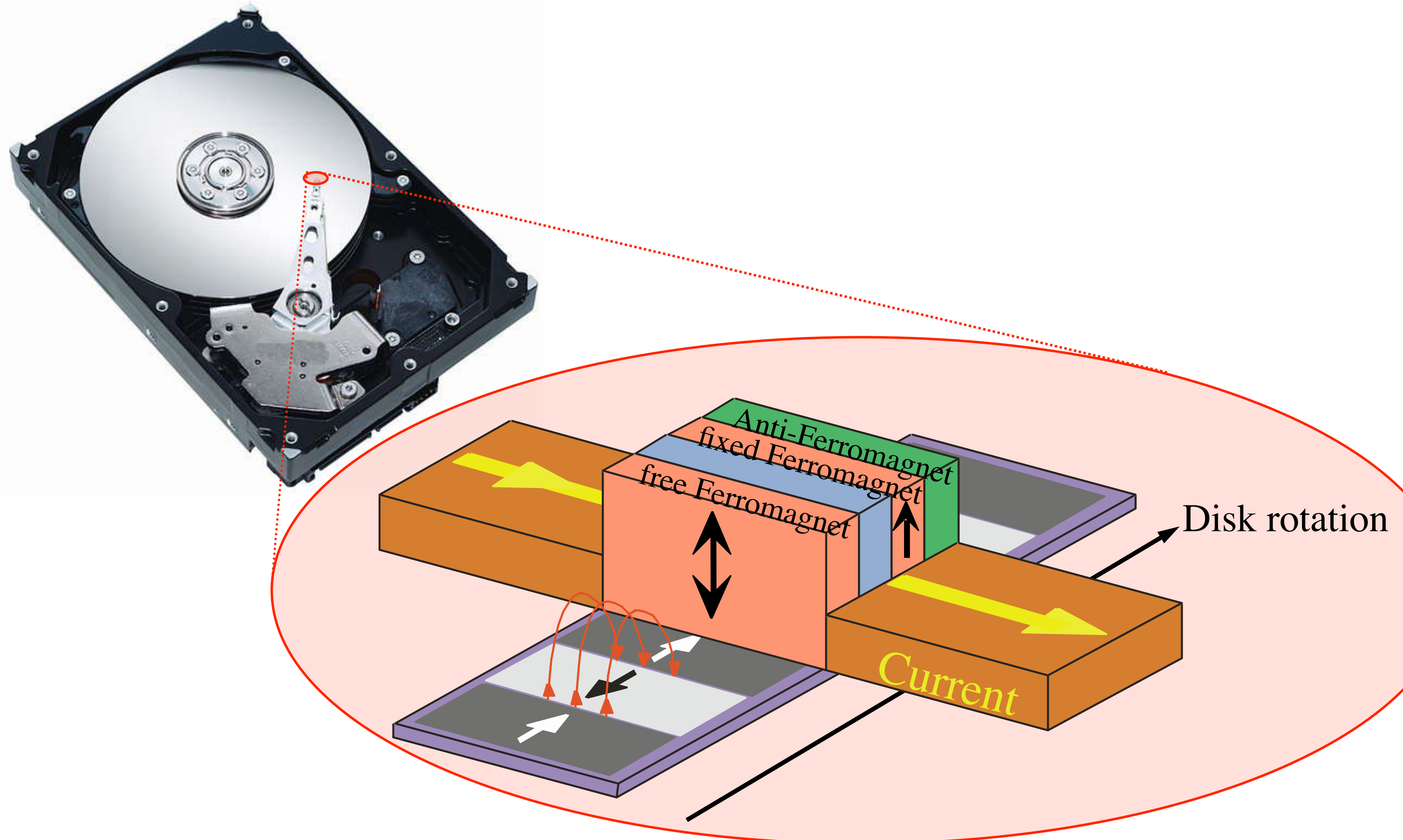

Application of GMR in hard-disks

Advantages of GMR-based read heads compared to AMR or inductive read heads:

1) Stronger MR signal
 ⇒ Better signal-to-noise
 ⇒ Smaller bits can be read

2) GMR is an interface effect (AMR is a bulk effect):
 ⇒ Thinner MR elements
 ⇒ Less demagnetization
 ⇒ Less wide MR elements
 ⇒ Higher sensitivity

AMR

GMR

Year	Areal Density Gbits/in2	Product
1991	0.132	Corsair
1992	0.260	Allicat
1993	0.354	Spitfire
1994	0.578	Ultrastar XP
1995	0.829	Ultrastar 2XP
	0.923	Travelstar 2LP
1996	1.32	Travelstar 2XP
	1.45	Travelstar VP
1997	2.64	Travelstar 5GS
	2.68	Deskstar 16GP
	3.12	Travelstar 6GN
1998	3.74	Travelstar 6GT
	4.1	Deskstar 25GP
	5.7	Travelstar 6GN
1999	5.3	Deskstar 37GP
	10.1	Travelstar 18GT
2000	7.04	Ultrastar 36LZX
	14.5	Deskstar 40GV
	17.1	Travelstar 30GT
2001	13.2	Ultrastar 73LZX
	25.7	Travelstarr 30GN
	29.7	Deskstar 120GXP
	34.0	Travelstar 40GN
2002	26.3	Ultrastar 146Z10
	45.5	Deskstar 180GXP
	29.7	Deskstar 120GXP
2003	70.0	Travelstar 80GN
2004	>100	
2005	>200	

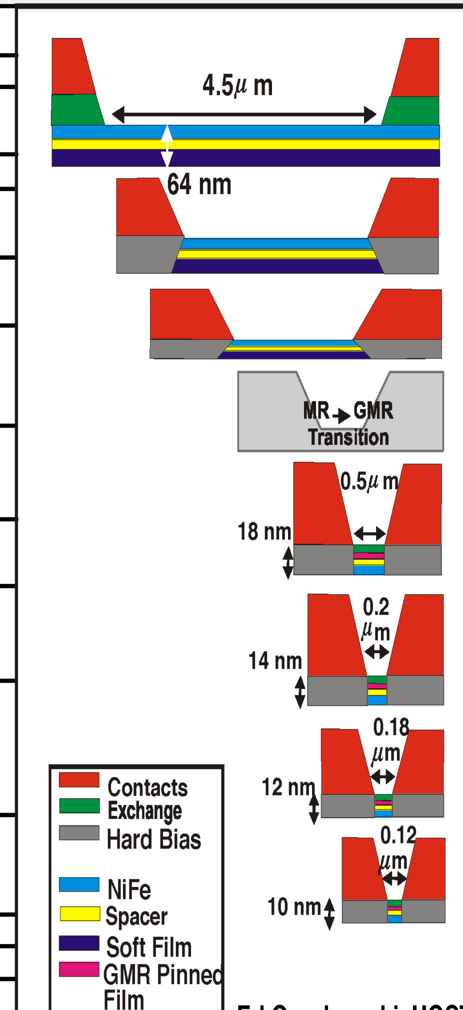

Ed Grochowski, HGST

Outline: Giant and tunneling magnetoresistance (GMR and TMR)

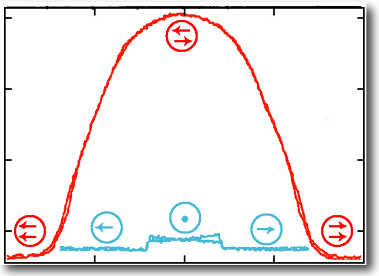

- Phenomenology of GMR
- Intermezzo: Ferromagnetic halfmetals
- Physical picture for GMR
- Applications of GMR
- Phenomenology of TMR
- Physical picture for TMR: Jullière and beyond
- Applications of TMR

Tunneling magnetoresistance (TMR)

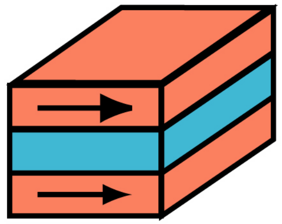

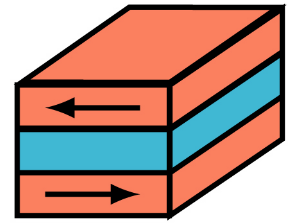

Ferromagnet
Insulator
Ferromagnet

Electrical resistance: $\mathbf{R_{Par}}$ **<(>)** $\mathbf{R_{AP}}$

The electrical resistance depends on the relative magnetic alignment of the ferromagnetic layers

Only for current perpendicular to the sample plane $\Rightarrow$ Tunneling current

Typical areal resistance: $RA \approx 1 - 10^6\ \Omega\ \mu m^2$

$$\text{TMR} = \frac{R_{AP} - R_P}{R_P}$$

60% for AlO_x barriers @RT

>600% for epitaxial MgO @ RT

Typical TMR structure and measurement

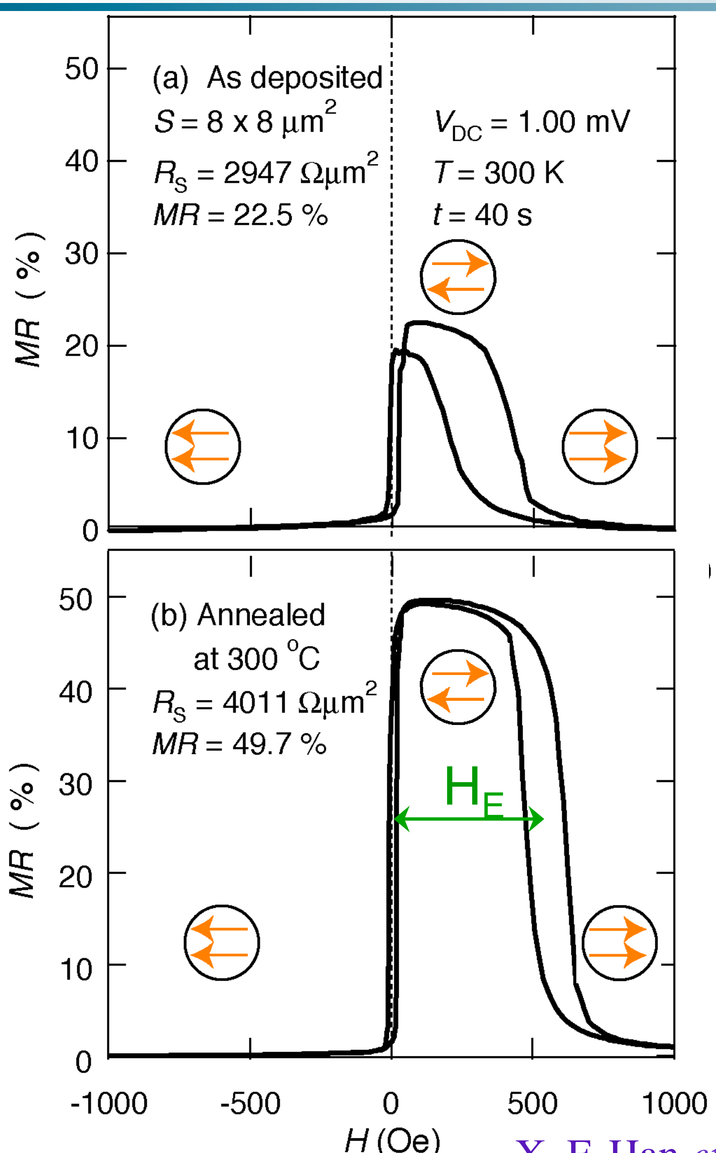

$Co_{75}Fe_{25}$(4 nm) /Al_2O_3(0.8 nm)/ $Co_{75}Fe_{25}$(4 nm) / IrMn (10 nm)

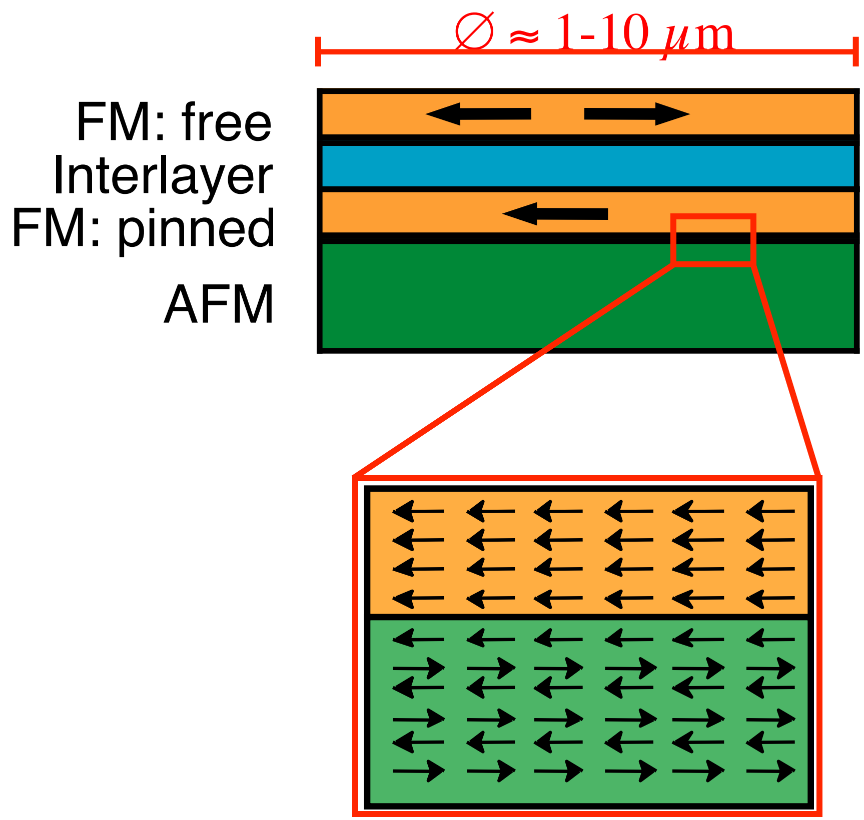

"Exchange Bias"

X. F. Han *et al*., Jpn. J. Appl. Phys. **39**, L439 (2000)

Intermezzo: Optical lithography of TMR junctions

Typical junction areas for TMR: 1 - $10^4\ \mu m^2$

Growth of the layered system

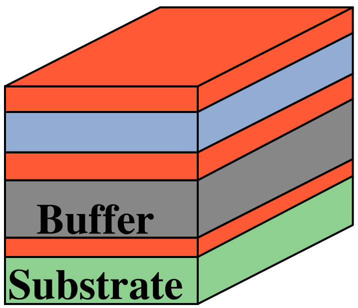

Optical lithography and ion beam etching

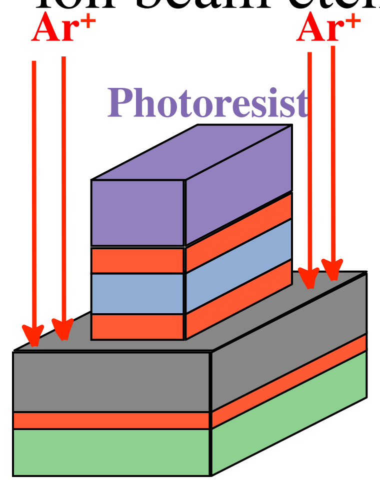

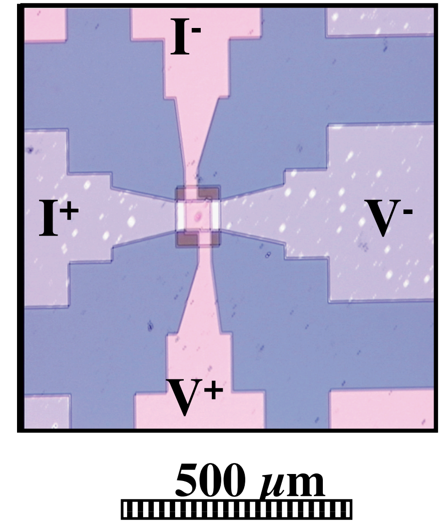

Insulator deposition, lift-off, deposition of top electrode

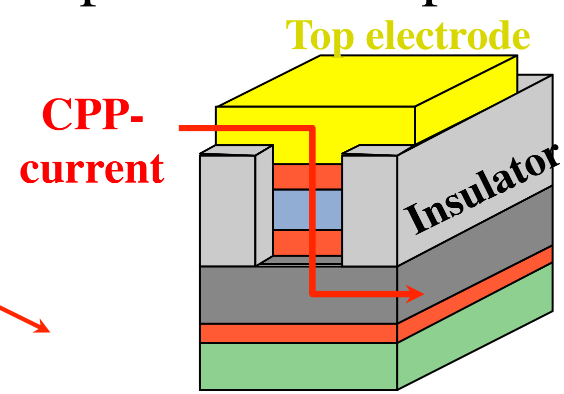

Junctions of layered structures and dimensions on the μm-scale for CPP transport measurements

Outline: Giant and tunneling magnetoresistance (GMR and TMR)

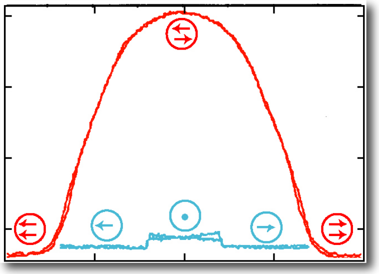

- Phenomenology of GMR
- Intermezzo: Ferromagnetic halfmetals
- Physical picture for GMR
- Applications of GMR
- Phenomenology of TMR
- Physical picture for TMR: Jullière and beyond
- Applications of TMR

Microscopic picture of TMR: Spin-dependent tunneling

TMR exploits spin-dependent tunneling probabilities across an insulating rather than spin-dependent scattering probabilities

Assumptions: Spin and energy conservation during tunneling

$\propto N_L^{\downarrow} N_R^{\downarrow}$

$\propto N_L^{\uparrow} N_R^{\uparrow}$

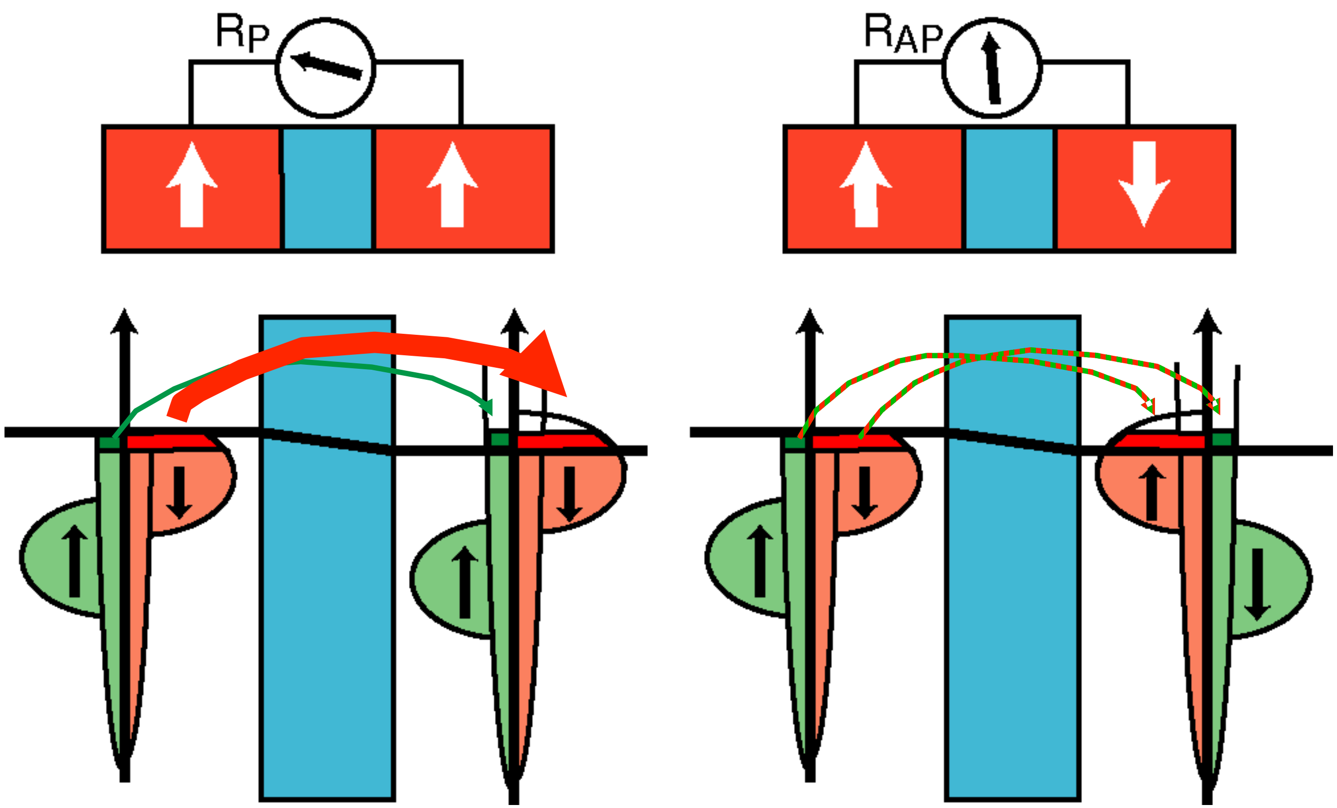

$\propto N_L^{\downarrow} N_R^{\uparrow}$

$\propto N_L^{\uparrow} N_R^{\downarrow}$

$\Rightarrow$ TMR depends on the spin-split DOS at the Fermi level $N_{L,R}^{\uparrow,\downarrow}$

Jullière's model

$$R_P = \frac{V}{I_P} \propto \frac{V}{N_L^{\uparrow} N_R^{\uparrow} + N_L^{\downarrow} N_R^{\downarrow}} \qquad R_{AP} = \frac{V}{I_{AP}} \propto \frac{V}{N_L^{\uparrow} N_R^{\downarrow} + N_L^{\downarrow} N_R^{\uparrow}}$$

Consider the polarization at the Fermi level: $P_{L,R} = \dfrac{N_{L,R}^{\uparrow} - N_{L,R}^{\downarrow}}{N_{L,R}^{\uparrow} + N_{L,R}^{\downarrow}}$

M. Jullière, Phys. Lett. **54A**, 225 (1975)

$$\Rightarrow \text{TMR} = \frac{R_{AP} - R_P}{R_P} = \frac{2P_L P_R}{1 - P_L P_R}$$ Jullière formula

[$P_L P_R > 0$: normal and $P_L P_R < 0$: inverse TMR effect]

BUT: What are the relevant polarizations P_i? Bulk? Interface?
Are interface states important?
What is the role of barrier material?

Beyond Jullière's model: Importance of barrier material

Co / X / $La_{0.7}Sr_{0.3}MnO_3$

X = $SrTiO_3$
Inverse TMR

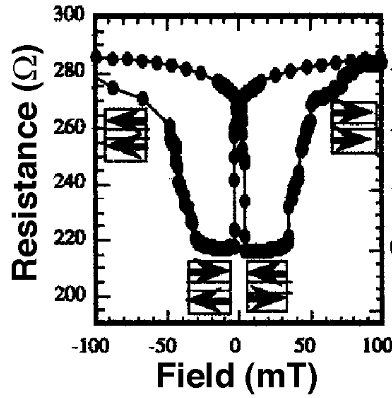

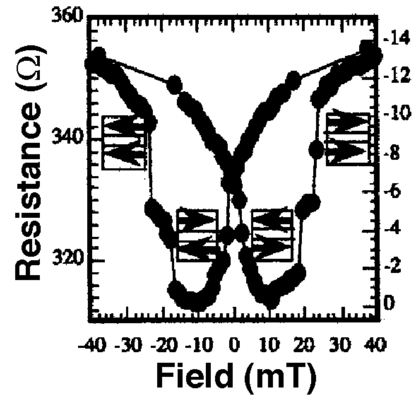

X = $Ce_{0.7}La_{0.3}TiO_{1.85}$
Inverse TMR

X = Al_2O_3
Normal TMR

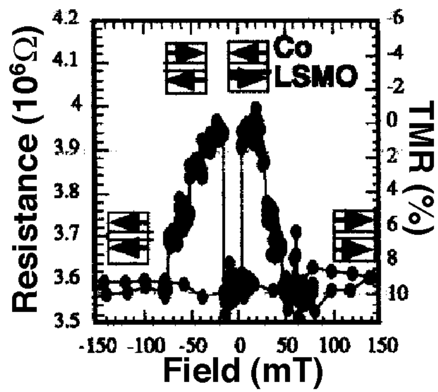

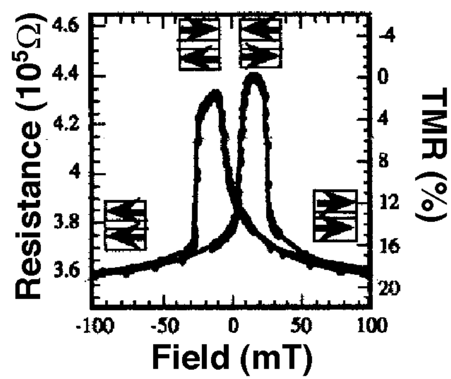

X = Al_2O_3/ $SrTiO_3$
Normal TMR

The strength and sign of TMR depend on the barrier material

P_L and P_R are related to the bonding details at the interface

J.M. de Teresa *et al*., Science **286**, 507 (1999)

Beyond Jullière's model: Epitaxial MgO barriers

Epitaxial [1] or highly oriented [2] MgO(001) barriers yield very high TMR ratios of up to 220% at RT.

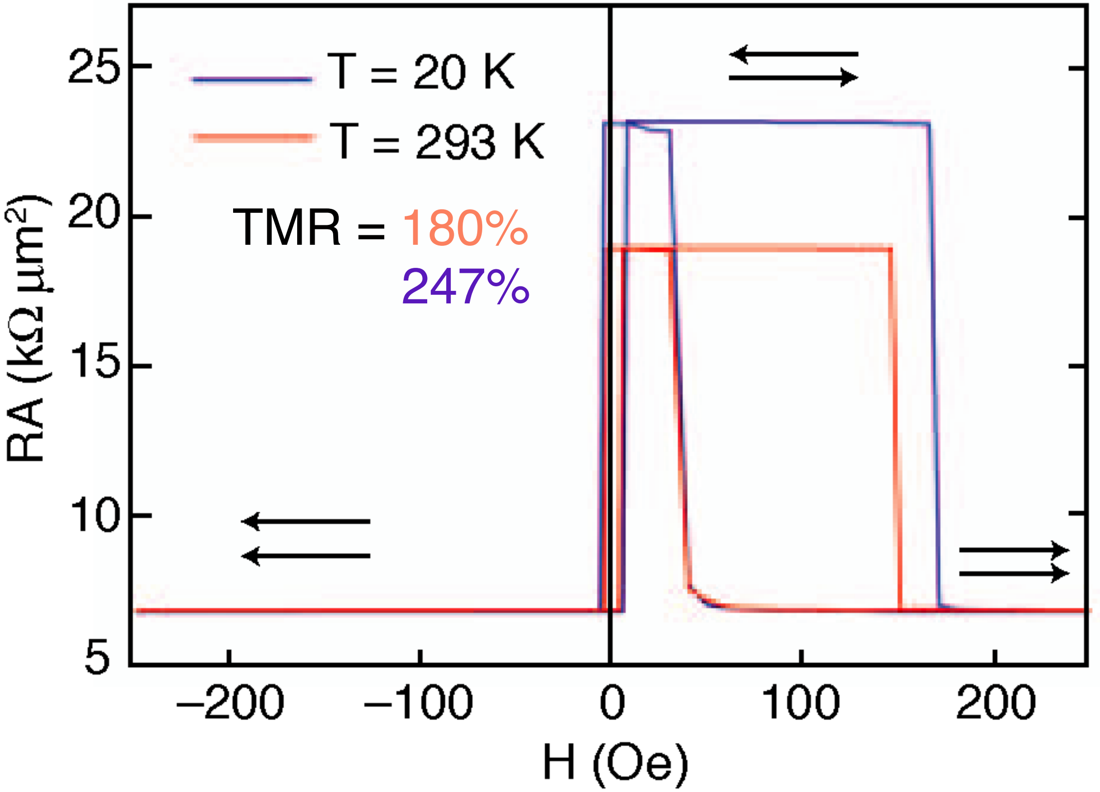

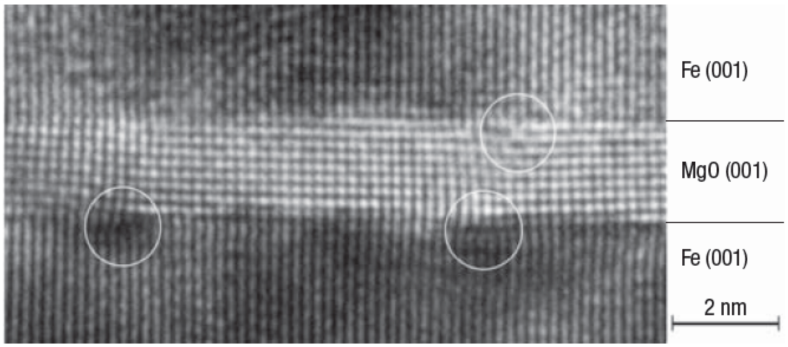

TEM of epitaxial MgO barrier [1]

High TMR ratios beyond what is expected from the Jullière's model

⇒ More realistic description of tunneling required

[1] S. Yuasa *et al.*, Nature Materials **3**, 868 (2004), [2] S.S.P. Parkin *et al.*, Nature Materials **3**, 862 (2004)

Beyond Jullière's model: Epitaxial MgO barriers

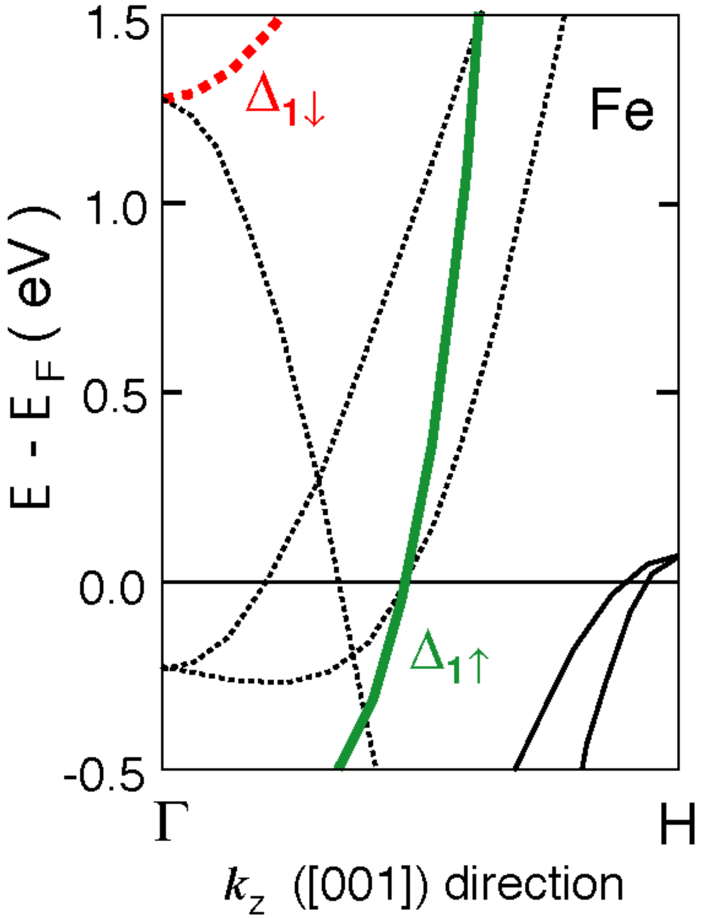

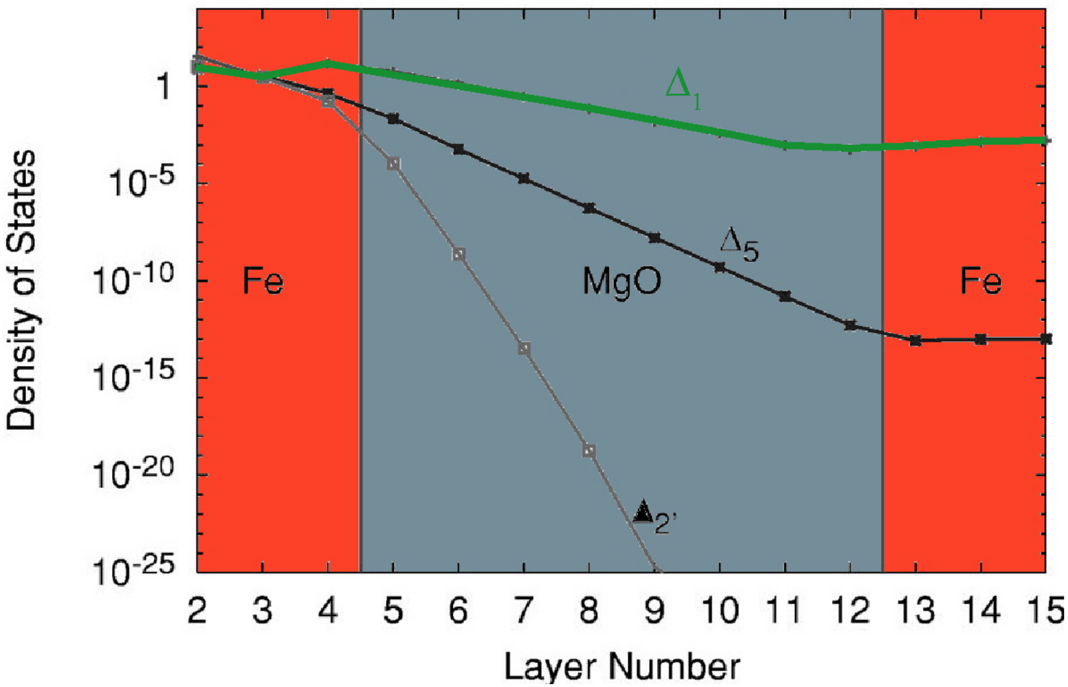

Δ_1 majority states decay slower and couple to propagating states in Fe

The high TMR is due to predominant and coherent tunneling of highly symmetric Fe Δ_1 majority states.

W.H. Butler et al., Phys. Rev. B 63, 054416 (2001)

"History" of TMR

There is always more to come…

1975 First observation of TMR in Fe/Ge/Co by Jullière
14% but only at low temperature

1995 Rediscovery of TMR by Miyasaki and Moodera
up to the "theoretical Jullière limit" for 3d ferromagnets
and AlO_x barriers of about 60% at RT in the following years

2004 Epitaxial structures with MgO barriers yield TMR
ratios of up to 600% at RT

Outline: Giant and tunneling magnetoresistance (GMR and TMR)

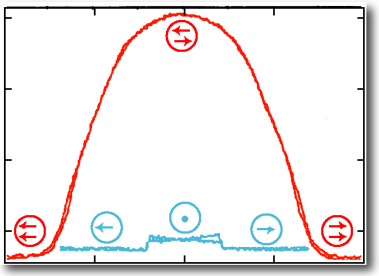

- Phenomenology of GMR
- Intermezzo: Ferromagnetic halfmetals
- Physical picture for GMR
- Applications of GMR
- Phenomenology of TMR
- Physical picture for TMR: Jullière and beyond
- Applications of TMR

Application of TMR: Magnetic RAM

Non-volatile, highly integrated solid-state device

Each TMR element represents one bit

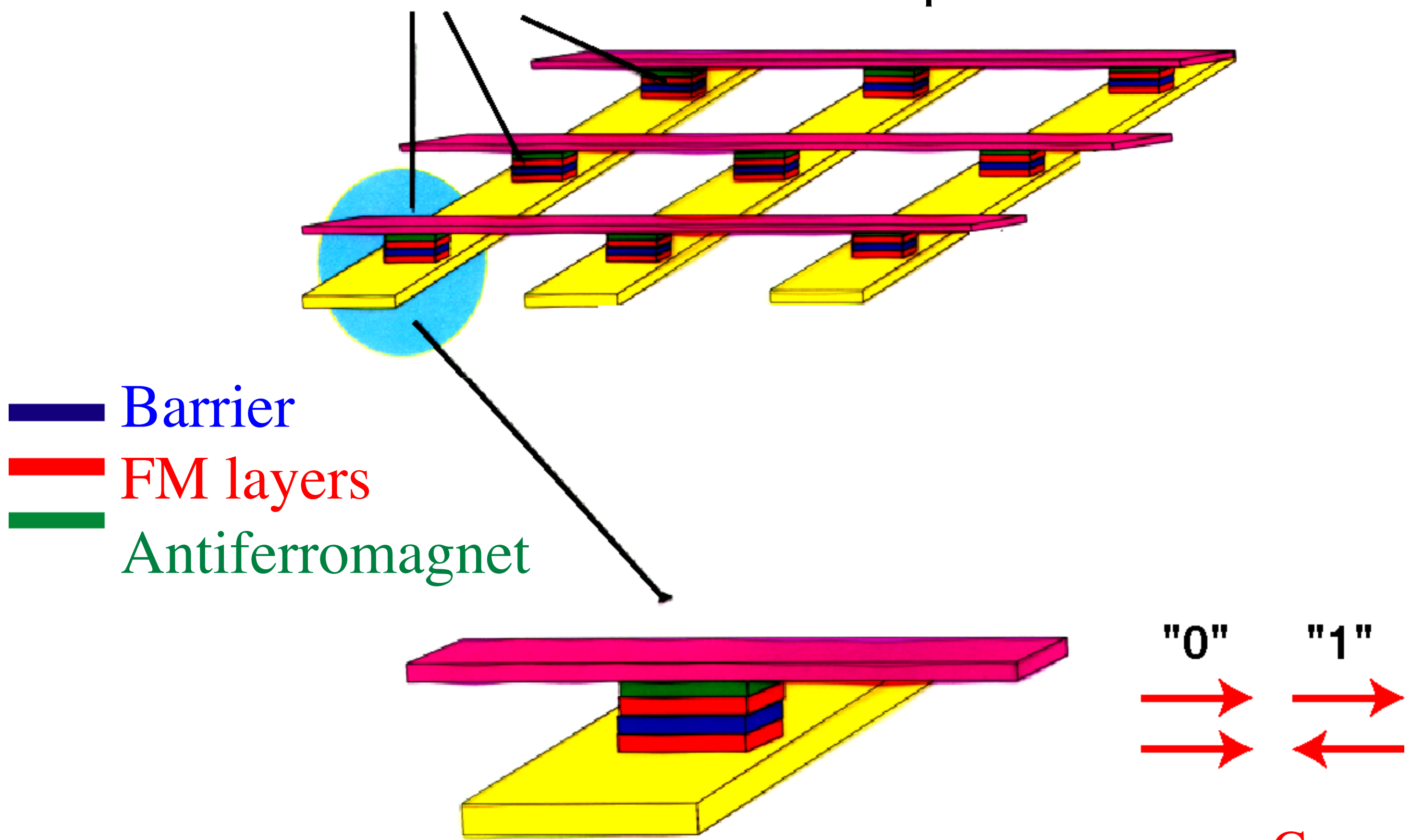

Commercialized 2006 by Freescale

Application of TMR: Magnetic RAM

Non-volatile, highly integrated solid-state device

Each TMR element represents one bit

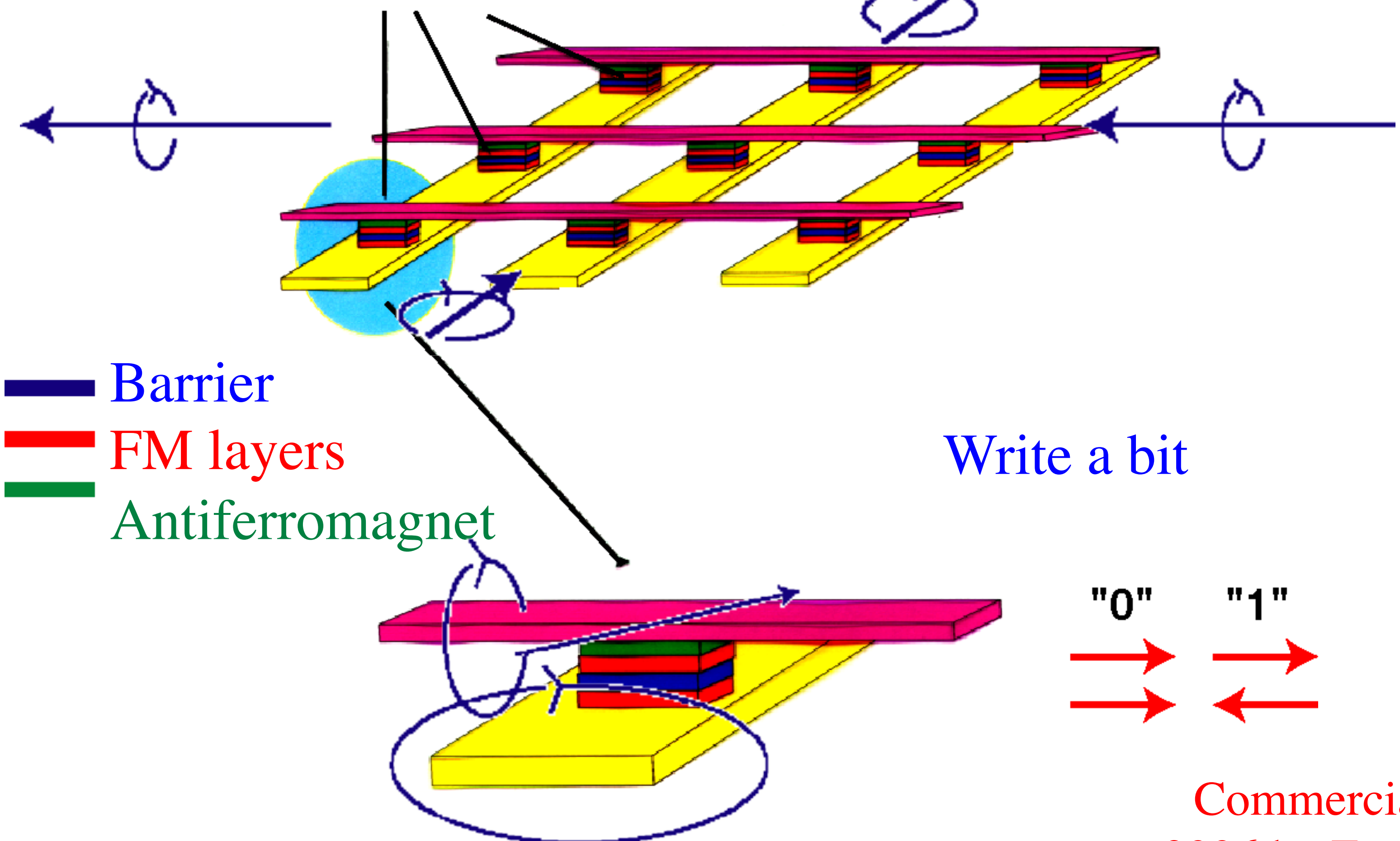

Commercialized 2006 by Freescale

Application of TMR: Magnetic RAM

Non-volatile, highly integrated solid-state device

Each TMR element represents one bit

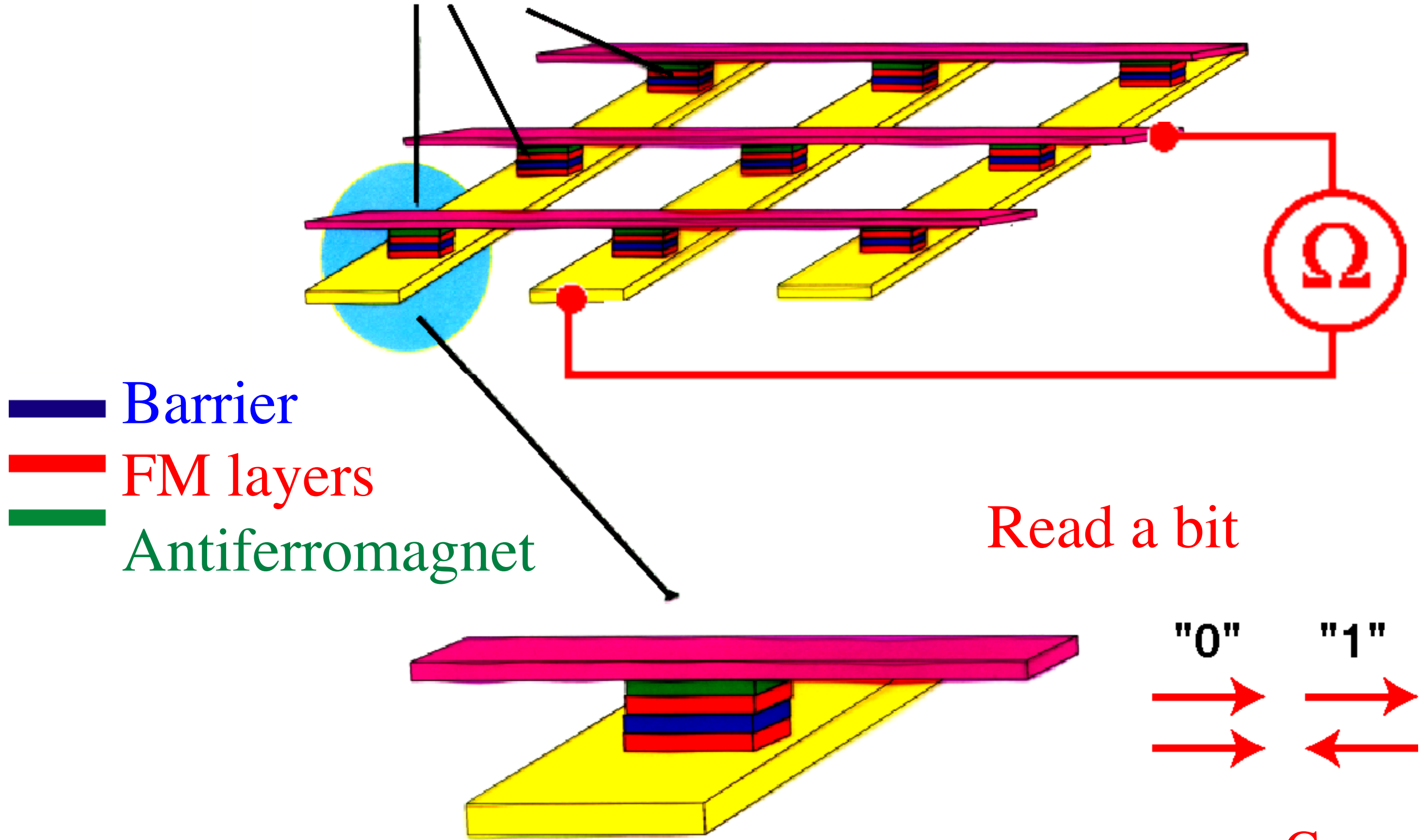

Commercialized
2006 by Freescale

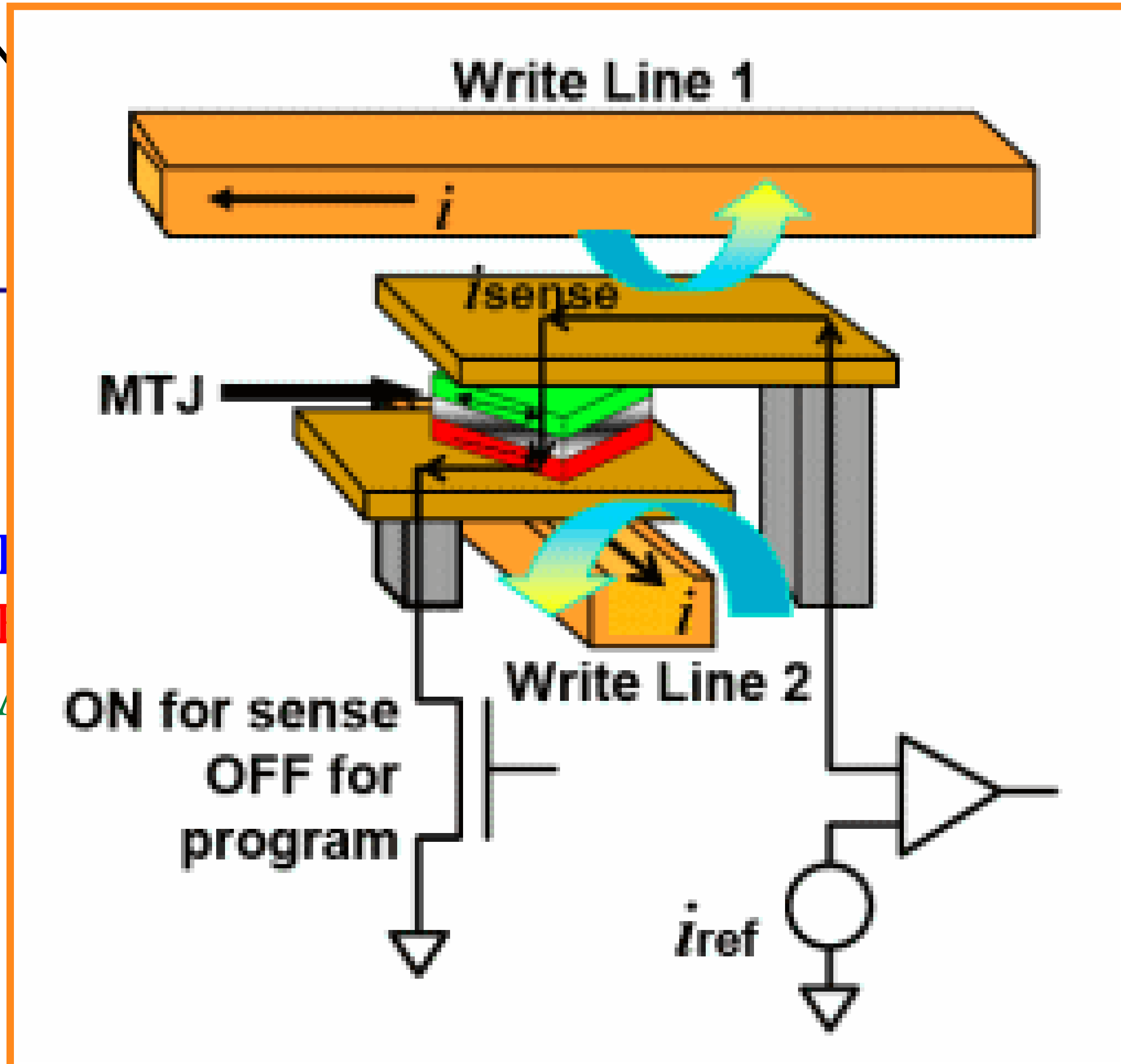

"1"

ommercialized
06 by Freescale

Advanced switching concept

Giant or tunneling magnetoresistance (GMR, TMR):
"*The magnetization state controls to the electric current flow*"

Parallel alignment
$\Rightarrow$ low resistive

Antiparallel alignment
$\Rightarrow$ high resistive

$R_P = \text{low}$
$I_P = \text{high}$

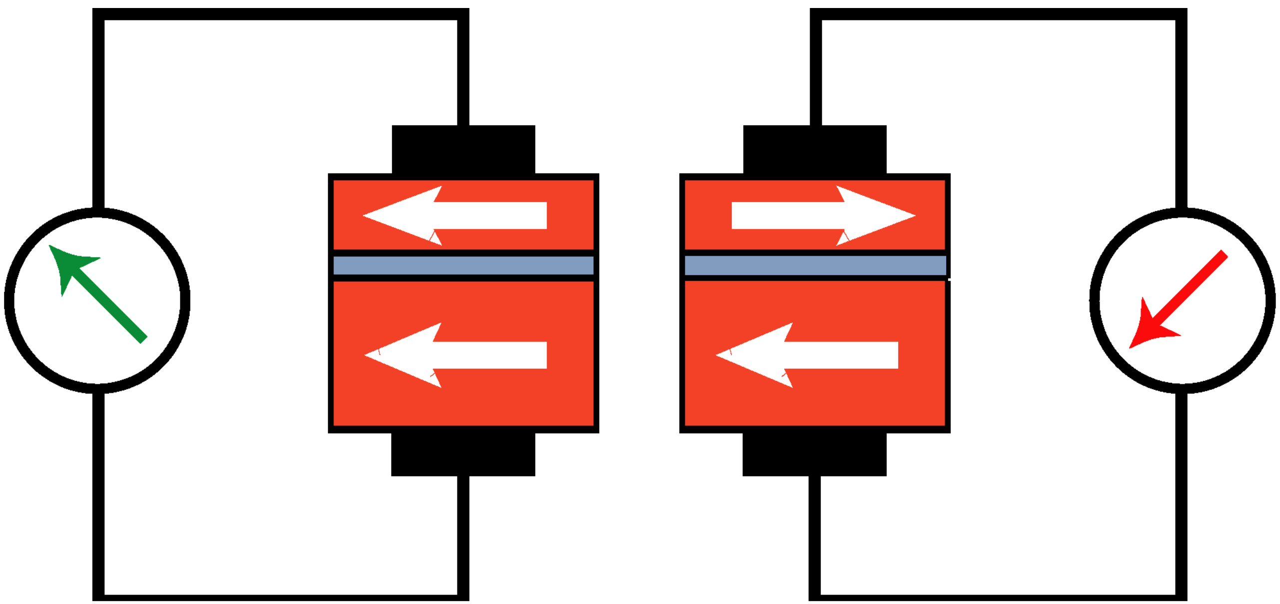

$R_{AP} = \text{high}$
$I_{AP} = \text{low}$

Apply Newton's third law "*Actio = Reactio*" to GMR/TMR:

"*The electric current flow controls the magnetization state*"

Negative current $\Rightarrow$ parallel alignment

Positive current $\Rightarrow$ Antiparallel alignment

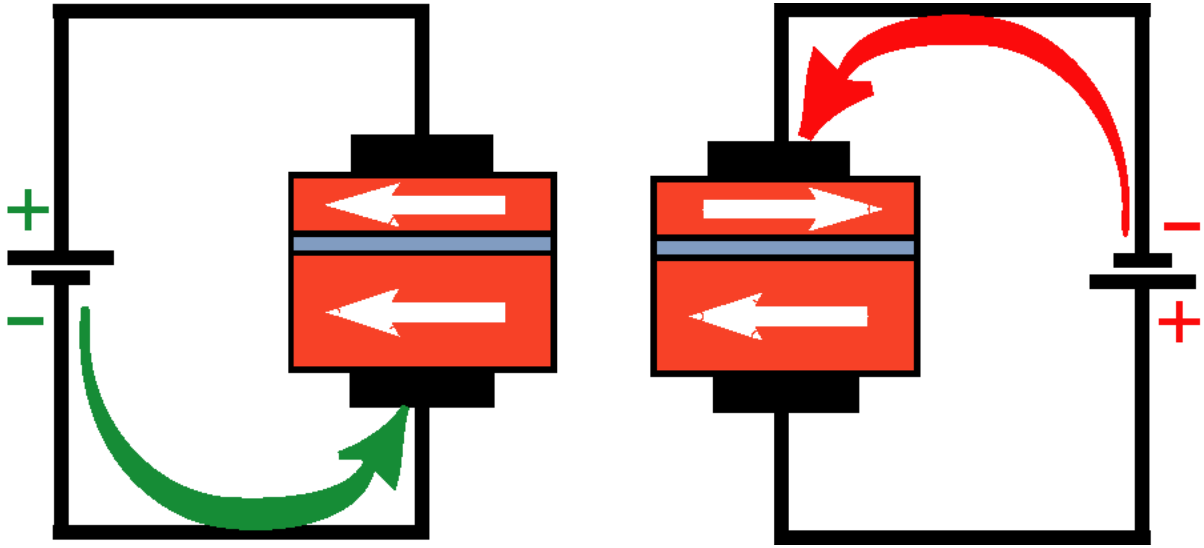

$\Rightarrow$ Current-induced magnetization switching by spin-transfer torque

J.C. Slonczewski, J. Magn. Magn. Mater. **159**, L1 (1996); L. Berger, Phys. Rev B **54**, 9353 (1996)

Magnetic random access memory (MRAM)

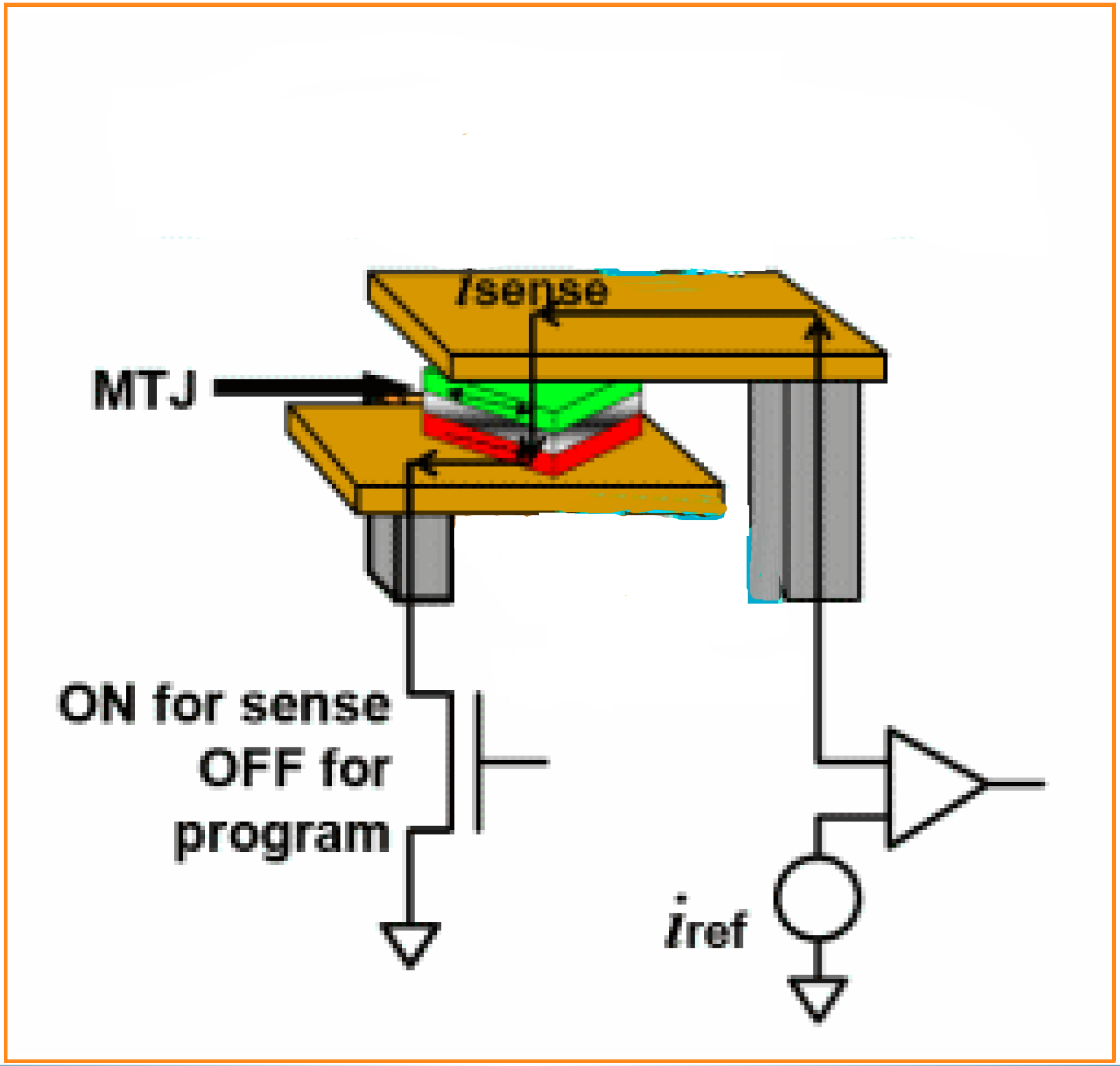

Overview

Introduction

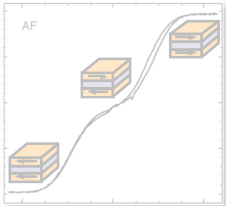

Interlayer exchange coupling

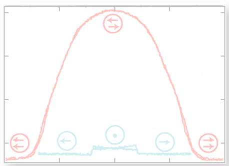

Giant and tunneling magnetoresistance

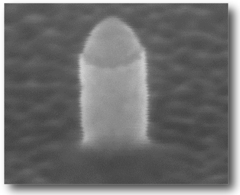

Current-induced magnetization dynamics

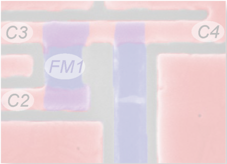

Pure spin current

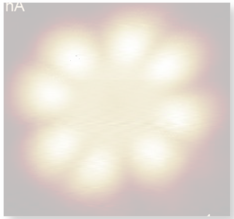

Magnetic molecules

Conclusions

Outline: Current-induced magnetization dynamics

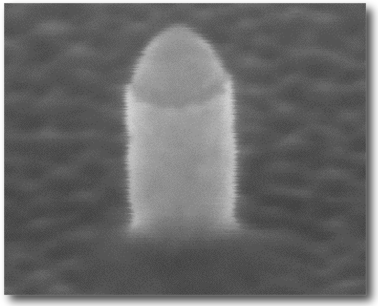

- Need for advanced magnetic switching concept
- Phenomenology of spin-transfer torque (STT)

  "Current-induced magnetization switching"
- Physical picture for STT
- Current-driven magnetization dynamics

  "Extended Landau-Lifshitz-Gilbert equation"

  "Spin-torque oscillators (STO)"
- STT in non-uniform magnetization structures

Advanced switching concept for spintronic devices

Spintronic devices employ the electron spin for data storage and processing.

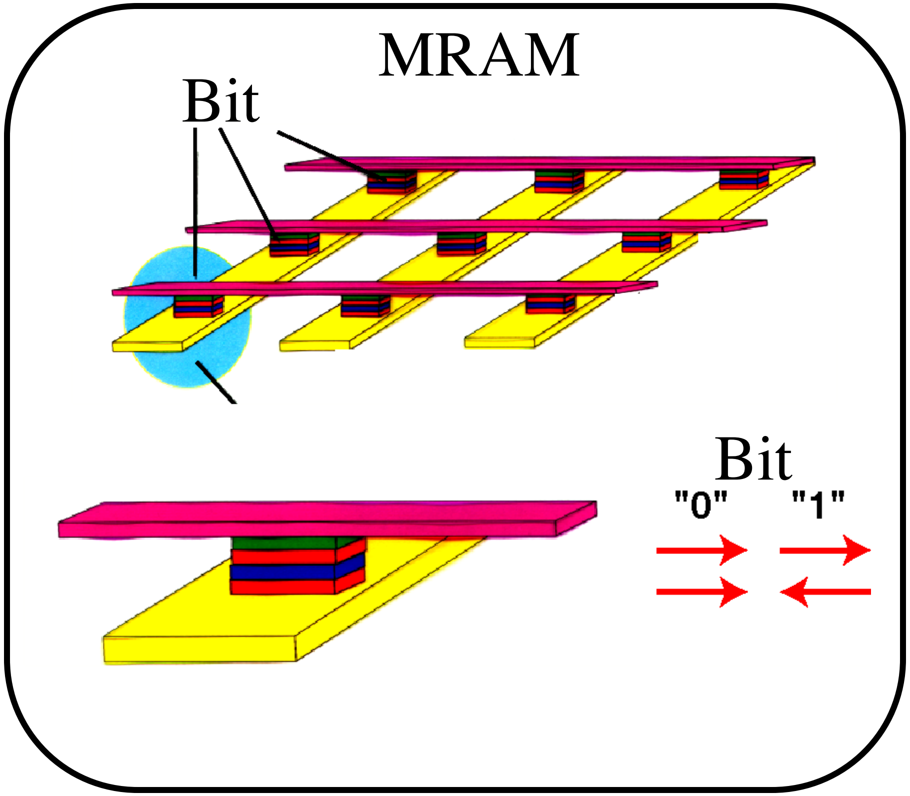

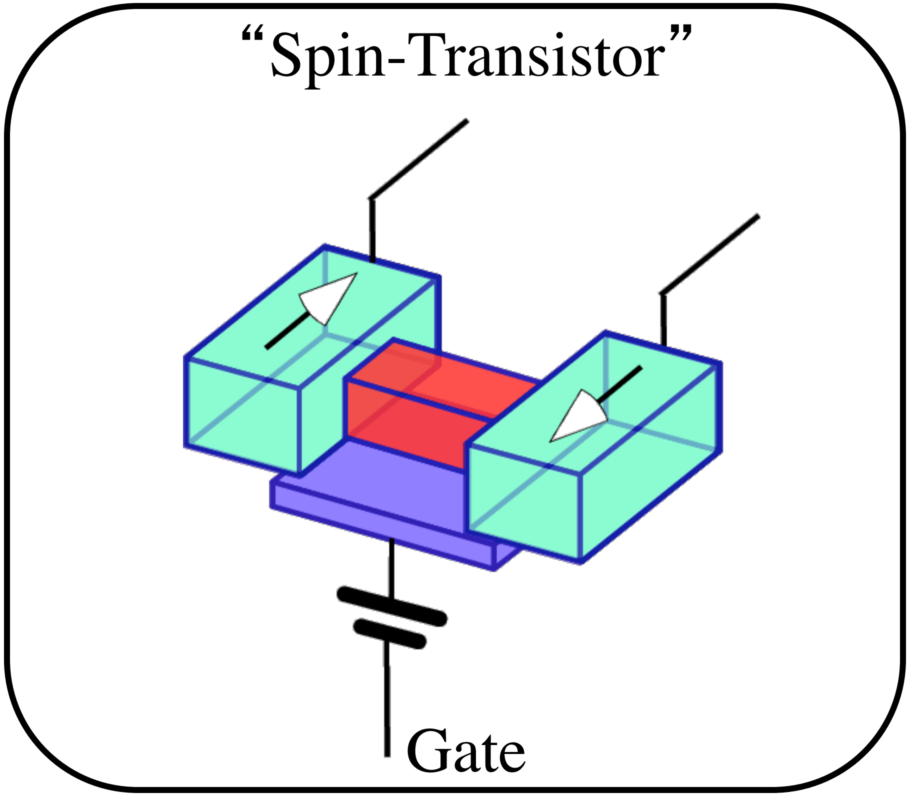

Manipulation of the magnetic state of ferromagnetic nano-scale objects, *e.g.* electrodes, is of crucial importance.

Conventional field-induced magnetization switching

Consider a constant magnetization $\boldsymbol{M}$ within a certain volume. The effective field $\boldsymbol{B}_{eff}$ gives rise to the energy density E and a torque $\boldsymbol{\Gamma}$:

$$E = -\overrightarrow{M} \cdot \overrightarrow{B}_{eff} \quad ; \quad \overrightarrow{\Gamma} = -(\overrightarrow{M} \times \overrightarrow{B}_{eff})$$

Parallel alignment

$E = \text{min.}, \boldsymbol{\Gamma} = 0$

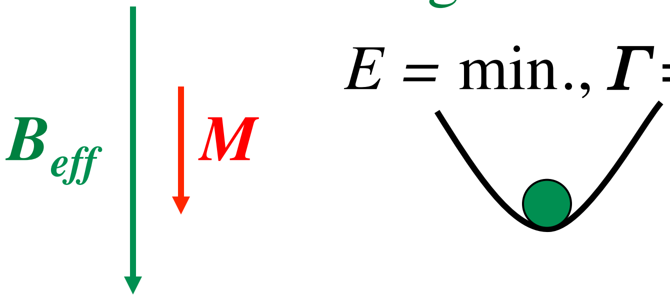

Stable equilibrium

Antiparallel alignment

$E = \text{max.}, \boldsymbol{\Gamma} = 0$

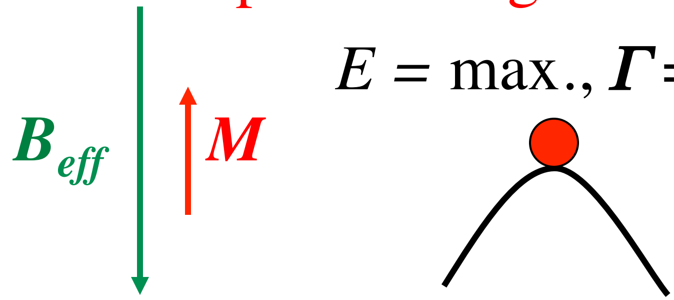

Unstable equilibrium

Conventional switching by applying an antiparallel field depends on perturbations (temperature, edges, magnetic inhomogeneities)

$\Rightarrow$ Slow, energetically inefficient, spatially incoherent

Conventional switching of a thin Ni nanowire

Ni wire, 40 nm diameter, 1 μm length, $\alpha = 0.1$ H = 200 mT.

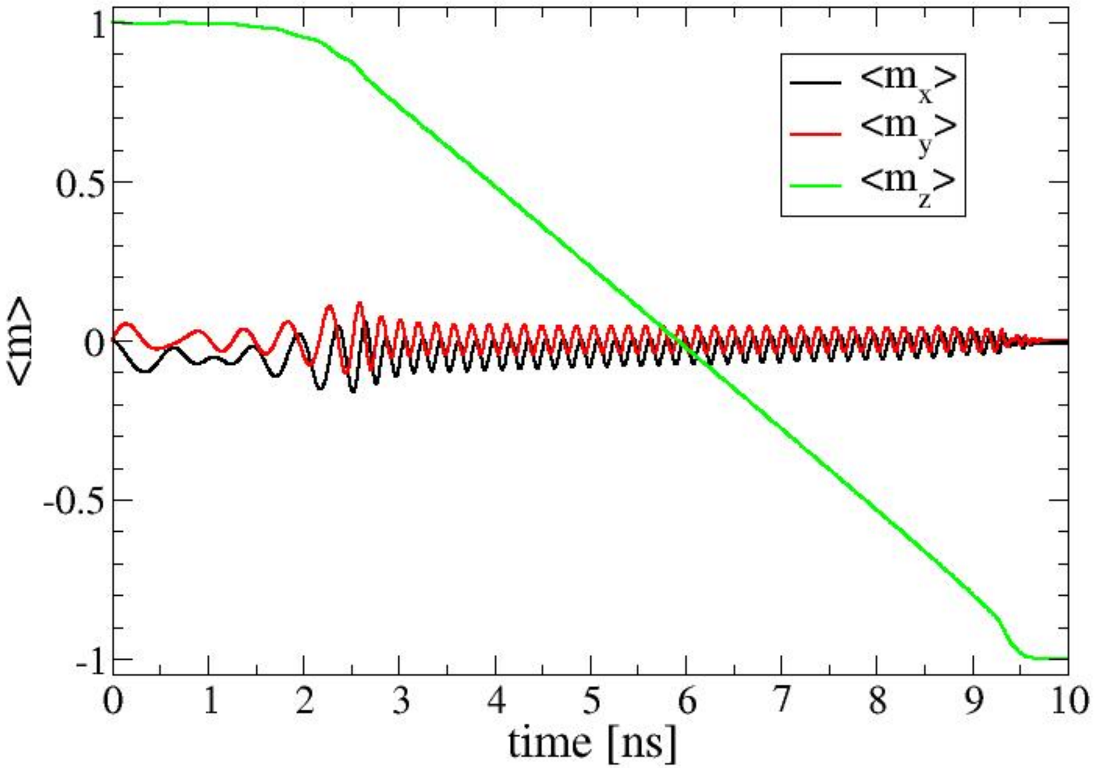

$t = 0 \ldots 4.5$ ns

H_{ext}

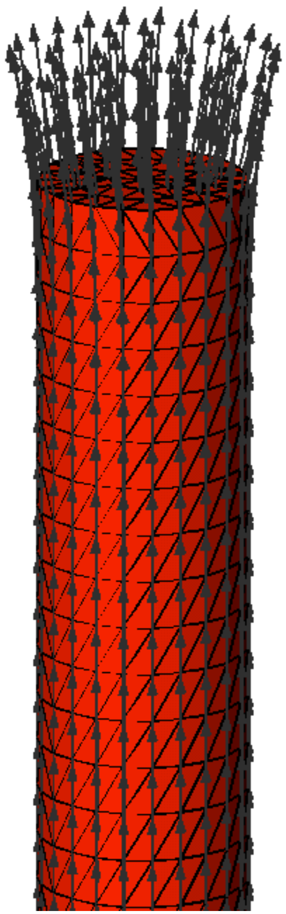

Nucleation, propagation, precession, ringing

$\Rightarrow$ slow, inefficient, incoherent

R. Hertel, J. Magn. Magn. Mater. **249**, 251 (2002).

Requirements for magnetization switching

- Local addressing and selection of single nano-scale objects

  ⇒ avoid external magnetic fields

  ⇒ switching by electrical means (gate voltage or current)

- Low dissipation to reduce power consumption and heat load

  ⇒ efficient mechanism

- Potential for down-scaling and semiconductor compatibility

  ⇒ solid-state environment

- Fast switching below 1 ns to keep up with increasing clock speeds

  ⇒ magnetization dynamics plays a role

⇒ Spin-transfer torque dynamics provides a route to advanced magnetization switching concepts

Field-induced *versus* current-induced writing of MRAM cells

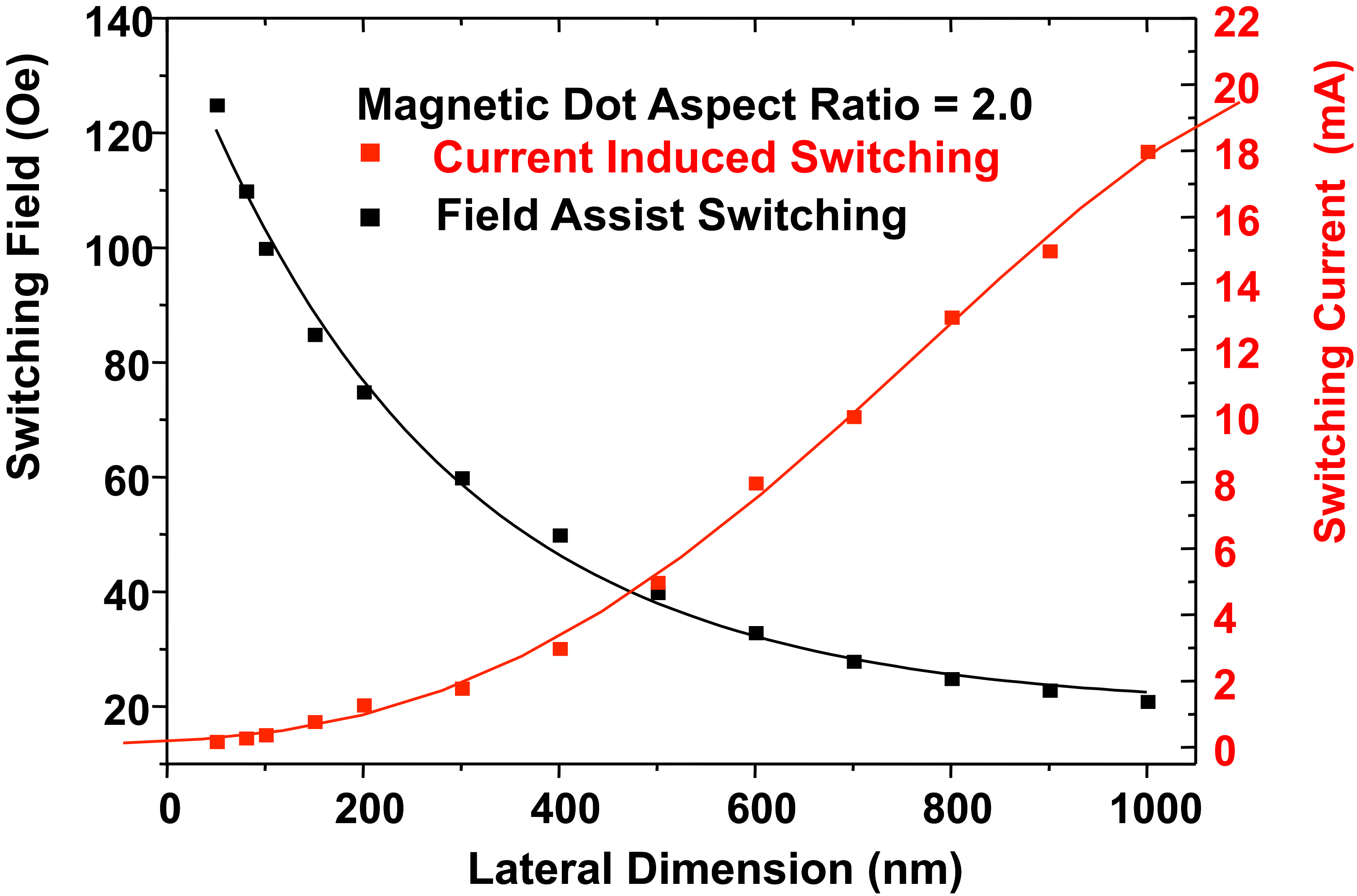

Kamel Ounadjela, Cypress Semiconductor

Outline: Current-induced magnetization dynamics

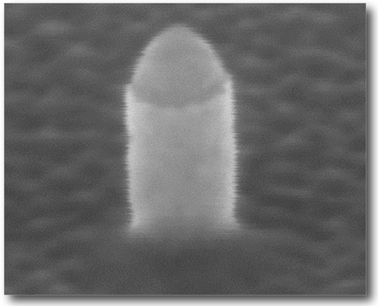

- Need for advanced magnetic switching concept
- Phenomenology of spin-transfer torque (STT)

  "Current-induced magnetization switching"
- Physical picture for STT
- Current-driven magnetization dynamics

  "Extended Landau-Lifshitz-Gilbert equation"

  "Spin-torque oscillators (STO)"
- STT in non-uniform magnetization structures

Current-induced magnetization switching

The polarity of the electric current flow controls
the magnetization state.

Negative current
⇒ parallel alignment

Positive current
⇒ Antiparallel alignment

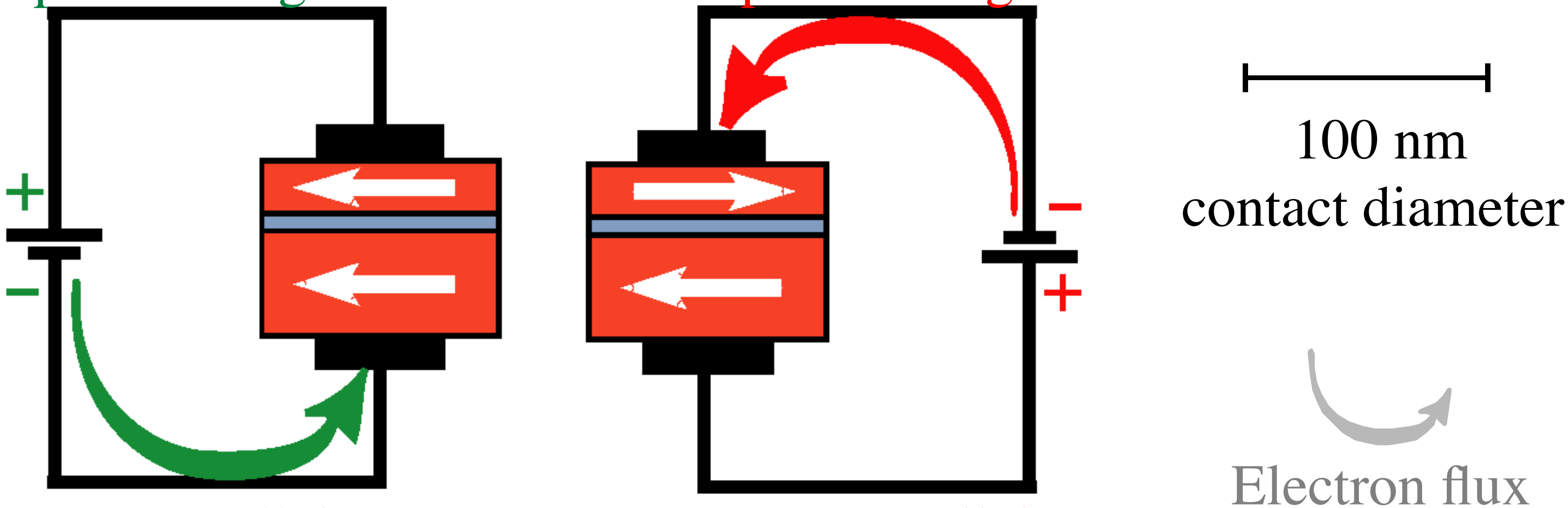

⇒ parallel

⇒ antiparallel

High current densities: $>10^7$ A/cm^2 or several mA per (100 nm)^2

J.C. Slonczewski, J. Magn. Magn. Mater. **159**, L1 (1996); L. Berger, Phys. Rev B **54**, 9353 (1996)
E.B. Myers *et al*., Science **285**, 867 (1999); J.A. Katine *et al*., Phys. Rev. Lett. **84**, 3149 (2000)

Pioneering work by the Cornell group

Columnar structure ("nanopillar") and measurement via GMR effect:

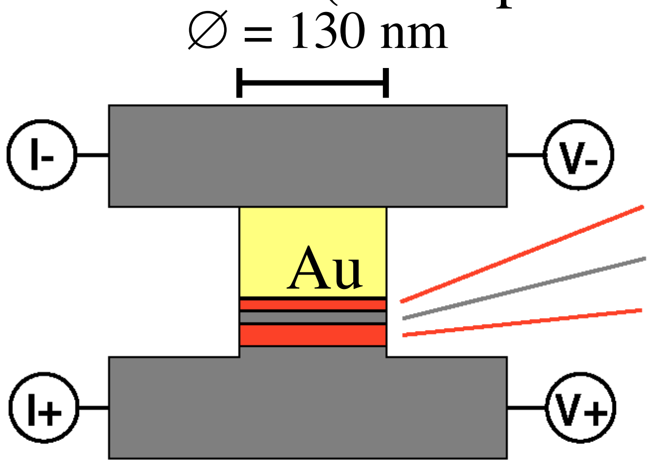

Sputtered, polycrystalline system:

2.5 nm Co: thin, "free" FM layer

6.0 nm Cu: spacer

10.0 nm Co: thick, "fixed" FM layer

low resistive, parallel state for negative current

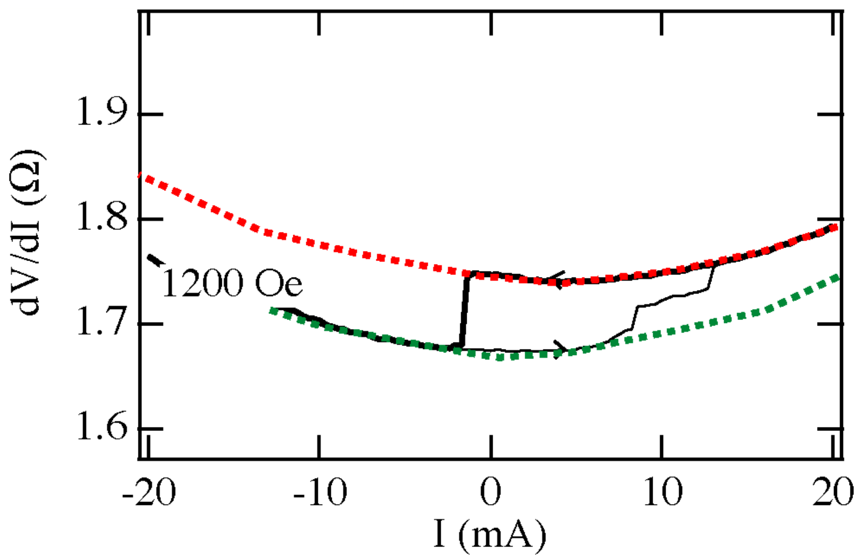

high resistive, antiparallel state for positive current

E.B. Myers *et al*., Science **285**, 867 (1999); J.A. Katine *et al*., Phys. Rev. Lett. **84**, 3149 (2000)

Nanopillars for spin-transfer torque effects

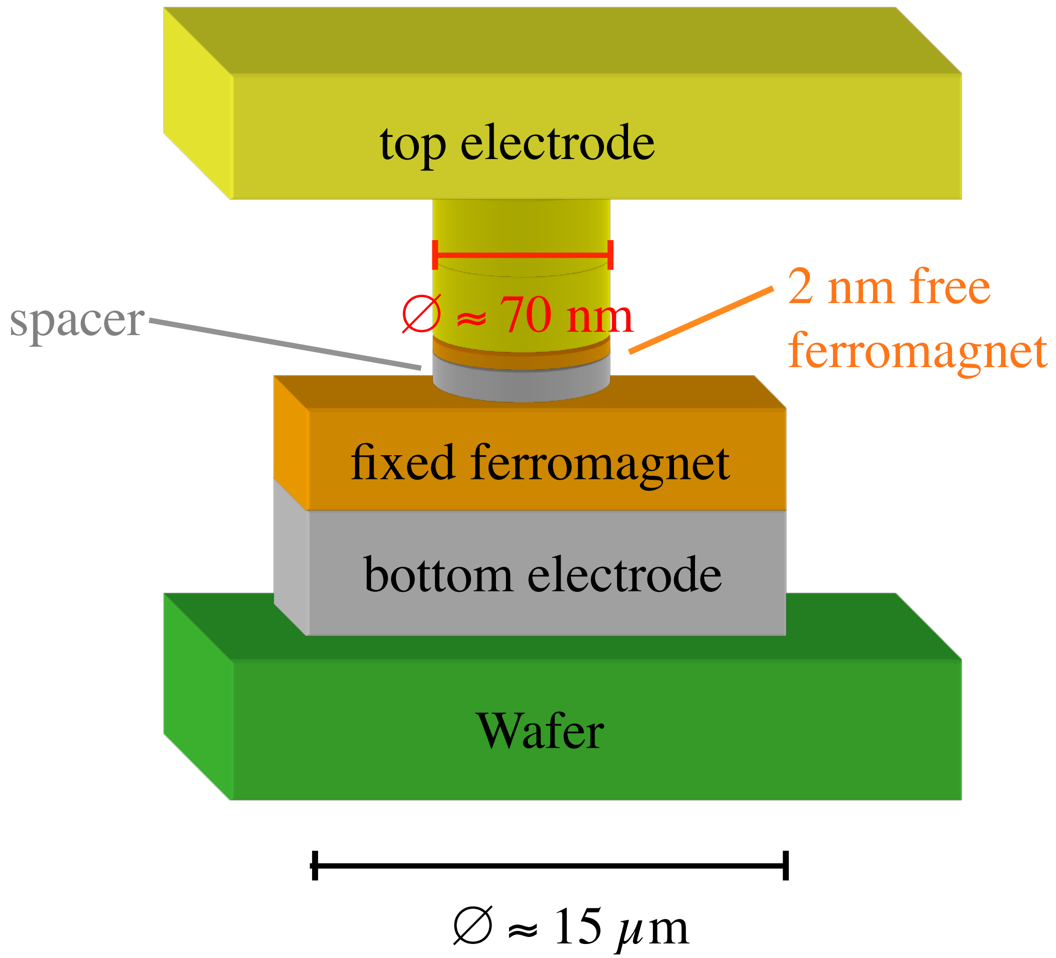

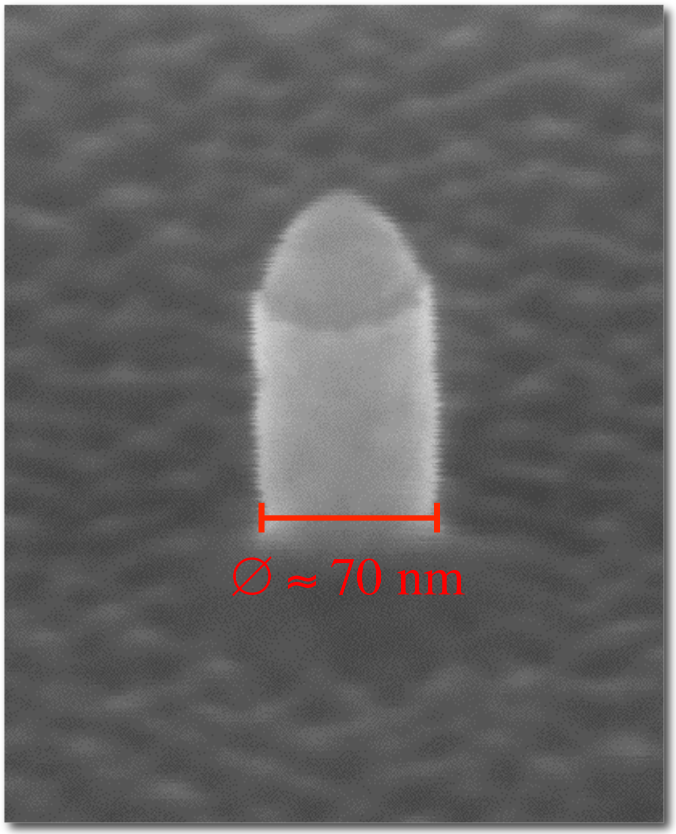

SEM micrograph

R. Lehndorff, D.E. Bürgler *et al.*, Phys. Rev. B **76**, 214420 (2007);
H. Dassow, D.E. Bürgler *et al.*, Appl. Phys. Lett. **89**, 222511 (2006)

Interplay between crystalline anisotropy and STT

2 nm Fe / 6 nm Ag / 20 nm Fe at 5 K; B_{ext} = 7.9 mT along hard axis

Magnetocrystalline anisotropy of Fe(001):

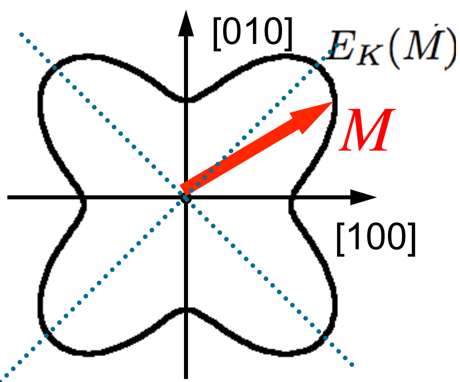

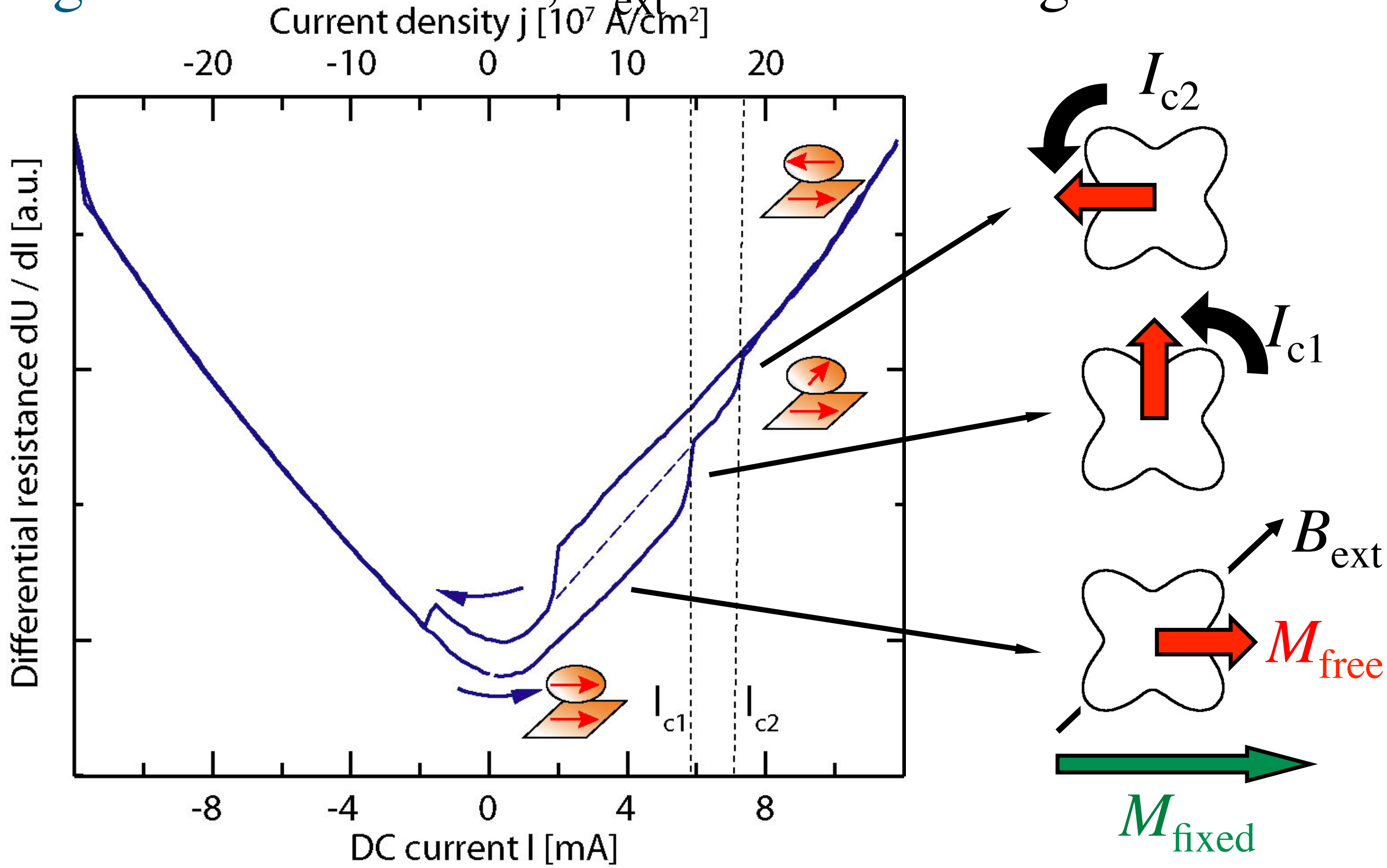

⇒ Precise control of magnetization alignment by current

R. Lehndorff, D.E. Bürgler *et al.*, Phys. Rev. B**76**, 214420 (2007)

Switching by Oersted field of current?

The current ($\approx 10^7$ A/cm^2) gives rise to a circular magnetic field, which favors a vortex-like magnetization state in the small magnetic elements.

BUT:

- The vortex state is symmetric with respect to the current polarity
- The maximum Oersted field at the edge scales like $\alpha I/d$
- The spin-torque transfer (STT) scales *like* $\beta I/d^2$

(current I, contact diameter d)

STT exceeds Oersted field *($\beta I/d^2 > \alpha I/d$)* for d below 1 μm

Contact diameters of several 100 nm …

… are needed to overcome Oersted fields

… provide sufficient current densities for several mA

… are feasible with electron-beam lithography

Switching by Oersted field of current?

The current ($\approx 10^7$ A/cm^2) gives rise to a circular magnetic field, which favors a vortex-like magnetization state in the small magnetic elements.

- The … polarity
  - … l/d

ST … m

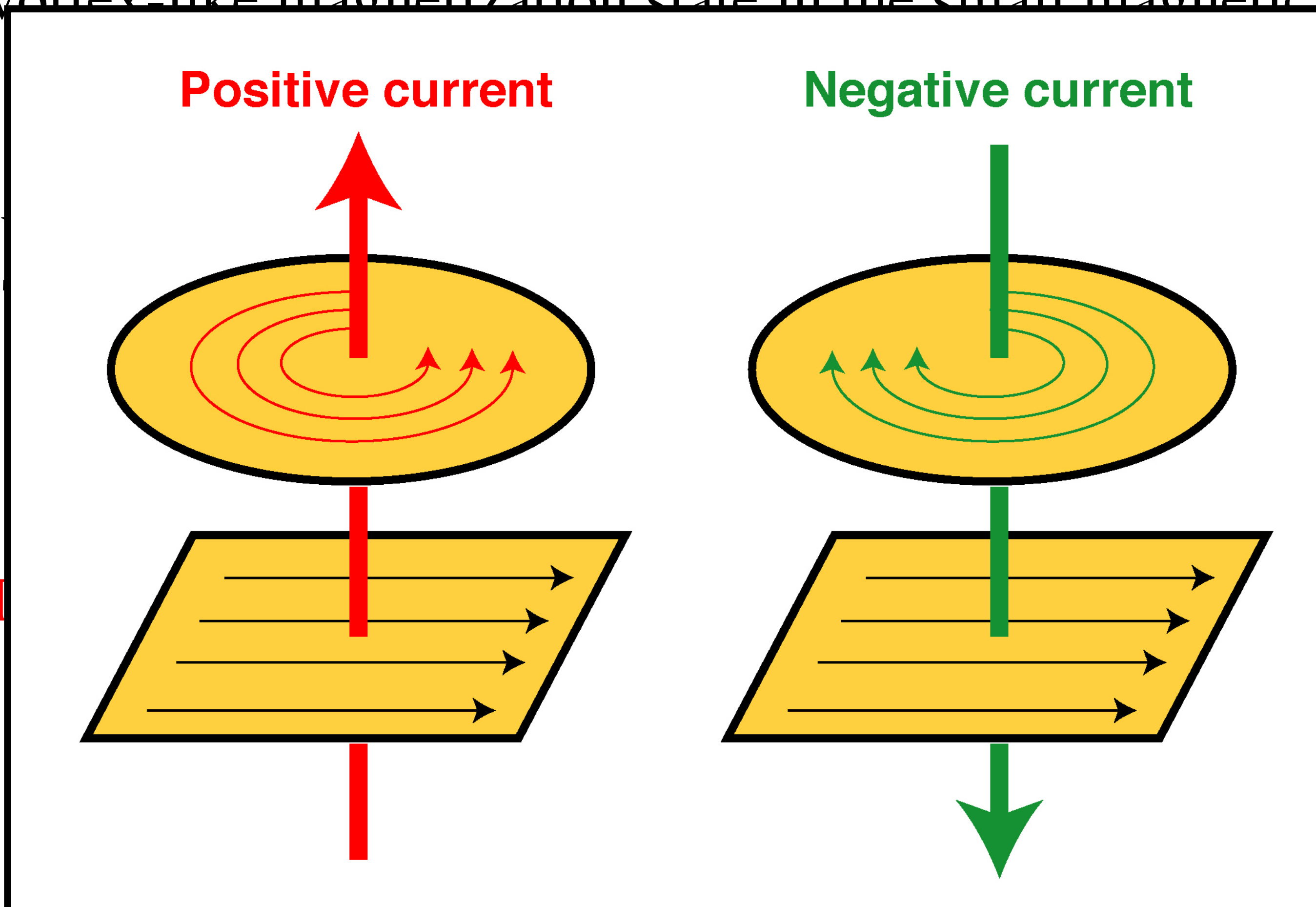

… are feasible with electron-beam lithography

Outline: Current-induced magnetization dynamics

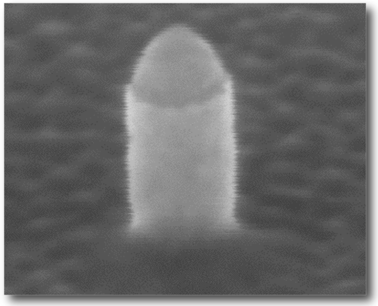

- Need for advanced magnetic switching concept
- Phenomenology of spin-transfer torque (STT)

  "Current-induced magnetization switching"
- Physical picture for STT
- Current-driven magnetization dynamics

  "Extended Landau-Lifshitz-Gilbert equation"

  "Spin-torque oscillators (STO)"
- STT in non-uniform magnetization structures

Absorption of transversal spin component I

Consider a polarized current entering from a non-magnet into a ferromagnet. The spin-split DOS gives rise to spin-dependent transmission and reflection at the interface:

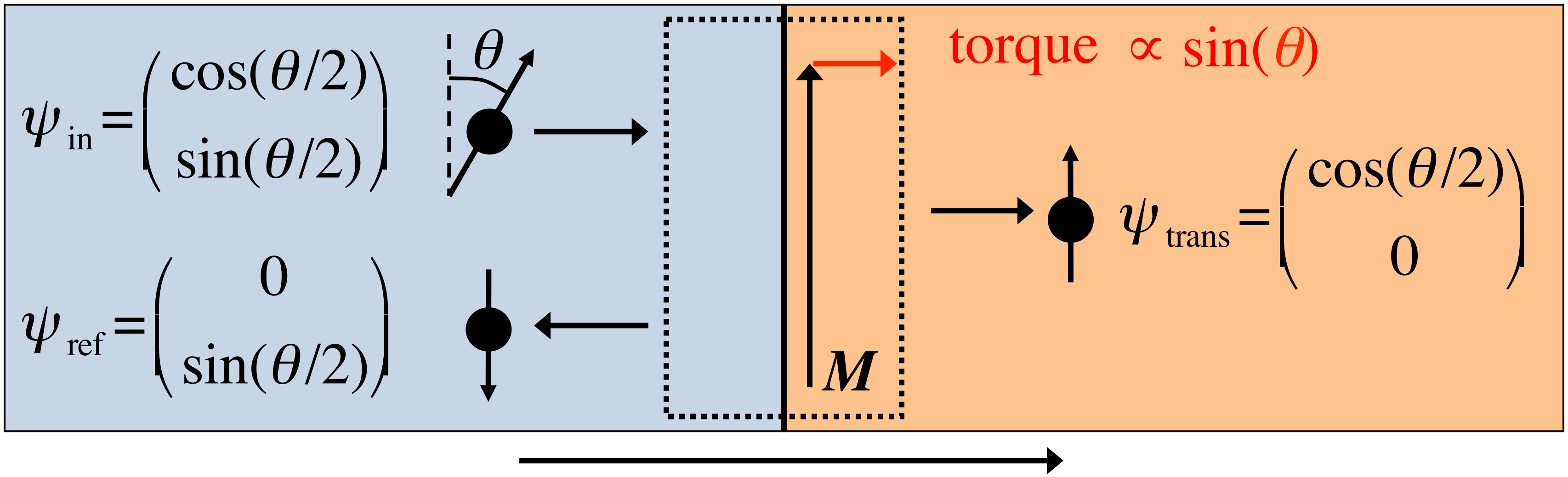

Transversal spin moment is absorbed and acts as a torque on the magnetization $\Rightarrow$ Spin filtering

Spinors for ideal spin filtering, *e.g.* for a half-metallic erromagnet

M. Stiles and A. Zangwill, Phys. Rev B **66**, 014407 (2002)

Absorption of transversal spin component I

Consider a polarized current entering from a non-magnet into a ferromagnet. The spin-split DOS gives rise to spin-dependent transmission and reflection at the interface:

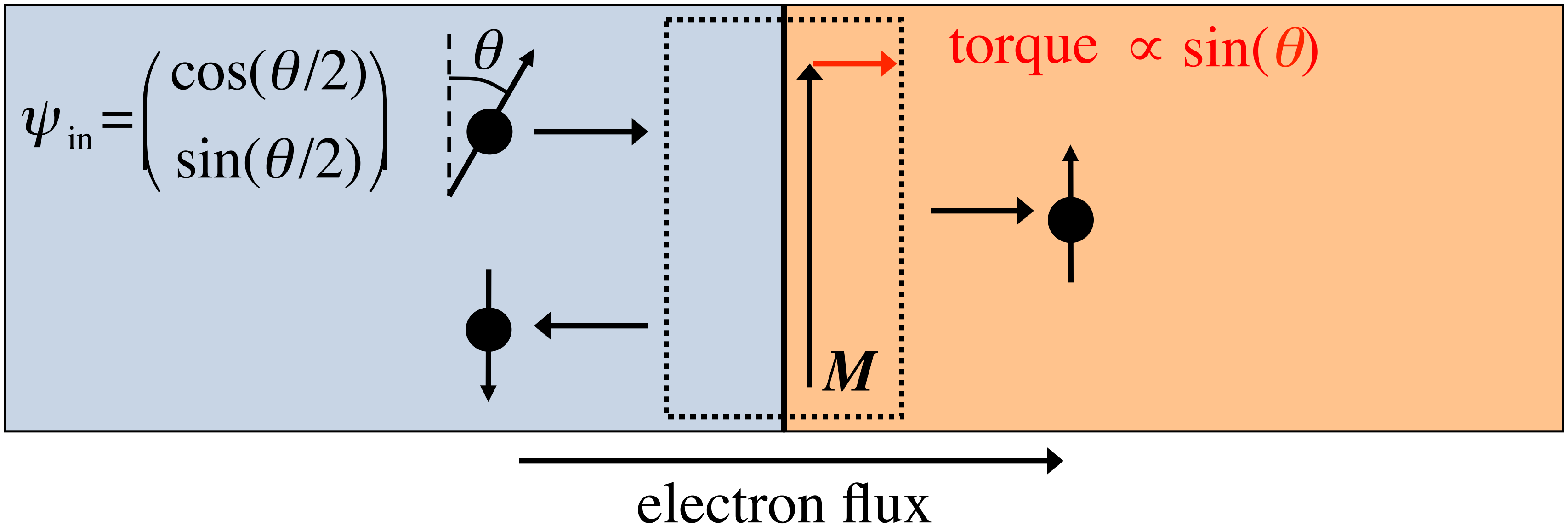

Transversal spin moment is absorbed and acts as a torque on the magnetization $\Rightarrow$ Spin filtering

In realistic cases, spin filtering absorbs about 50% of the transversal spin component. The other 50% are transmitted or reflected.

M. Stiles and A. Zangwill, Phys. Rev B **66**, 014407 (2002)

Absorption of transversal spin component II

Spin-up and spin-down waves of the transmitted electrons have in the ferromagnet different k vectors, $k^{\uparrow}$ and $k^{\downarrow}$.

$\Rightarrow$ Each spin precesses in space and acquires a k-dependent phase ξ

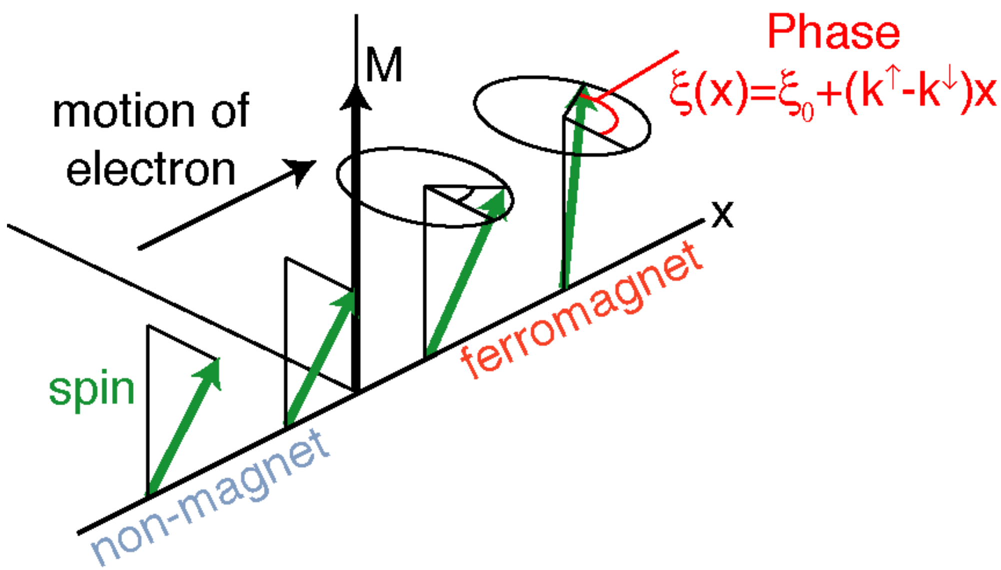

Summing over all k, different ξ reduce the transversal spin component

$\Rightarrow$ Absorption of the transversal spin component due to spatial spin precession in the ferromagnet

M. Stiles and A. Zangwill, Phys. Rev B **66**, 014407 (2002)

Absorption of transversal spin component III

Quantum-mechanically, a reflected or transmitted spin is rotated by some *k*-dependent angle

Summing over all *k*, different rotation angles reduce the transversal spin component

⇒ Absorption of the transversal spin component due to spin rotation of reflected and transmitted electrons

All three effects together
–(i) spin filtering, (ii) spin precession, and (iii) spin rotation–
completely absorb near the interface the transversal spin component of the incident current, which acts as a torque on the magnetization

M. Stiles and A. Zangwill, Phys. Rev B **66**, 014407 (2002)

A second FM layer with tilted magnetization polarizes the incident current. One layer ($\boldsymbol{M}_{free}$) is easier to switch than the other ($\boldsymbol{M}_{fixed}$):

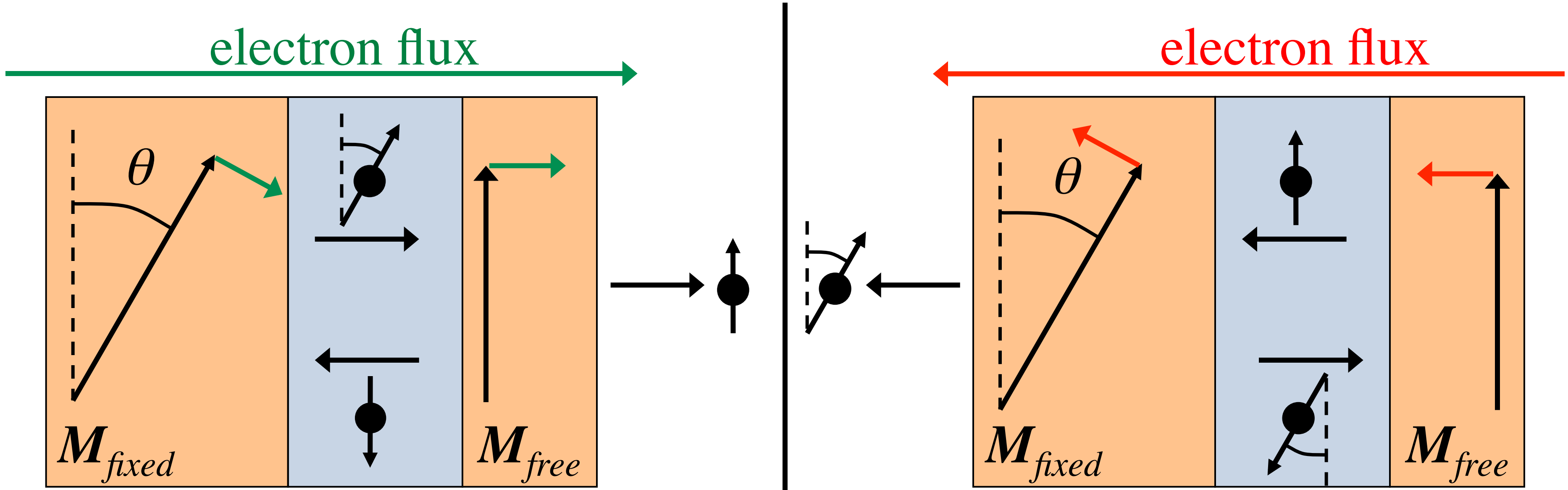

$\boldsymbol{M}_{free}$ rotates towards $\boldsymbol{M}_{fixed}$
⇒ stabilization of
parallel alignment

$\boldsymbol{M}_{free}$ rotates away from $\boldsymbol{M}_{fixed}$
⇒ destabilization of
antiparallel alignment

Note importance of reflected current and asymmetry of FM layers

X. Waintal *et al.*, Phys. Rev. B **62**, 12317 (2000)

Confirmation of picture: Dependence on spacer thickness

Spin-flip scattering in the spacer reduces the spin-torque transfer efficiency g and requires larger critical current densities J_c^+, J_c^-.

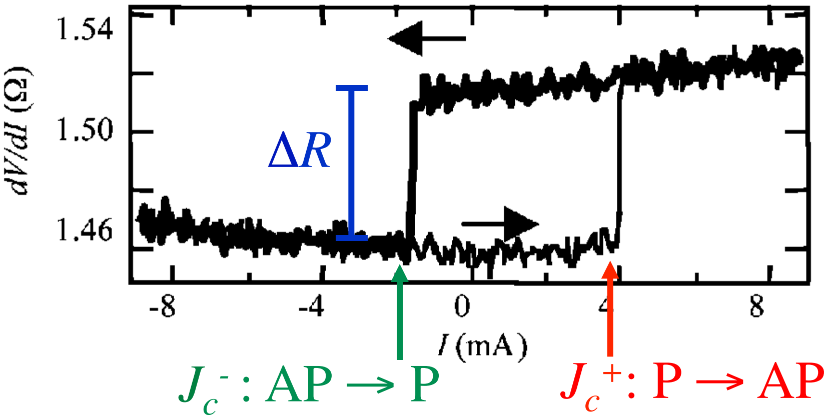

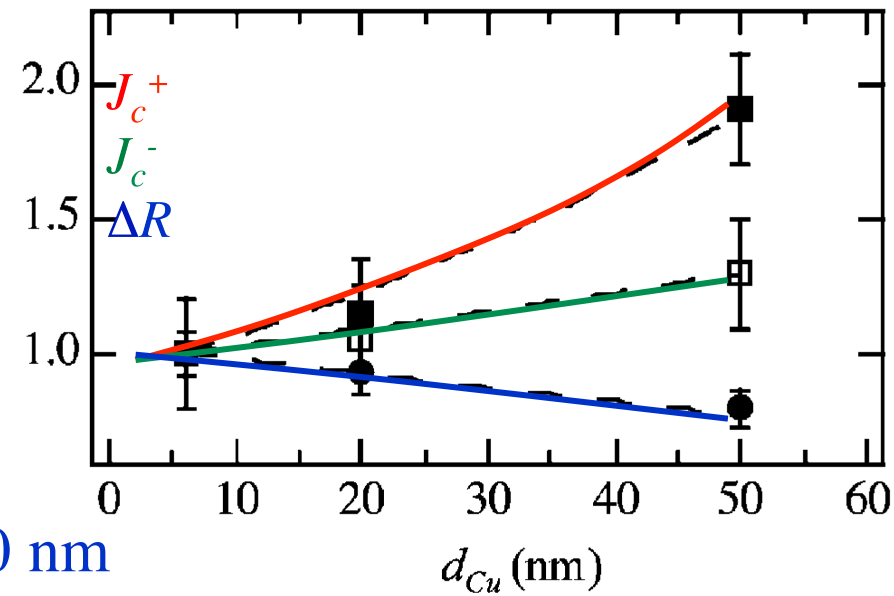

$\Delta R \propto \exp(-d_{Cu}/\lambda)$ $\Rightarrow \lambda = 190 \pm 20$ nm

$J_c^- \propto \exp(d_{Cu}/\lambda)$ $\Rightarrow \lambda = 170 \pm 40$ nm

$J_c^+ \propto \exp(2d_{Cu}/\lambda)$ $\Rightarrow \lambda = 140 \pm 30$ nm (70 ± 20 nm without factor 2)

Reflected electron must cross the spacer layer twice!

F.J. Albert *et al.*, Phys. Rev. Lett. **89**, 226802 (2002)

Confirmation of picture: Dependence on spacer thickness

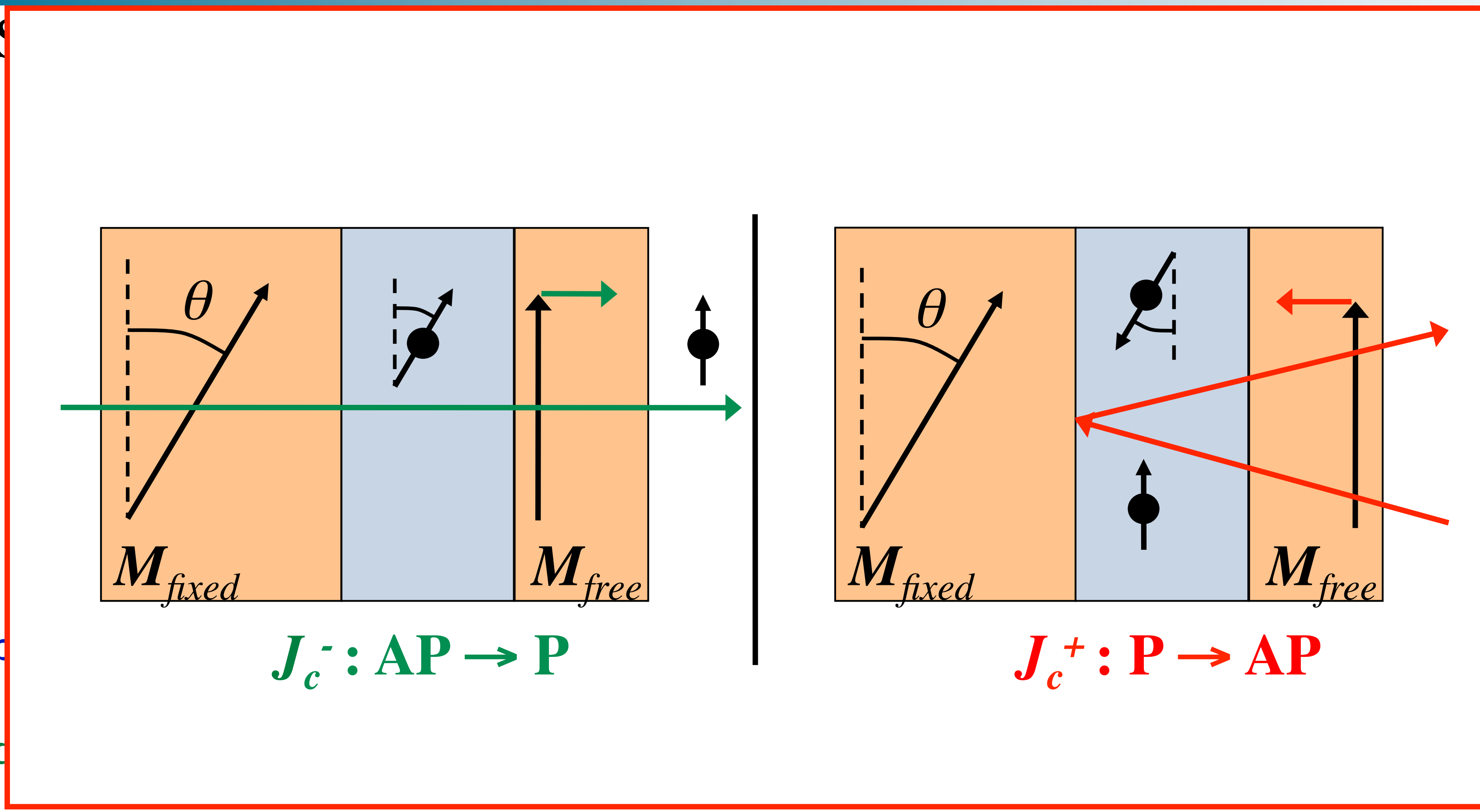

$\Delta R \propto$

$J_c^- \propto$

$J_c^+ \propto \exp(\boxed{2} d_{Cu}/\lambda)$ $\Rightarrow \lambda = 140 \pm 30$ nm (70 ± 20 nm without factor 2)

Reflected electron must cross the spacer layer twice!

F.J. Albert *et al*., Phys. Rev. Lett. **89**, 226802 (2002)

Above consideration is correct for any spin-polarized current:

- Ballistic current due to drift motion in an electric field
- Diffusive current due to spin accumulation δm_z

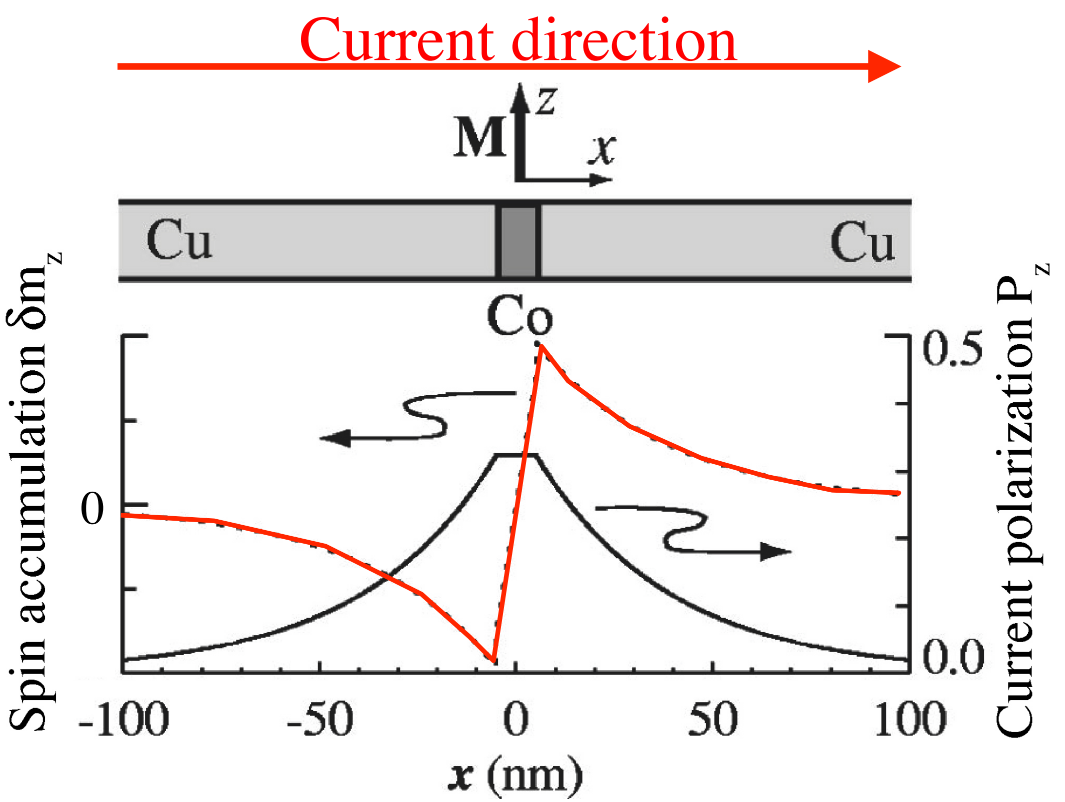

Spin accumulation δm_z decays due to spin-flip scatting over distances given by the spin scatting length λ

$\Rightarrow$ gradient in δm_z

$\Rightarrow$ diffusive spin-polarized current

Outline: Current-induced magnetization dynamics

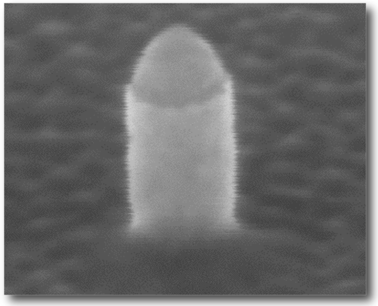

- Need for advanced magnetic switching concept
- Phenomenology of spin-transfer torque (STT)

  "Current-induced magnetization switching"
- Physical picture for STT
- Current-driven magnetization dynamics

  "Extended Landau-Lifshitz-Gilbert equation"

  "Spin-torque oscillators (STO)"
- STT in non-uniform magnetization structures

Landau-Lifshitz-Gilbert (LLG) equation

Landau-Lifshitz-Gilbert equation describes the motion of $\vec{M}$ in $\vec{H}_{\text{eff}}$:

$$\frac{d\vec{M}}{dt} = -\frac{\gamma}{1+\alpha^2}\left[\vec{M}\times\vec{H}_{\text{eff}}\right] - \frac{\alpha\gamma}{M_S\left(1+\alpha^2\right)}\vec{M}\times\left[\vec{M}\times\vec{H}_{\text{eff}}\right] \; ; \; \vec{H}_{\text{eff}} = -\frac{1}{\mu_0}\frac{\delta E_{tot}}{\delta\vec{M}}$$

Precession around $\boldsymbol{H}_{\text{eff}}$
with Larmor frequency
of typically several GHz
($e.g.$ Fe, Co, Ni)
$\Rightarrow \tau \approx 0.1$ ns

Damping towards $\boldsymbol{H}_{\text{eff}}$
with a typically time
constant (for $\alpha = 0.001$)
of several ns

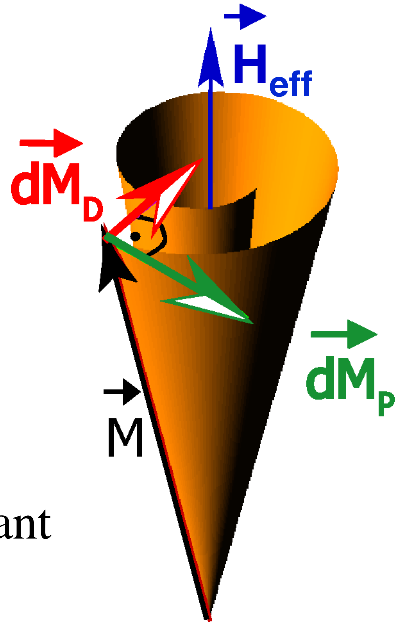

μ_0: permeability of vacuum
α: phenomenological damping constant
γ: gyromagnetic ratio
M: saturation magnetization

L. Landau and E. Lifshitz, Phys. Z. Sowjetunion **8**, 153 (1935)
T. L. Gilbert, PhD thesis (1956); T. L. Gilbert, IEEE Trans. Magn. **40**, 3443 (2004)

Extended Landau-Lifshitz equation

The spin-transfer torque can be written as:

$$\frac{d\vec{M}_{\text{free}}}{dt} = \frac{I}{A} \cdot g(\theta) \cdot \vec{M}_{\text{free}} \times \left[\vec{m}_{\text{free}} \times \vec{m}_{\text{fixed}}\right] \; ; \quad \vec{m}_{\text{free,fixed}} = \frac{\vec{M}_{\text{free,fixed}}}{M_S}$$

$g(\theta)$ is the material-dependent efficiency of the spin-transfer effects

J.C. Slonczewski, J. Magn. Magn. Mater. **159**, L1 (1996)

Compare to LLG damping term:

$$\frac{d\vec{M}}{dt} = -\frac{\alpha\gamma}{M_S\left(1+\alpha^2\right)} \vec{M} \times \left[\vec{M} \times \vec{H}_{\text{eff}}\right]$$

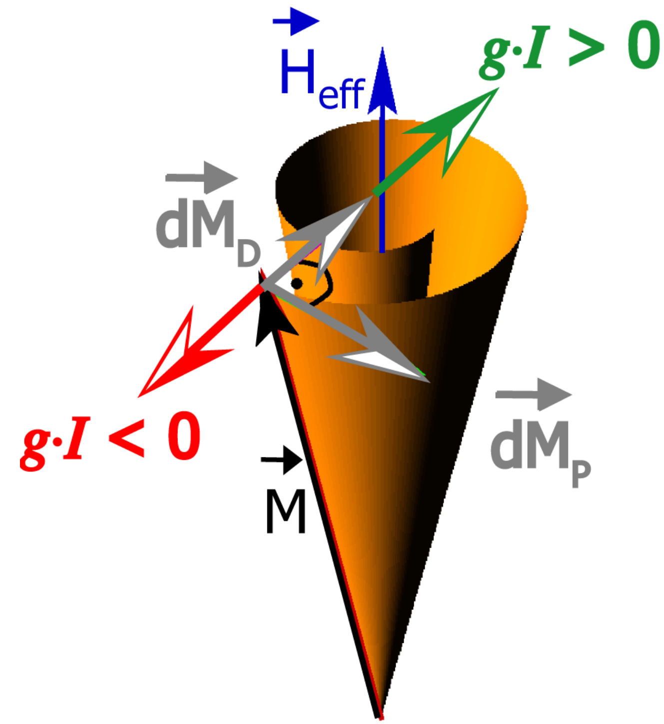

Spin-transfer torque

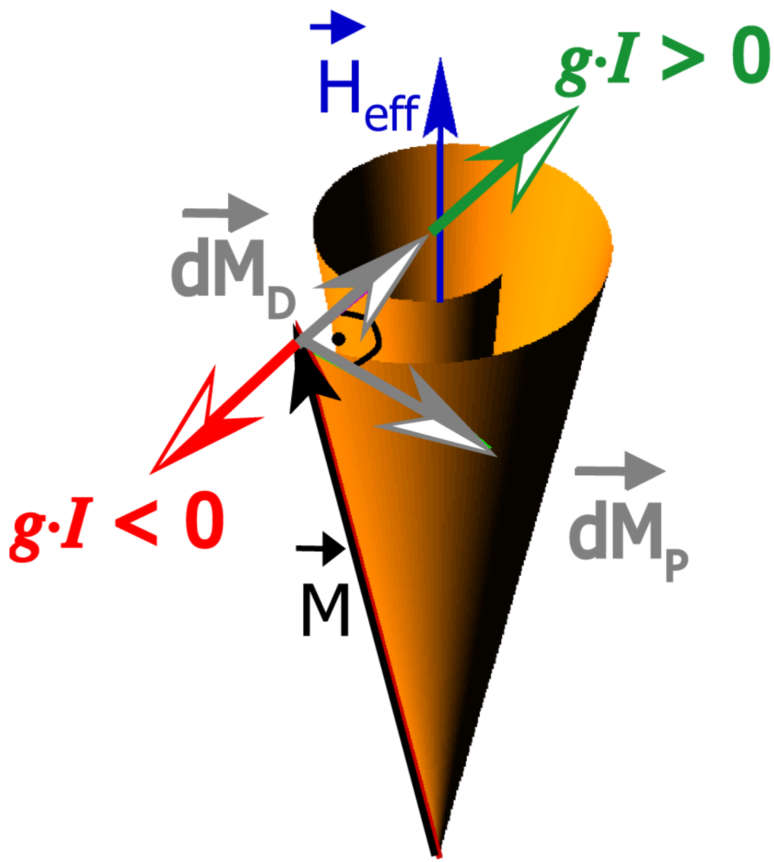

Depending on the polarity of *I* and *sign(g)*, the spin-transfer torque increases or compensates the intrinsic damping.

Microwave oscillations driven by spin-polarized currents

Spin-transfer torque can excite oscillatory motions of $\boldsymbol{M}_{free}$ with frequencies of several GHz.
$\Rightarrow$ GHz voltage signal due to GMR

$\Rightarrow$ dc currents in magnetic nanostructures give rise to microwave signals

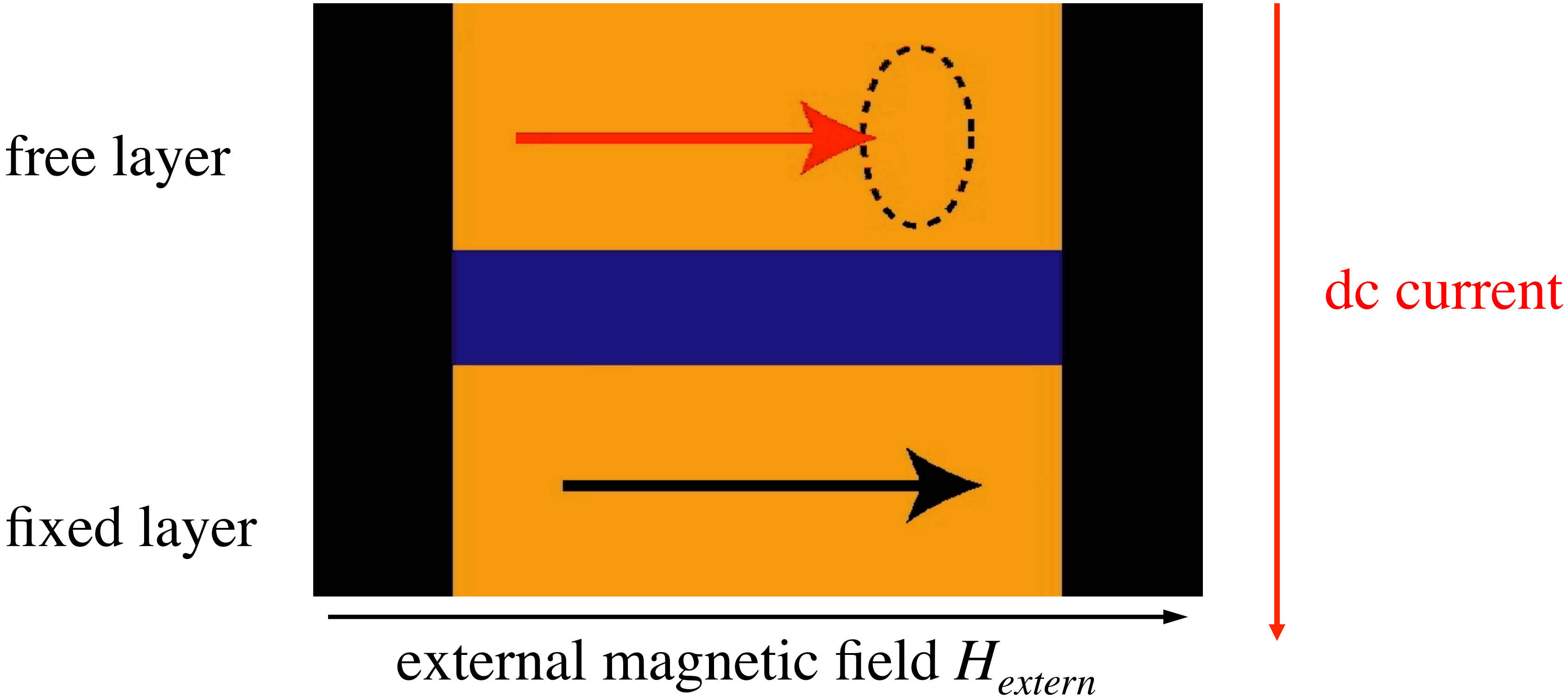

Microwave oscillations driven by spin-polarized currents

Spin-transfer torque can excite oscillatory motions of $\boldsymbol{M}_{free}$ with frequencies of several GHz.

⇒ dc curre wave signals

free laye

c current

fixed lay

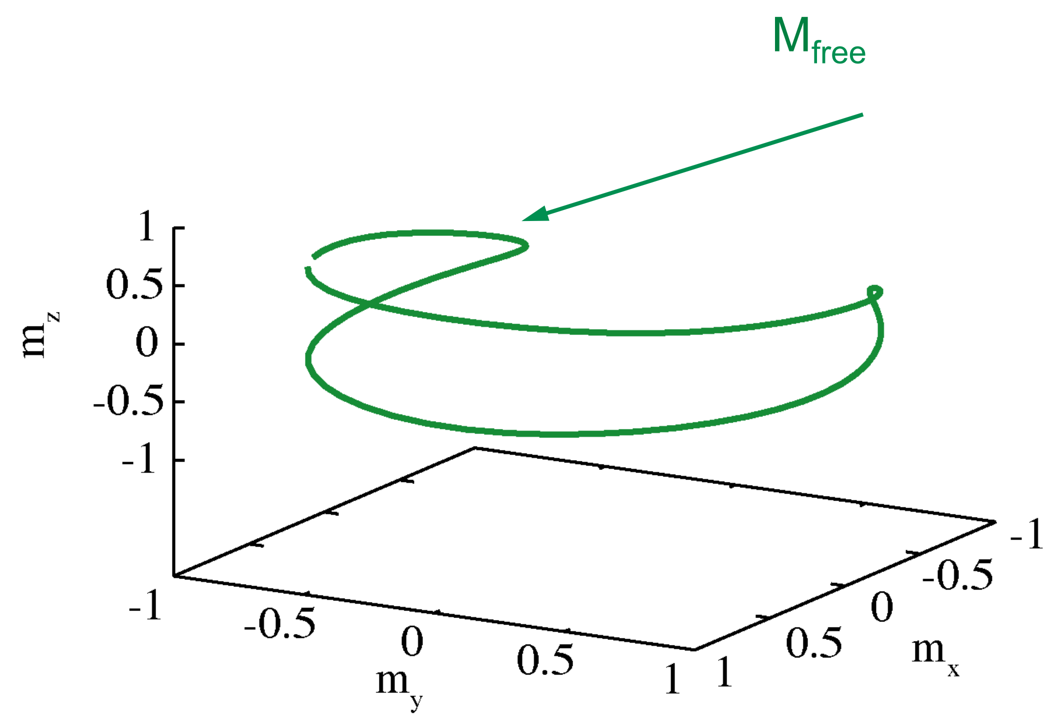

Novel magnetization dynamics
not accessible with magnetic fields!

external magnetic field H_{extern}

Wiring diagram for HF measurements

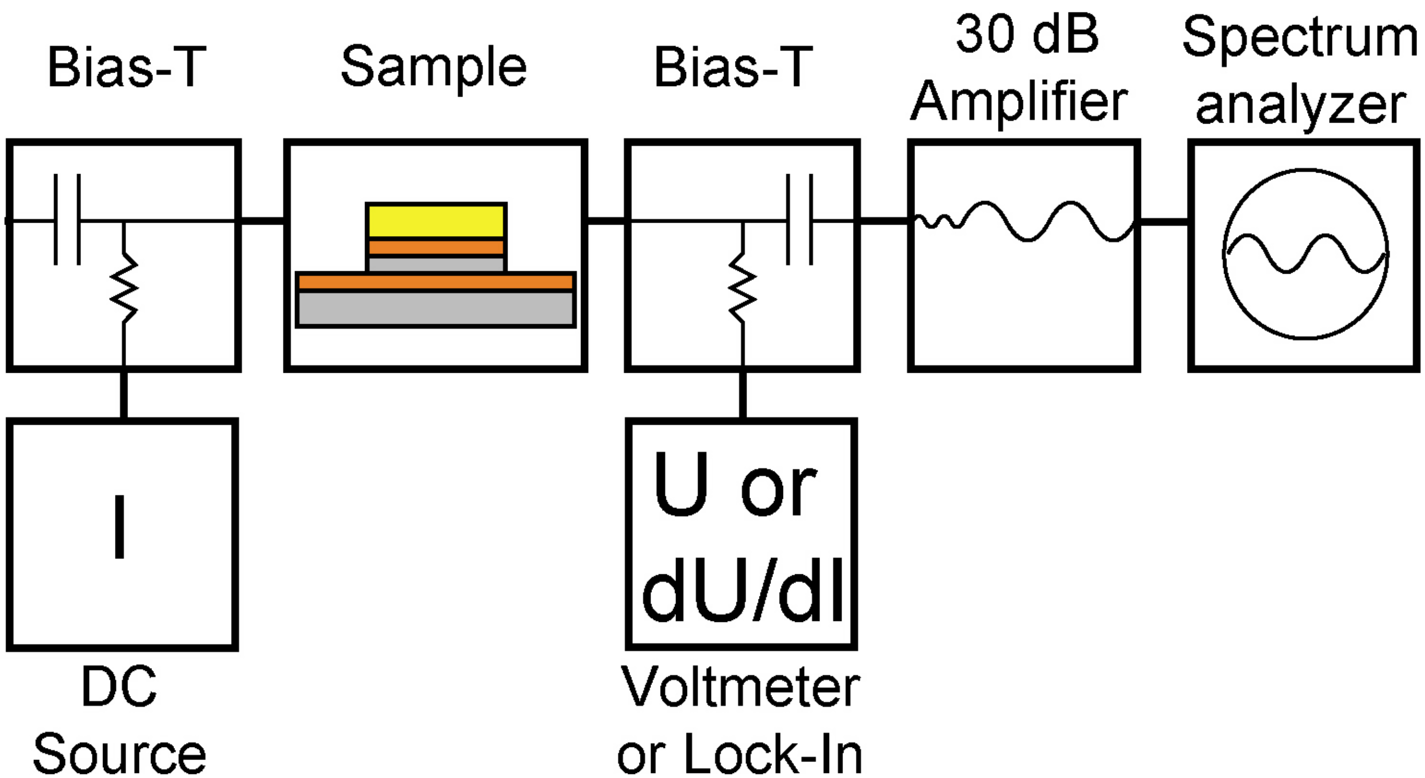

Setup similar to Kiselev *et al*., Nature **425**, 380 (2003)

Pioneering work by the Cornell group

First observation of current-driven magnetization dynamics

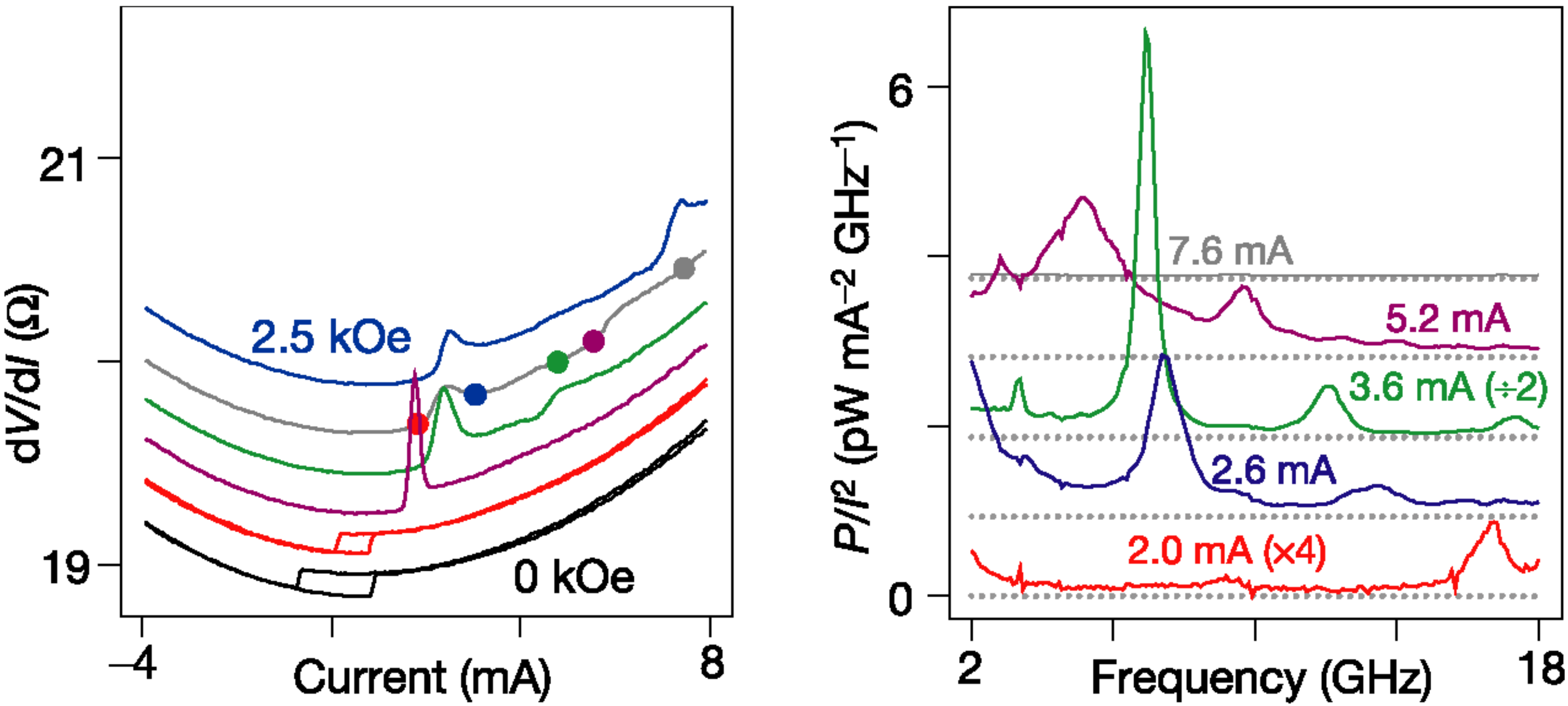

S.I. Kiselev *et al.*, Nature **425**, 380 (2003)

JARA|FIT

JÜLICH FORSCHUNGSZENTRUM

Current-driven magnetization dynamics: Macrospin model

Oscillatory motion of $\boldsymbol{M_{free}}$ and the *H-I* phase diagram can qualitatively be understood by applying the extended LLG to a macrospin:

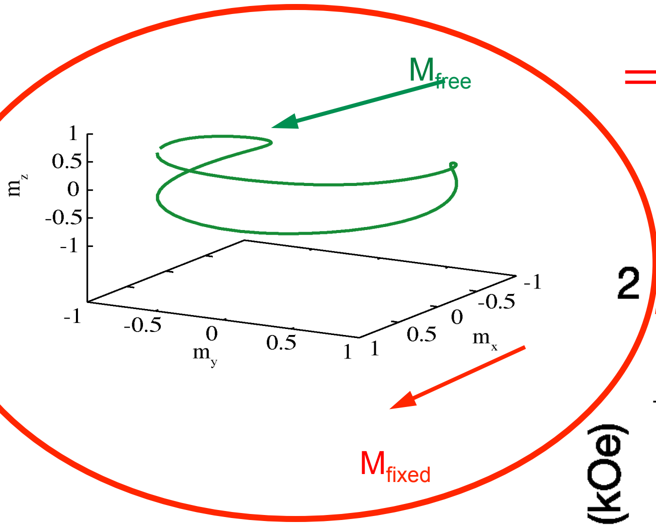

$\Rightarrow$ much larger "precession angles" than in FMR

$\Rightarrow$ new type of magnetization dynamics

R. Lehndorff, D.E. Bürgler *et al.*, IEEE Trans. Magn. **44**, 1951 (2008)

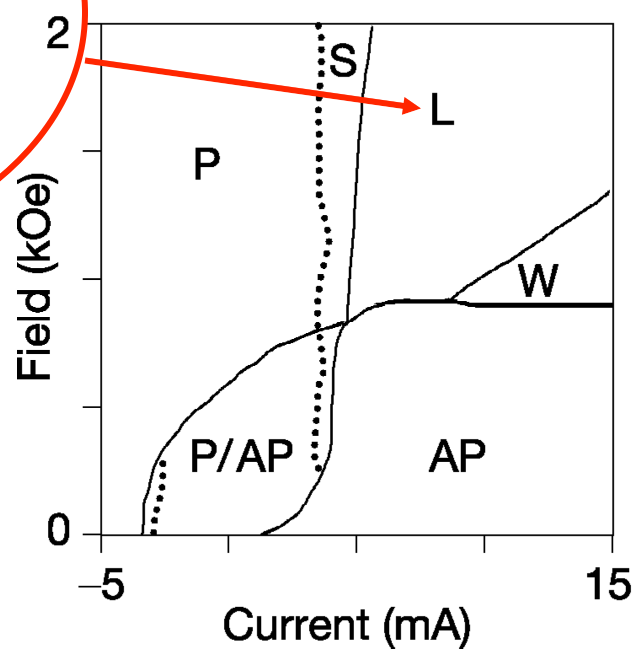

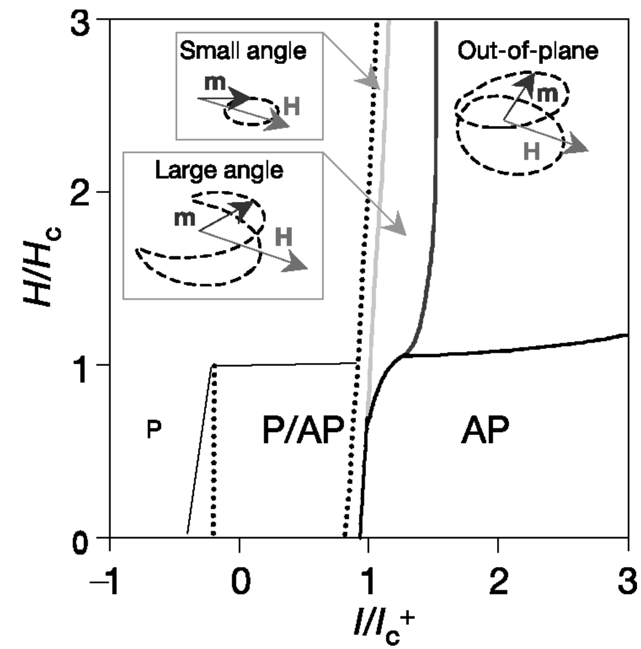

S.I. Kiselev *et al.*, Nature **425**, 380 (2003)

FEM micromagnetic simulation

2 nm-thick Fe nanomagnet with ∅ 150 nm

50 mT external field along Fe(110), $\alpha = 0.02$

5×10^7 A/cm^2, 30% spin-polarization

t = 0 ns | t = 5.4 ns | t = 8.3 ns

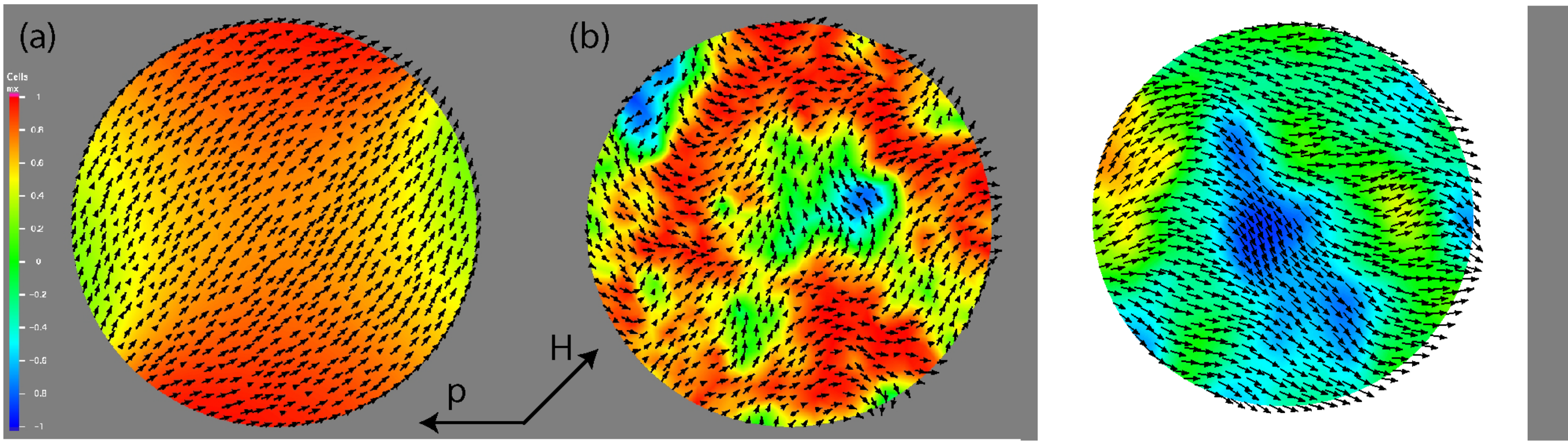

⇒ Very inhomogeneous magnetization structures

⇒ Different from what we know from field-induced dynamics

R. Hertel *et al*., Forschungszentrum Jülich;

K.-J. Lee *et al*., Nature Materials **3**, 877 (2004)

FEM micromagnetic simulation

Time evolution of spatially averaged magnetization components

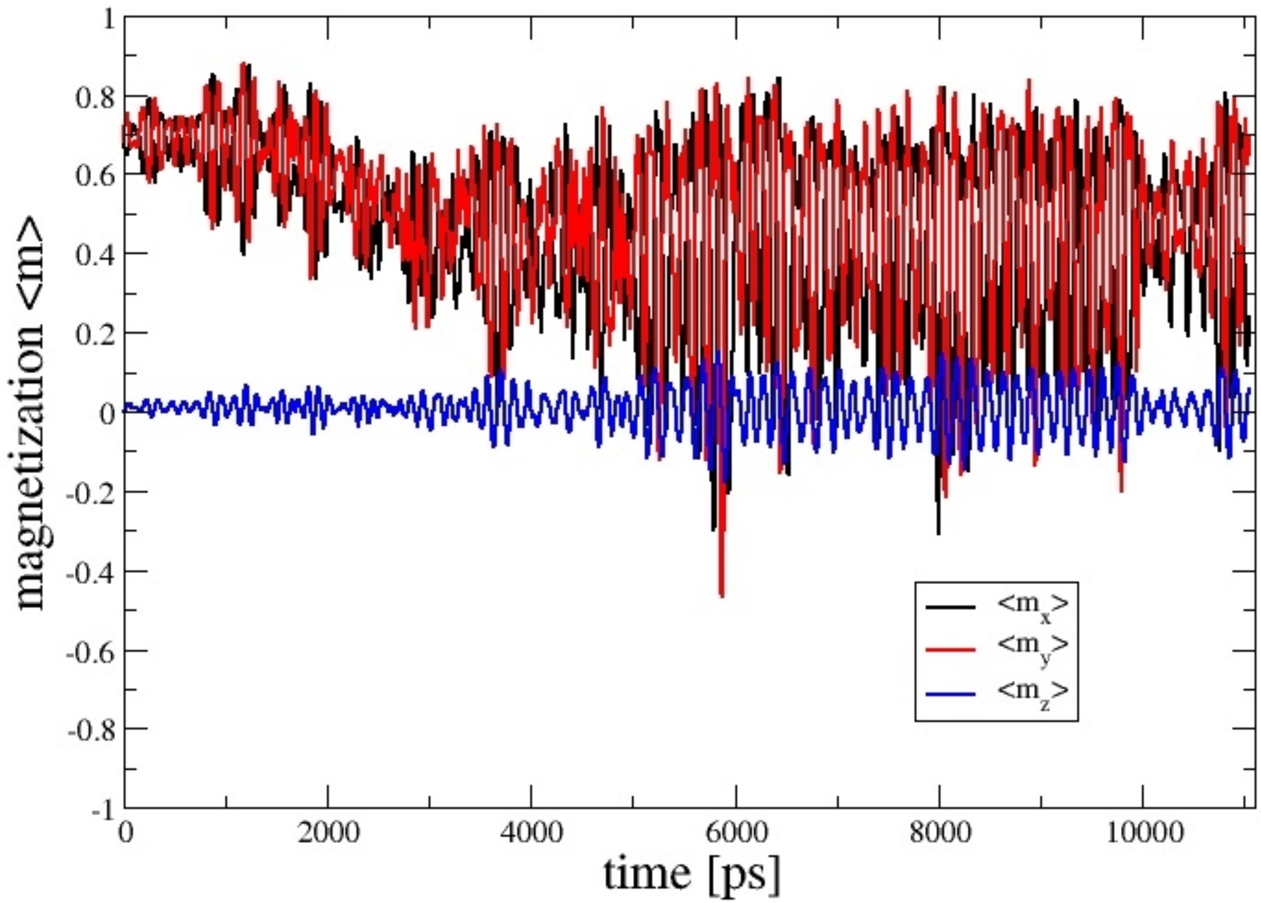

⇒ Oscillations with strongly varying amplitude

Fourier transform of spatially averaged components

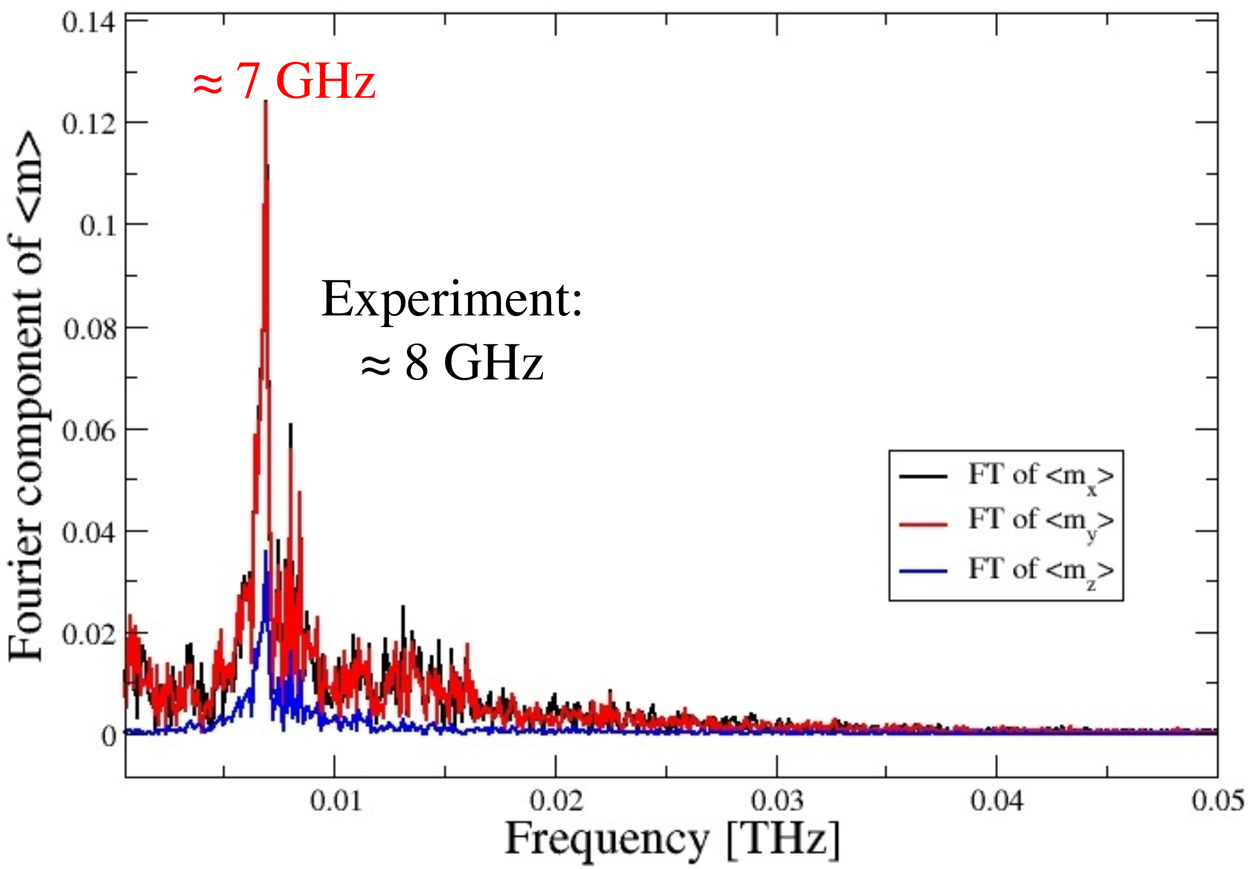

Fe nanomagnet:
2 nm-thick, ∅ 150 nm
50 mT along Fe(110)
$5\text{x}10^7\,\text{A/cm}^2$, $P = 30\%$
$\alpha = 0.02$

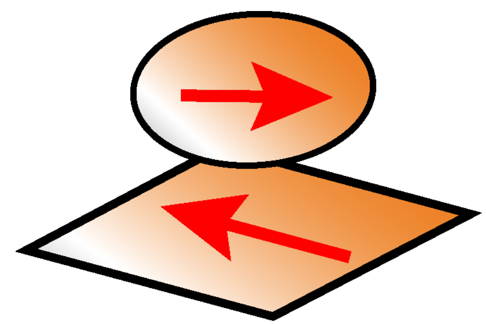

⇒ Clearly visible peaks in Fourier spectrum

Spin-torque oscillator (STO)

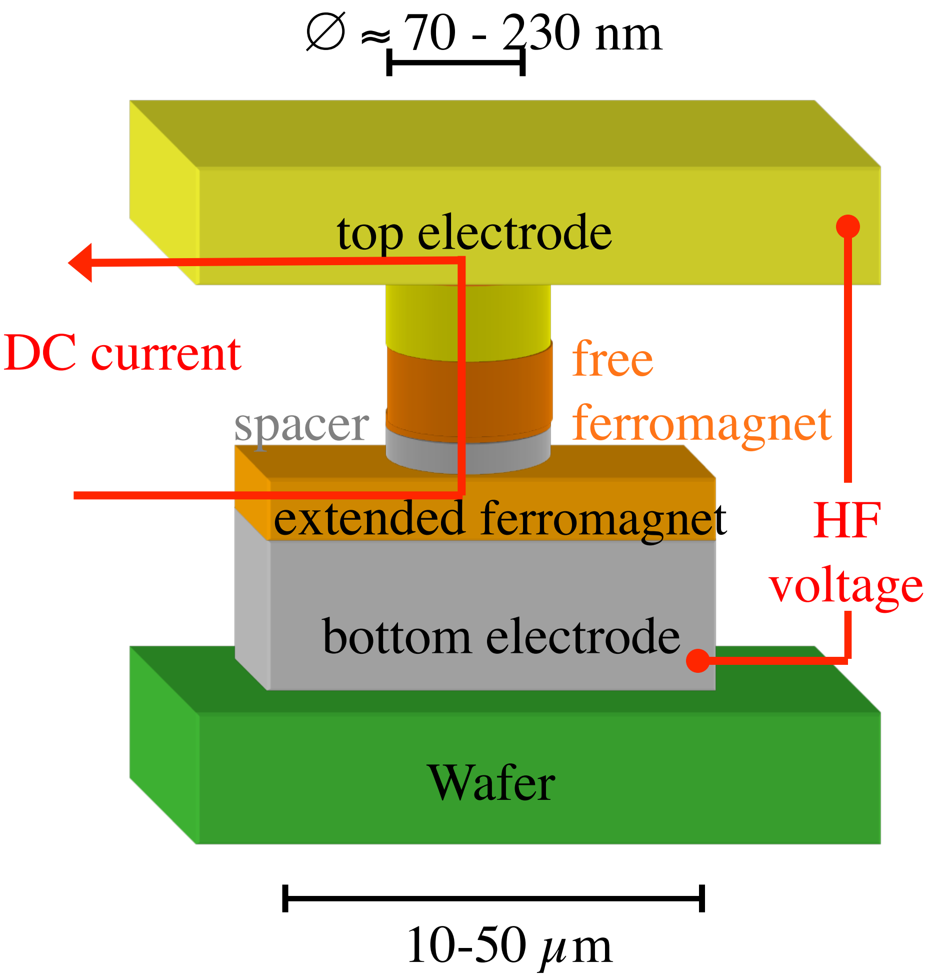

Excitation of free ferromagnet due to spin-transfer torque

Spin-torque oscillators (STO) as microwave sources:

- solid-state realization
- nano-scale
- tunable by field and current
- RT operation
- envisaged for applications in
- communication and
  quantum information technology

BUT: Output power needs to be significantly increased:

- Optimizing STOs properties
- Synchronization of many STOs

Synchronization of several pillars to increase output power

IDEA:

Create an array of coupled and thus coherently oscillating STNOs:
N oscillators produce up to N^2-fold output power
due to coherency

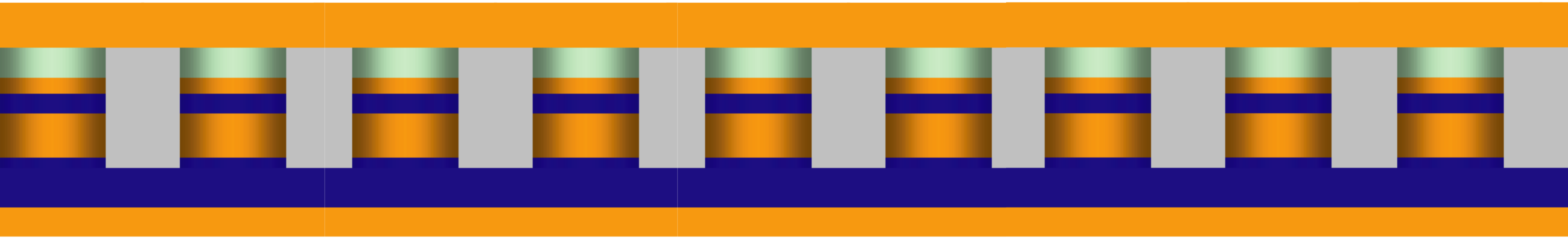

Coupling via
- magnetic interaction (spin-waves) in common magnetic layer
S. Kaka *et al*., Nature **437**, 389 (2005)
F.B. Mancoff *et al*., Nature **437**, 393 (2005)
- electric interaction (microwaves) in common electrodes
-J. Grollier *et al*., Phys. Rev. B **73**, 060409 (2006)

Wiring diagram for injection locking

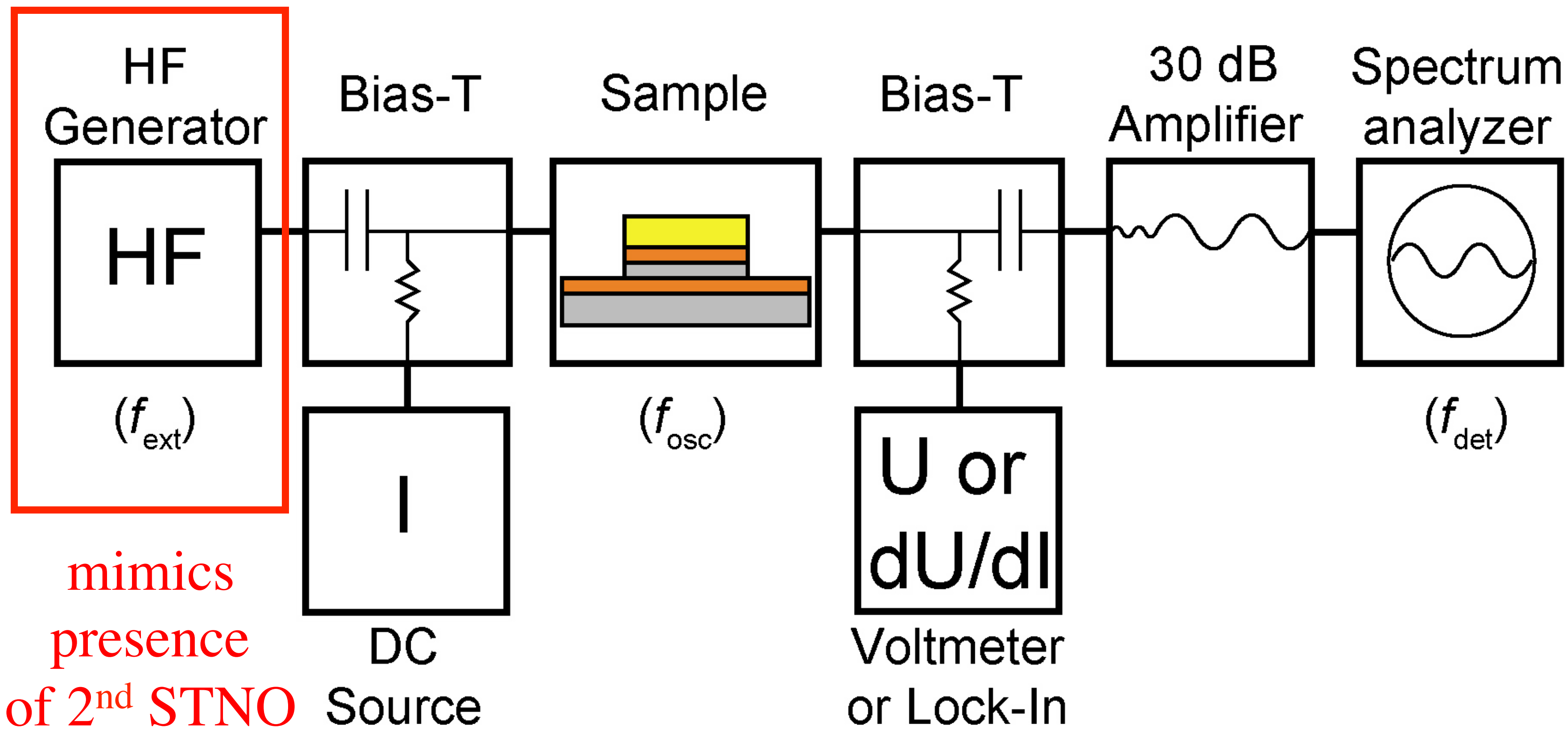

Phase-locking of gyrotropic motion to external HF signal

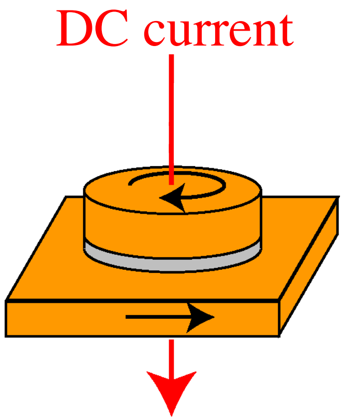

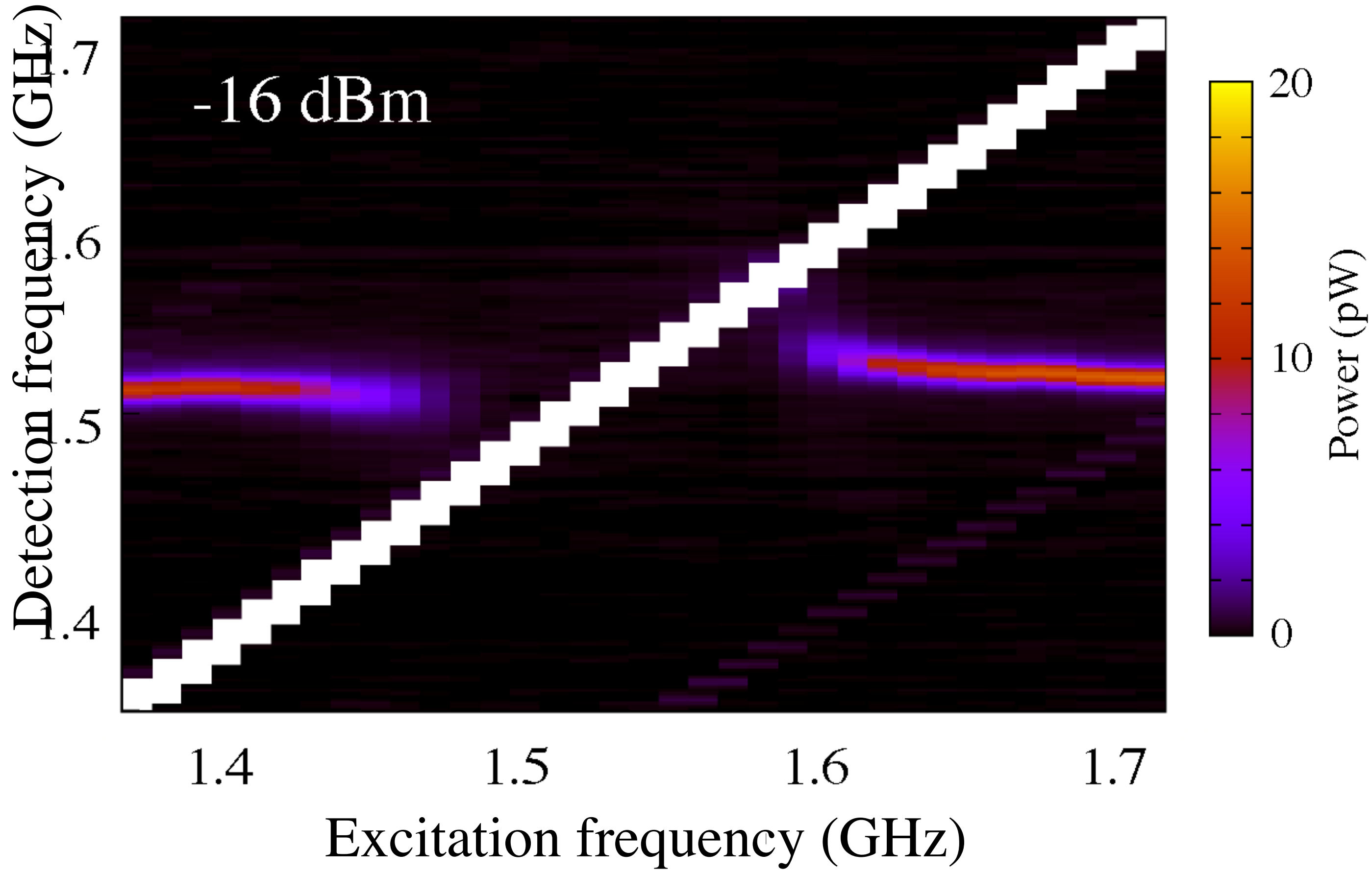

Vortex STNO phase-locks to the externally applied HF signal in a rather large frequency range of about 100 MHz

R. Lehndorff, D.E. Bürgler *et al.*, Appl. Phys. Lett. **97**, 142505 (2010)

Frequency versus external HF amplitude

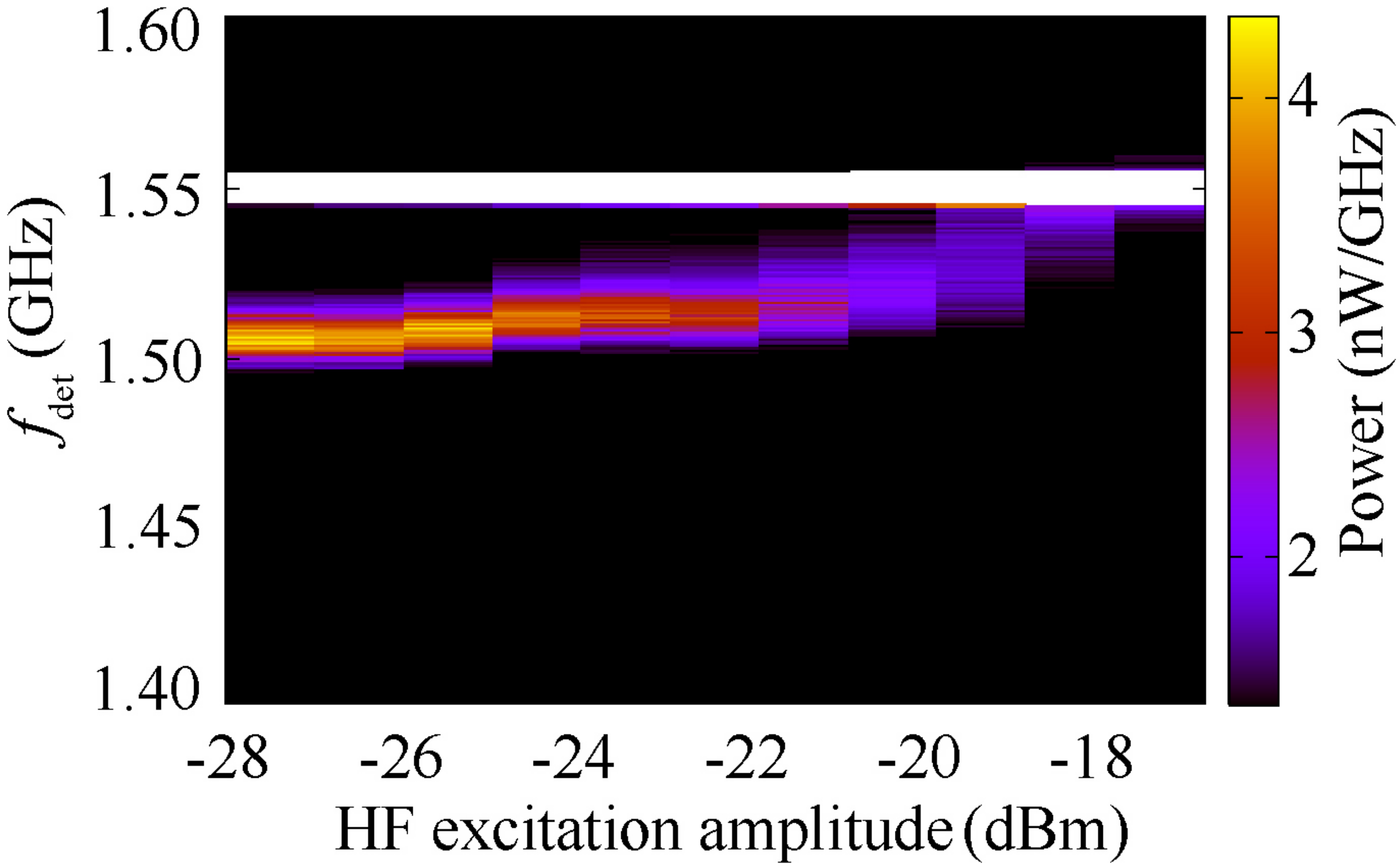

Estimated HF power emitted from STNO: 0.4 nW

Estimated external HF power required for phase-locking: 1.3 μW

R. Lehndorff, D.E. Bürgler *et al*., Appl. Phys. Lett. **97**, 142505 (2010)

JARA|FIT

JÜLICH FORSCHUNGSZENTRUM

HF output power scales with (MR-ratio)^2

$\Rightarrow$ Use TMR instead of GMR

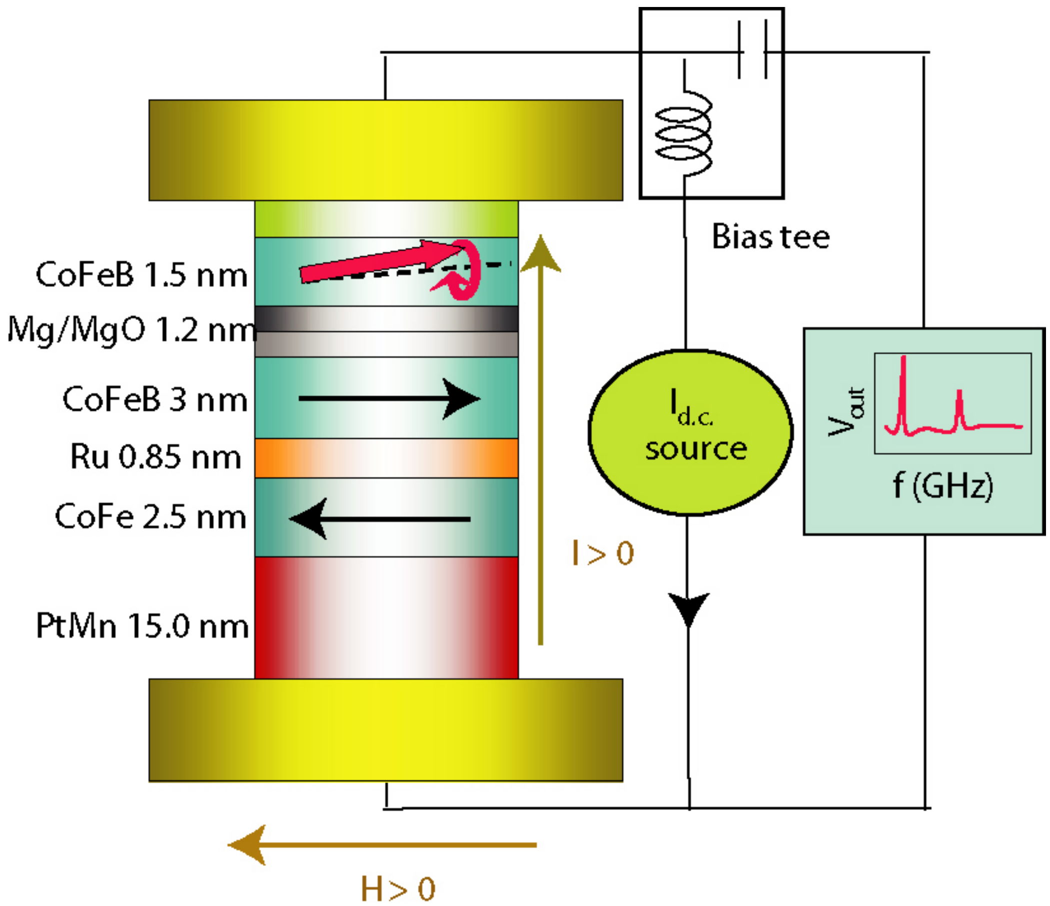

- Elliptical cross-section 160 nm x 70 nm
- $RA = 4\ \Omega\mu\mathrm{m}^2$

A.M. Deac *et al*., Nature Physics **4**, 803 (2008)

TMR-based spin-torque nano-oscillator

Field-induced switching:

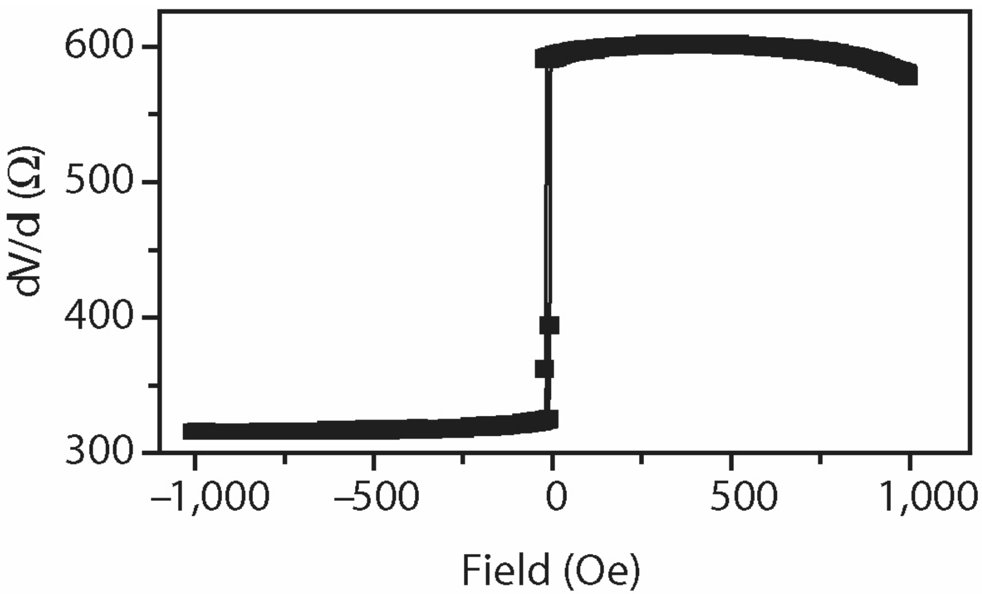

STT-induced switching:

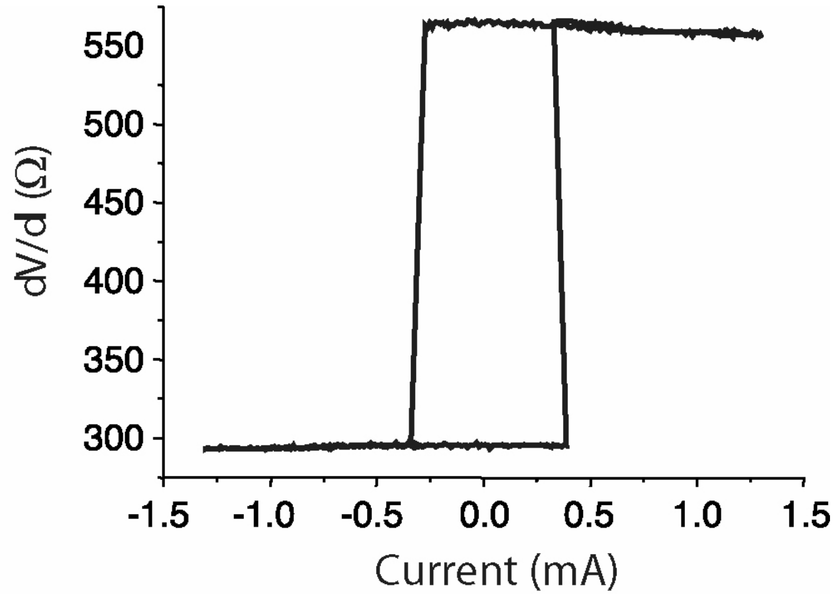

- 110% TMR ratio

- Critical current density: 3×10^6 A/cm^2

A.M. Deac *et al*., Nature Physics **4**, 803 (2008)

TMR-based spin-torque nano-oscillator

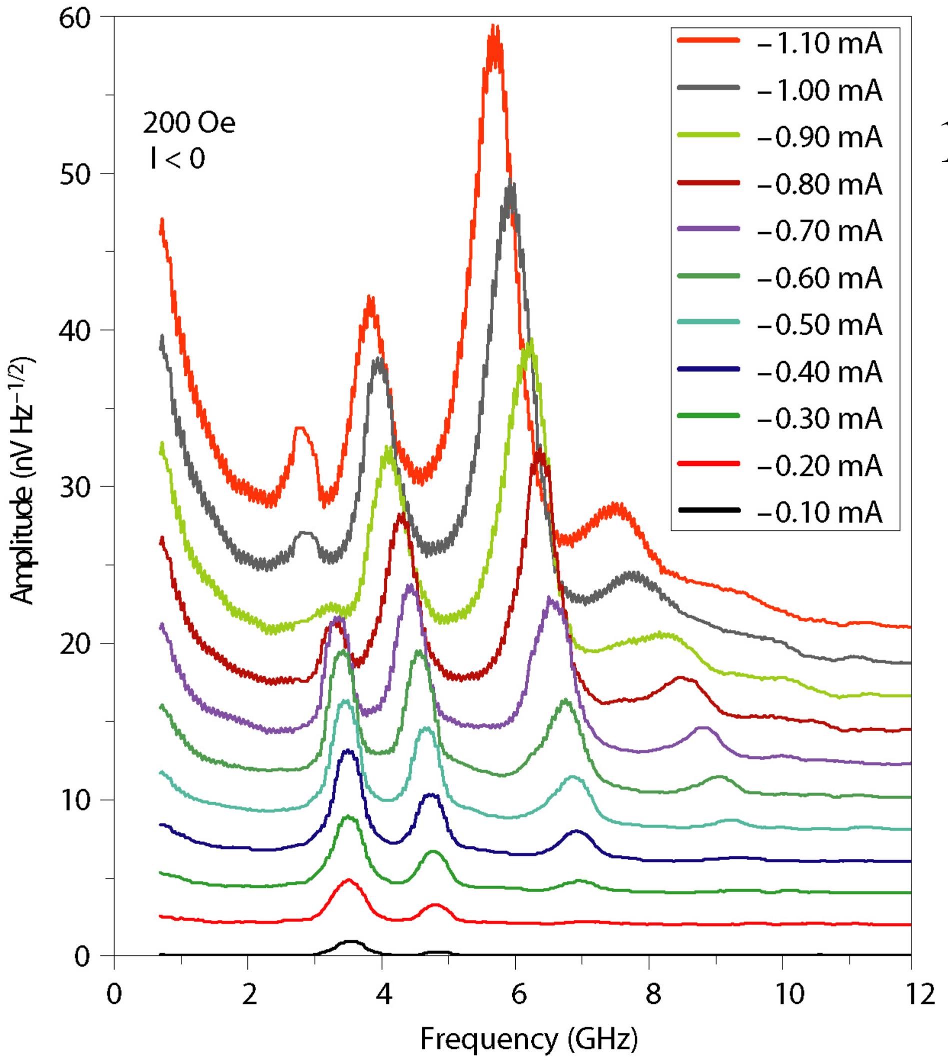

- Different peaks correspond to 1st and 2nd order of modes at the center and at the "tips" of the elliptical magnetic element

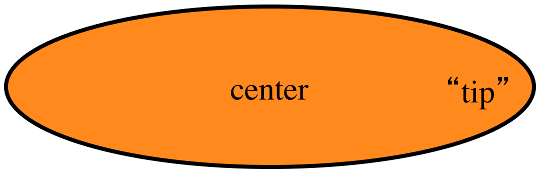

- Maximum output power: 0.48 μW (although a significant fraction is lost due to poor impedance matching)

A.M. Deac *et al*., Nature Physics **4**, 803 (2008)

Outline: Current-induced magnetization dynamics

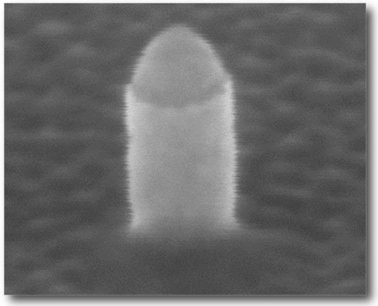

- Need for advanced magnetic switching concept
- Phenomenology of spin-transfer torque (STT)

  "Current-induced magnetization switching"
- Physical picture for STT
- Current-driven magnetization dynamics

  "Extended Landau-Lifshitz-Gilbert equation"

  "Spin-torque oscillators (STO)"
- STT in non-uniform magnetization structures

Current-driven domain wall motion

Domain walls are intrinsically non-uniform magnetization structures

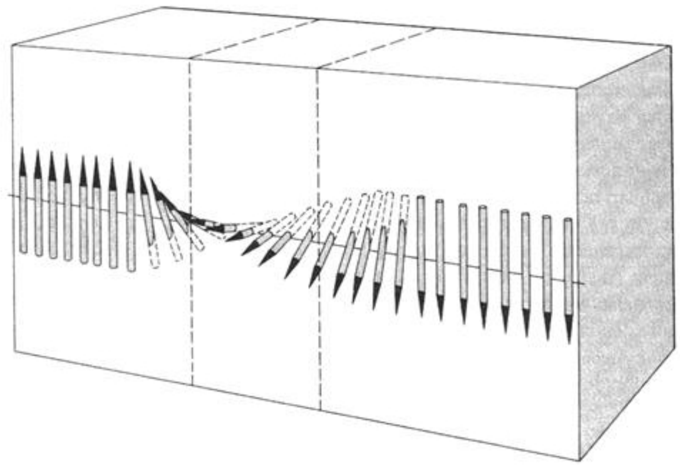

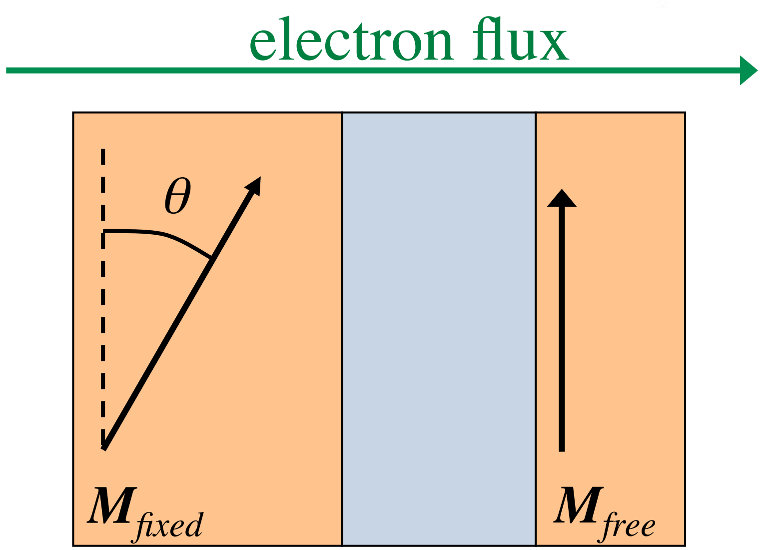

Current-driven domain wall motion

MFM observation of current-induced domain wall motion

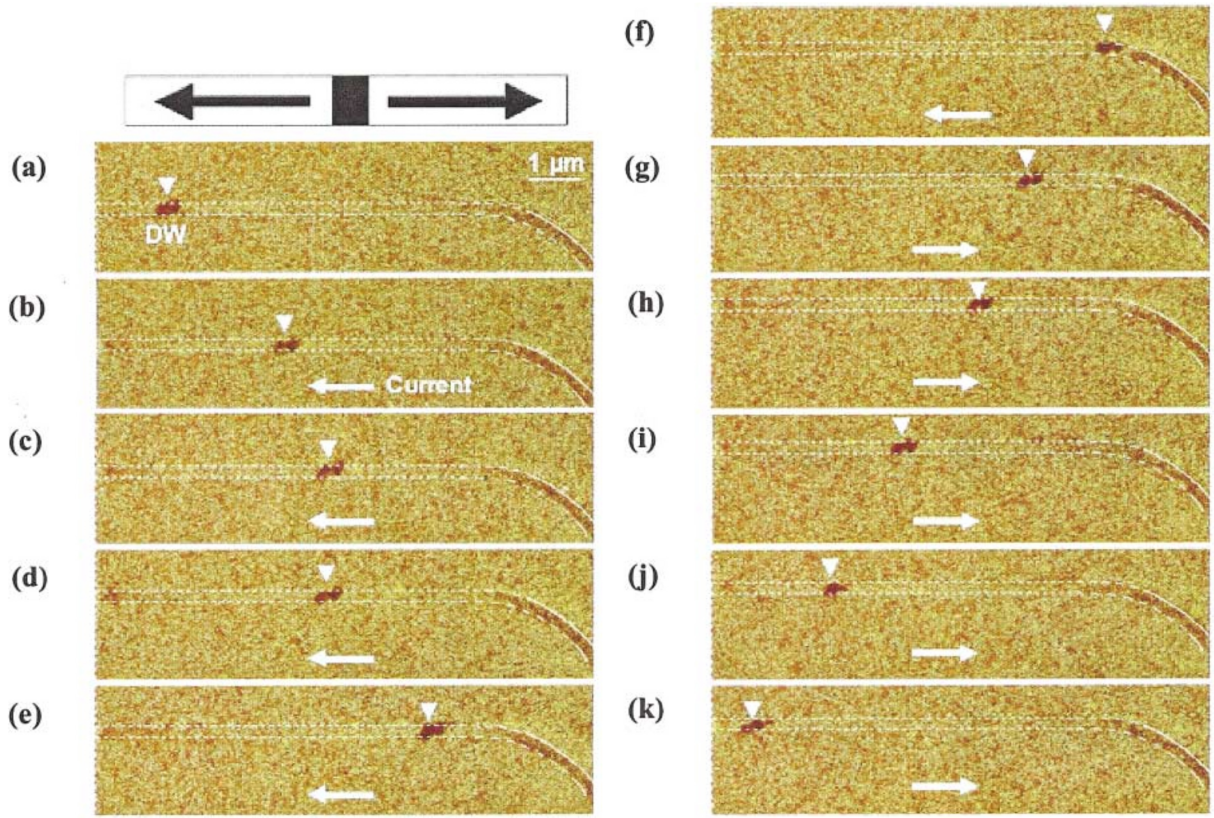

Here, arrows indicate the technical current direction

Current pulses: 1.2×10^8 A/cm^2, 0.5 μs

A. Yamaguchi *et al*., Phys. Rev Lett. **92**, 077205 (2004)

STT term in continuous limit

STT acting on a magnetization distribution $\vec{M}(\vec{x})$ due to a current given by the current density $\vec{j}$ and polarization P:

$$\left(\frac{d\vec{M}}{dt}\right)_{\mathrm{STT}} = -(\vec{u}\cdot\nabla)\cdot\vec{M} + \frac{\beta}{M_{\mathrm{S}}}\left[\vec{M}\times(\vec{u}\cdot\nabla)\cdot\vec{M}\right] \quad ; \quad \vec{u} = -\frac{\mu_B P}{eM_{\mathrm{S}}}\vec{j}$$

Slonczewski-like	field-like
in-plane	out-of-plane
adiabatic	non-adiabatic

$\Rightarrow$ Non-adiabatic STT is required to explain experimental observation of current-induced domain wall motion

A. Thiaville *et al*., Europhys. Lett. **69**, 990 (2005)

Current-driven domain wall motion: Racetrack memory

current

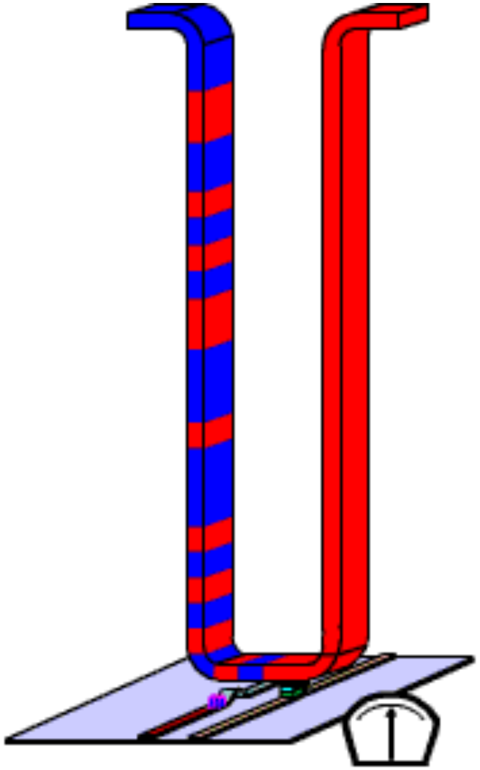

- powerful storage-class memory
- solid-state device
- cost and storage capacities rivaling that of HDDs
- but much improved performance and reliability

Current-driven vortex core switching

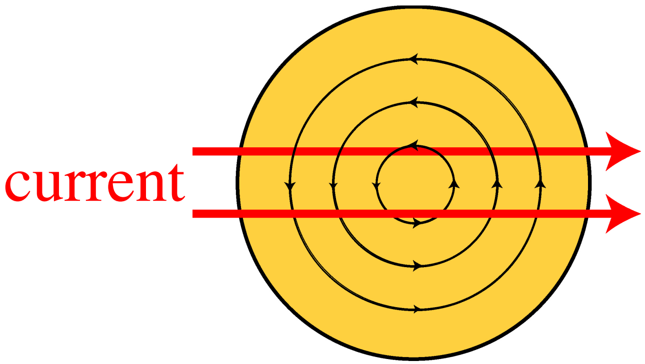

Current pulses applied to magnetic vortices can

- excite the gyrotropic mode of the vortex
- switch the core polarization

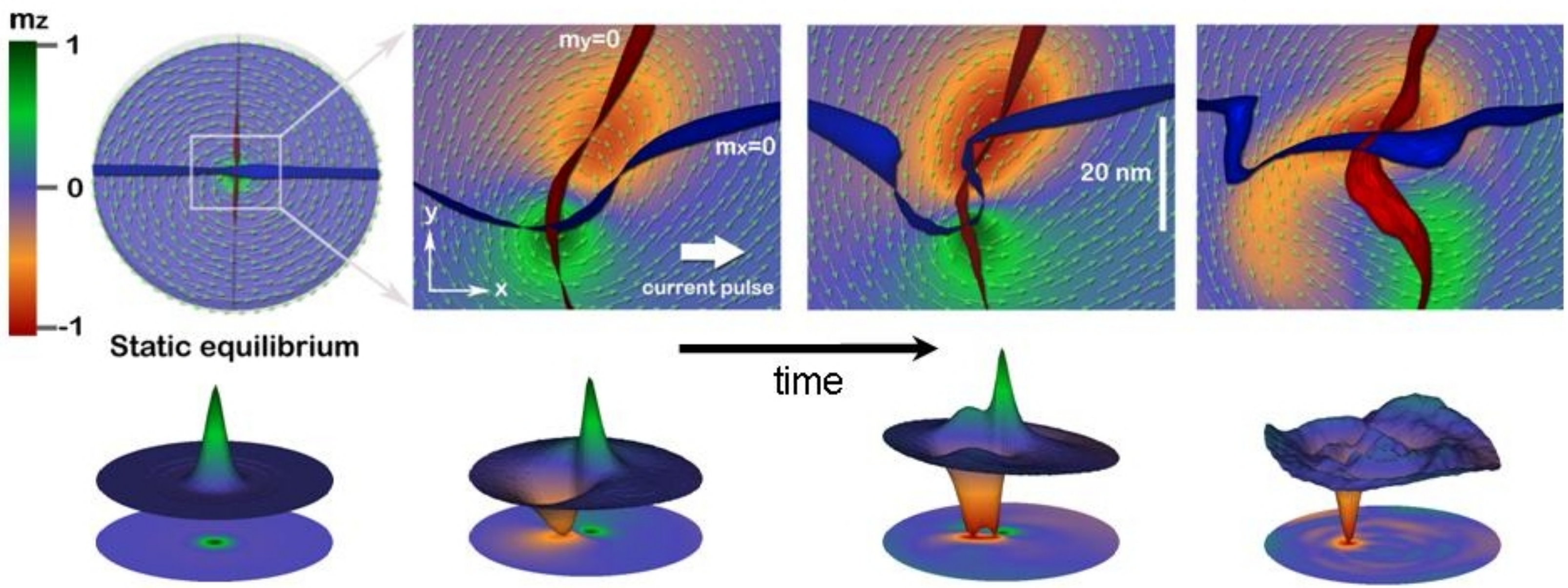

Simulation: Liu *et al*., Appl. Phys. Lett. **91**, 112501 (2007)
Experiment: K. Yamada *et al*., Appl. Phys. Lett. **93**, 152502 (2008)

STT and GMR in metallic antiferromagnets

PHYSICAL REVIEW B **73**, 214426 (2006)

Theory of spin torques and giant magnetoresistance in antiferromagnetic metals

A. S. Núñez,* R. A. Duine,† Paul Haney,‡ and A. H. MacDonald§
Department of Physics, The University of Texas at Austin, 1 University Station C1600, Austin, Texas 78712-0264, USA
(Received 26 April 2006; published 14 June 2006)

PRL **100**, 226602 (2008) PHYSICAL REVIEW LETTERS week ending 6 JUNE 2008

Spin-Transfer Torques in Antiferromagnetic Metals from First Principles

Yuan Xu, Shuai Wang, and Ke Xia
State Key Laboratory for Surface Physics, Institute of Physics, Chinese Academy of Sciences, P.O. Box 603, Beijing 100080, China
(Received 15 August 2007; published 3 June 2008)

PHYSICAL REVIEW B **75**, 174428 (2007)

Ab initio giant magnetoresistance and current-induced torques in Cr/Au/Cr multilayers

P. M. Haney,[1,*] D. Waldron,[2,†] R. A. Duine,[3,‡] A. S. Núñez,[4,§] H. Guo,[2,‖] and A. H. MacDonald[1,¶]

Conclusions on STT

- STT is understood in terms of spin momentum transfer and angular momentum conservation
- Current-induced STT enables a novel, highly non-linear magnetization dynamics
- Current-induced magnetization switching and STOs are of high technological relevance